UNCLASSIFIED

~~OFFICIAL USE ONLY~~

UCRL 9243

UNIVERSITY OF CALIFORNIA

Ernest O. Lawrence

Radiation Laboratory

CONTROLLED THERMONUCLEAR RESEARCH
QUARTERLY REPORT
March, April, May 1960

LIVERMORE AND
BERKELEY, CALIFORNIA

UNCLASSIFIED

~~OFFICIAL USE ONLY~~

For Reference

Not to be taken from this room

Bldg. 50

DISCLAIMER

This document was prepared as an account of work sponsored by the United States Government. While this document is believed to contain correct information, neither the United States Government nor any agency thereof, nor the Regents of the University of California, nor any of their employees, makes any warranty, express or implied, or assumes any legal responsibility for the accuracy, completeness, or usefulness of any information, apparatus, product, or process disclosed, or represents that its use would not infringe privately owned rights. Reference herein to any specific commercial product, process, or service by its trade name, trademark, manufacturer, or otherwise, does not necessarily constitute or imply its endorsement, recommendation, or favoring by the United States Government or any agency thereof, or the Regents of the University of California. The views and opinions of authors expressed herein do not necessarily state or reflect those of the United States Government or any agency thereof or the Regents of the University of California.

OFFICIAL USE ONLY

UCRL-9243
Controlled Thermonuclear
Processes (UC-20)
TID-4500 15th Ed.

UNIVERSITY OF CALIFORNIA

Lawrence Radiation Laboratory
Berkeley, California

Contract No. W-7405-eng-48

CONTROLLED THERMONUCLEAR RESEARCH QUARTERLY REPORT

March, April, May 1960

June 20, 1960

Classification changed to UNCLASSIFIED
by authority of memo. from Tech Info. Div.
on 10-27-60 B. Fokett
Date Person making change

OFFICIAL USE ONLY

Printed in USA. Price $2.50. Available from the
Office of Technical Services
U. S. Department of Commerce
Washington 25, D.C.

OFFICIAL USE ONLY

CONTROLLED THERMONUCLEAR RESEARCH QUARTERLY REPORT

March, April, May 1960

Contents

GENERAL INTRODUCTION 4

I. PYROTRON (MAGNETIC MIRROR) PROGRAM . . . . . .

1. Introduction and Summary 7
2. Table Top Magnetic-Compression Experiment 8
3. Radial Scintillation Probe Measurements on Table Top II . . 11
4. Plasma Calorimetry and Electric Field Measurements on Table Top 20
5. Table Top Diagnostics 22
6. Magnetic High-Compression Experiments 23
7. Adiabatic Low-Energy Injection and Capture Experiment (Alice) 25
8. Molecular-Beam Experiment 30
9. Vacuum and Surface Studies 32
10. P-4 (Steady-State Plasma) System 36

II. ASTRON PROGRAM

1. Introduction 38
2. Astron E-Layer Calculations 39
3. Astron-Model Plasma Parameters 42
4. Astron Dry Run Experiment 48
5. 10-Inch Cathode Development 51

III. LIVERMORE PINCH PROGRAM

1. Summary 54
2. Electron-Beam Pinch 55
3. Conical Pinch Plasma Accelerator 59
4. Liquid Sodium Experiment 60
5. 12-Inch Levitron 62
6. Ion Heating by Torsional Waves in a Mirror Machine . . . 64

IV. BERKELEY PLASMA RESEARCH

1. Sheet Pinch Studies 66
2. Homopolar Program 73
3. Crossed-Field Breakdown Studies 76
4. Plasma Physics and Microwave Diagnostics 77
5. Hydromagnetic Wave and Cyclotron Heating 78
6. Ion Magnetron 80
7. Experiments with Pulsed Magnetic Cusps 83

---

* Preceding Quarterly Reports: UCRL-9106, UCRL-9002

OFFICIAL USE ONLY

V. THEORETICAL AND BASIC EXPERIMENTAL PLASMA PHYSICS

1. Energy Transfer from Hot Ions to Cold Electrons in a Plasma 95
2. Densities of Electrons Trapped by the Geomagnetic Field . . 99
3. End Losses in Mirror Machines 100
4. The Magnetic Mirror Instability 101
5. Stability Calculation for a Diffuse Linear Pinch 102
6. Magnetic Shocks 103
7. The Effects of Space Charge on the Shape of Laminar Beams. . 106
8. Energy Dependence of the Critical Pressure for Neutral Injection 109
9. Theory of Scattering of Charged Particles by Atoms 113
10. Atomic and Molecular Beam Research 114

VI. ENGINEERING AND TECHNOLOGICAL DEVELOPMENT

1. Ultrahigh-Vacuum Development 115
2. Mechanical Engineering Development 117
3. Electrical Engineering Development 126

VII. TALKS AND PUBLICATIONS. 135

OFFICIAL USE ONLY

UCRL-9243

CONTROLLED THERMONUCLEAR RESEARCH QUARTERLY REPORT*

March, April, May 1960

Lawrence Radiation Laboratory
University of California
Berkeley and Livermore, California

June 20, 1960

GENERAL INTRODUCTION

C. M. Van Atta

During the period covered by this report on controlled thermonuclear research new results have been obtained in various components of the program. Some of the more significant of these results are mentioned briefly in the following outline.

1. A series of papers is in preparation describing the transverse adiabatic stability theory and applying it to specific cases. Of particular interest is the instability which develops in the magnetic-mirror confinement of a plasma of greater transverse than axial pressure. For a given ratio of the transverse component of the pressure to the axial component a critical value of the ratio of P/B^2 is predicted, above which enhanced radial diffusion due to instability occurs.

2. A fairly complete theoretical treatment of a plasma with nonisotropic pressure confined in a mirror field has been carried out. For comparison with the observation of nonisotropic instabilities produced in the Table Top machine the axial distribution of the plasma for various ratios of transverse to axial pressure components has been computed. Theoretical predictions of the critical values of P/B^2 for various ratios of transverse to axial pressure components can now be compared with the experimental results obtained on the Table Top machine.

3. Additional results have been obtained on the energy transfer from energetic ions to cold electrons in a plasma. It is found that for 20-kev deuterons the rate of energy transfer to electrons from 10 ev to 1 kev temperature is appreciably less than that derived by Lyman Spitzer in "Physics of Fully Ionized Gases." These results are comparable to those described in the preceding report for 200-kev deuterons.

4. In the Baby Alice energetic neutral atomic injection facility there is good agreement between the observed mean life (25 to 30 μsec) of the captured ions as measured by observation of the energetic neutral particles lost due to charge exchange on the background gas and that expected from the pressure of the residual gas and the charge-exchange cross section. This result is significant not only in confirming the expected behavior of the Baby Alice experiment but also in providing a calibration of the energetic-neutral-particle probes which will be used in the full-scale Alice machine.

*Work done under the auspices of the U. S. Atomic Energy Commission.

OFFICIAL USE ONLY

5. The character and causes of rf oscillations in the experimental Astron injection system have been identified and the oscillations have been very greatly suppressed. The oscillations were traced to several causes: the broad energy distribution of the electrons as initially injected, rf modulation of the electron beam in the injector due to klystron-like oscillations in the electrode structure, and shock excitation of transverse electric modes in the beam-trapping cavity by the incoming beam pulse. The first two causes were reduced substantially by injecting electrons of very narrow energy range and by correcting the causes of oscillation in the accelerating column. Shock-excited oscillations have been suppressed by introduction of radial fins near the outer wall of the cavity.

6. The electron-beam probe apparatus for exploring the magnetic field of a linear magnetically stabilized pinch is now working reliably. Indications are that the electron beam follows the magnetic field lines "adiabatically," so that interpretation of motions of the beam spot is now possible. The apparatus is particularly well suited to the measurement of diffusion of the B_θ into the B_z field, for which preliminary observations are in progress.

7. Further study of the output of the conical pinch plasma accelerator indicates that the average energy of the plasma deuterons is from 3000 to 100 ev, the plasma density from 10^{14} to 2×10^{15} deuterons/cm^3 for operation in the pressure range from 100 to 400 μ of D_2. The total output ranges from 10^{17} to 10^{18} deuterons per pulse and represents from 1 to 10% of the initial gas in the discharge. The output plasma velocity is found to depend upon the direction of the applied potential. If the voltage is reversed so that the output electrode is the anode, the mean output velocity is reduced to about one-half the figures given above, indicating that electrostatic as well as hydromagnetic forces play a role in the plasma propulsion in this device.

8. Measurement of the radial current flow at the boundary of the plasma in the hydromagnetic-wave experiment demonstrates that the oscillating-current circuit is completed in the plasma and not in the wall of the tube that contains the plasma. This measurement yields the boundary condition, which has been in doubt, and in particular proves that the azimuthal magnetic field goes to zero at the boundary. These conditions can now be put into the solution for the modes that are first-order Bessel functions for the radial current with zero values at the central axis and at the wall. Higher modes can be experimentally separated from the fundamental because of differences in attenuation.

9. With an input of about 200 kw of 9-Mc rf power into the hydromagnetic wave in the Hothouse II plasma-heating experiment for periods of about 100 μsec, microwave measurements indicate that about 30% of the neutral gas is ionized by the rf alone. A substantial increase in rf power input will result from modifications now in progress.

10. The formation time for low-pressure breakdown at 100 kv in the Homopolar IV device at magnetic field intensity of 10 to 20 kilogauss is found to be from 100 to 200 μsec. This period appears quite adequate for injecting a puff of gas and ionizing it to form a rotating plasma.

11. The fast cusp compression of a section of a linear-discharge (moderate-pinch) column has resulted in the formation of a disc of plasma in the median plane of the cusp field. The combination of a linear-discharge column with a fast-rising cusp field may provide a more valid means of studying cusp confinement of a high-β plasma than other experiments previously described.

An interesting occurrence toward the end of this report period was the visit of the thermonuclear visiting team from the USSR. The group--consisting of Boris I. Gavrilov, Il'ya F. Kvartskhava, Yevgeniy V. Piskarev, Vladimir T. Tolok, and Natan A. Yavlinskiy--represented those in the USSR who are more interested in fundamental plasma physics experiments than in the immediate construction of large thermonuclear devices. Aside from reports on their own experimental research, the Russian group brought with them a manuscript by B. A. Trubnikov on the calculation of electron-cyclotron radiation from a plasma, which appears to substantiate the results of Trubnikov and Kudryavtsev published in Volume 31 of the proceedings of the Geneva Conference of 1958. Exchange of technical information proceeded in an atmosphere of cordiality and mutual respect.

A list of publications by members of the controlled thermonuclear group issued during the quarter is given at the end of this report.

I. PYROTRON (MIRROR MACHINE) PROGRAM

1. INTRODUCTION AND SUMMARY

Richard F. Post

In the last quarter much of the construction and initial electrical testing of the multistage compression experiment was accomplished, the "Baby Alice" fast-atom injection experiment yielded some preliminary experimental results, and significant new results were obtained in the theoretical understanding and experimental elucidation of the compression-induced velocity-space instability observed in Table Top when very large compression ratios are used.

In the supporting research for the full-scale ALICE experiment, more reliable and very encouraging results were obtained on the pumping of hydrogen gas by molybdenum surfaces. Indicated pumping speeds of 10^5 liters per second were obtained at pressures below 10^{-9} mm Hg. These results now encourage us to believe that the stringent vacuum requirements of the ALICE experiment should be achievable through the use of these and other techniques now developed.

The question of plasma stability continues to be uppermost in the investigations. As a result of the Table Top experiments, we feel that instabilities of a purely hydromagnetic origin (either flute instabilities or the velocity-space "mirror instability") can be avoided, at least in selected circumstances, in our experiments. We are applying the present theoretical understanding of these instabilities (particularly the "mirror" instability) as a yardstick in the coming multistage compression and in the ALICE experiment. It appears that in neither case will this particular instability be troublesome, although it can be seen that it might have been in ALICE had the design magnetic field been lower. But hydromagnetic instabilities may not be the only types that can occur in a Mirror Machine. Still unanswered experimentally or theoretically are the effects of raising the ion temperature above the electron temperature, or the effects of the ambipolar potentials expected in such a case. These answers must await the operation of the multistage compression experiment or ALICE.

2. TABLE TOP MAGNETIC-COMPRESSION EXPERIMENT

Robert E. Ellis and Norris W. Carlson

Electron Energy Distribution and Scintillator-Probe Calibration

Preliminary measurements have been made for the absolute calibration of a scintillator probe of the type used in making electron energy distribution measurements previously reported. The variable-energy 50-kev electron beam apparatus, also mentioned in previous progress reports, has been used for this purpose. It consists of a glass vacuum system containing an electron gun of the type used in cathode-ray tubes. The gun is maintained at negative high voltage. The beam from the gun is accelerated through a stack of accelerating electrodes, then passed through a 1/16-in. collimating hole into a region between electrostatic deflecting plates.

The undeflected beam impinges on the fluor in the scintillator probe, which is at ground potential. A pulse circuit provides voltage to the deflector plates in such a way that the beam normally is deflected into a Faraday cup (designed to prevent secondary emission losses) located off the axis of the undeflected beam. The deflector voltage may then be pulsed off at intervals from a fraction of a second to 100 seconds, with square pulse widths up to approx 10 msec. With appropriate beam currents, the electron energy flux into the probe can be made to simulate the electron energy flux intercepted by the probe in experiments on the Table Top machine. The probe aperture itself is collimated with a 1/8-in. hole in front of the plastic fluor detector.

If one ascertains that the beam has a small enough cross section so that it enters the probe fluor without loss of beam to the probe collimator, and if all the deflected beam is collected in the Faraday cup, then we may determine the probe signal as a function of electron beam current and electron energy.

The equation expressing the signal observed in an oscilloscope in terms of the probe and beam parameters is

$Q = 6.25 \times 10^{12} K \epsilon I [E - E_A]$, where

Q = scope signal, in volts;

K = constant, determined by the absolute scintillation efficiency of the fluor, the photomultiplier gain, efficiency of conversion into electrons at the photocathode of light emitted by the fluor (dimensions are volts/μa/kev);

ϵ = relative efficiency of the fluor in converting electron energy into photons—a function of electron energy and electron beam current—assumed to be essentially unity at sufficiently high energy and low enough beam current (dimensionless);

I = beam current, in μa;

E = beam energy, in kev;

E_A = energy (in kev) given up by an electron of energy E when passing though the thin aluminum coating (approx 2000 Å) on the fluor. Also included in this quantity should be any energy loss not associated with creation of photons, which might be caused by deterioration of the fluor surface or other surface effects.

Preliminary runs have been made with two different fluors to determine the quantity K in the above equation. The first fluor was that used in obtaining much of the data upon which previously reported electron energy distribution calculations were based. (For example, see Quarterly Report, UCRL-9106, March 1960.) Data were obtained only to to E = 22 kev for this fluor because of problems with the electron beam. The 1/16-in. beam collimator had not yet been installed. After the change to a new fluor, with the beam collimator installed, further experience with the apparatus enabled us to obtain a somewhat better set of data, up to E = 40 kev. A pulse width of 1 msec was used. Although the new fluor (prepared in the same way as the other) showed a significantly greater scintillation response, we will have to check this effect by further calibration runs with the old fluor or make further runs on Table Top.

The object of determining the constant K in the equation for Q is, of course, to enable us to determine the absolute flux of electrons escaping through a mirror of the Table Top machine as a function of time during a machine pulse. Using the value of electron flux as a function of time, we may then integrate the flux from some initial time--say, t = 1 msec after the initiation of the magnetic field pulse--to the end of the pulse. The result should give us the total number of electrons intercepted by the fluor during the pulse. If we assume that all the electrons originally in the core of the plasma (a small-diameter region of the plasma along the axis of the plasma spindle, which is the portion of the plasma our probe "sees") eventually escape through the mirror, and if we estimate the volume of the plasma they inhabited before escaping, then we can determine the plasma density at t = 1 msec. Taking into consideration the value of magnetic field at the probe relative to the field in the plasma, and the manner in which the magnetic field decays in time, we can estimate the volume of the plasma from which the electrons escape to enter the 1/8-in.-diameter probe collimator. Typical values of the plasma volume seen by the probe will be a few cubic centimeters, depending on the probe position with respect to the mirror and the mirror ratio. The constant K has been evaluated on the basis of extrapolations of data taken thus far with the calibrating beam. It has not yet been possible, however, to extend the data to sufficiently high beam energies to assure that we can safely assume that the relative scintillation efficiency has been adequately determined for various beam intensities. A few minor changes now being made in the equipment will enable us to do this.

Because of the apparent difference in scintillation efficiency of the two fluors so far tested, the newest fluor was subjected to approx 18,000 pulses from the calibrating electron beam at a rate of 150 ppm, with a pulse width of 1 msec, beam energy of 10 kev, and a beam current of 0.05 μa (approx 3×10^8 electrons per msec). No deterioration in signal was observed. Further tests of the scintillation response as a function of integrated electron energy flux will be made more closely to determine to what extent it is necessary to "condition" a fluor before it is used. It may be noted that beam

currents of a few tenths of μa to a few μa, at a beam energy of approx 25 kev (corresponding to estimates of the mean energy of the escaping electrons detected in some Table Top experiments), produced pulses of substantially the same magnitude as those observed at Table Top. There is some evidence that the probe signal output per microampere of beam current at a given beam energy does not vary more than about 10% for beam currents ranging from approx 0.05 to approx 1 μa during a given run, whereas the effect of several hundred to thousands of pulses may be to lower the scintillation response by something like 20%. These effects have been noted in the process of making several runs through a range of energies, as contrasted to the test made at a beam energy of 10 kev mentioned above. A program of testing and calibrating both single- and multiple-channel probes, using both plastic and cesium iodide fluors, as well as the evaluation of light-piping methods for increased probe sensitivity, continues; some of the probes are ready and others nearly so.

Additional computer runs have been made on Table Top electron-energy-distribution data to obtain values for the escaping electron flux from $t = 1$ msec out to $t = 5$ msec, as detected by a scintillator probe. The results indicate that for the two extreme values assumed for θ (angle of entry of electrons into aluminum absorbers used in electron energy determination—see Quarterly Report, UCRL-9106, March 1960) the electron flux varies by a factor of two, as does the mean energy of the escaping electrons. The case of higher mean energy, corresponding to a larger θ and thus to a longer range in the absorber, yields the smaller flux value. Thus it appears that a correction of that type to account for the effect of using the probe in a high-magnetic-field region should result in a change of a factor of about two in the earlier plasma-density estimates.

3. RADIAL SCINTILLATION PROBE MEASUREMENTS ON TABLE TOP II

Richard F. Post and Walton A. Perkins

The theoretical prediction and first observation of a velocity-space hydromagnetic instability in Table Top was reported in the preceding Quarterly report. This instability is induced by the magnetic compression process itself, provided it is carried out in a density-compression time regime in which collisions are relatively unimportant, and the compression ratio is large. In such a case, a very high ratio of "temperature" perpendicular to the magnetic lines to "temperature" along the lines can be generated, leading to local hydromagnetic instabilities provided a critical value of β (plasma pressure $\div$ $(B^2/8\pi)$ is exceeded (see discussion by William Newcomb, this report, p. 90).

We have used theoretical methods developed by Newcomb to calculate the values of critical β, and its dependence on the quantities $T_{\parallel}/T_{\perp}$ and R (mirror ratio) and on spatial position along the field lines between the mirrors in the confinement region. A closed analytic expression for β_{crit} was derived, which was shown to apply to a broad class of distribution functions, namely those representable as a one-dimensional Fourier integral over Maxwellian functions,

$$f = \int_0^\infty g(\alpha) \exp - \left[\frac{m}{2} \left(\frac{V_{\parallel}^2}{T_{\parallel}} + \frac{V_{\perp}^2}{T_{\perp}} \right) \alpha \right] d\alpha ,$$

i.e., as an arbitrary function of the variable $V_{\parallel}^2/T_{\parallel} + V_{\perp}^2/T_{\perp}$. It is found that the value of β_c is smallest at the midplane of the machine, where it approaches $T_{\parallel}/T_{\perp}$ for small $T_{\parallel}/T_{\perp}$ at all values of R, and for large R at all values of $T_{\parallel}/T_{\perp}$. A plot of β_c vs $T_{\parallel}/T_{\perp}$ at the midplane (point of lowest magnetic field between the mirrors) is shown in Fig. 1 for various values of R.

In the course of determining the values of β_c a calculation was made which yielded a "universal" density-distribution function for any confined equilibrium plasma in a Mirror Machine which can be described by a distribution function of the form above. These curves are plotted in terms of the variable $\psi = B/B_0$, i.e., the local value of B divided by the value of the magnetic field at the midplane. Thus $1 < \psi < R$. To calculate the actual spatial distribution of the plasma, it is necessary to know only the relation between ψ and position, i.e., to possess a normalized plot of field strength vs position. Examples of the "universal" density curves are shown in Fig. 2. The utility of the curves is that they can be compared with experimental density-position curves to determine the parameter $T_{\parallel}/T_{\perp}$. This can then in turn be used to calculate the value of β_c. This is being done in the instability experiment here reported.

The experimental arrangement is shown in Fig. 3. An axial (end) scintillator and a radial scintillator probe protruding into the vacuum system at the midplane monitored the electron fluxes. The stainless steel coating in the vacuum chamber was absent during this experiment.

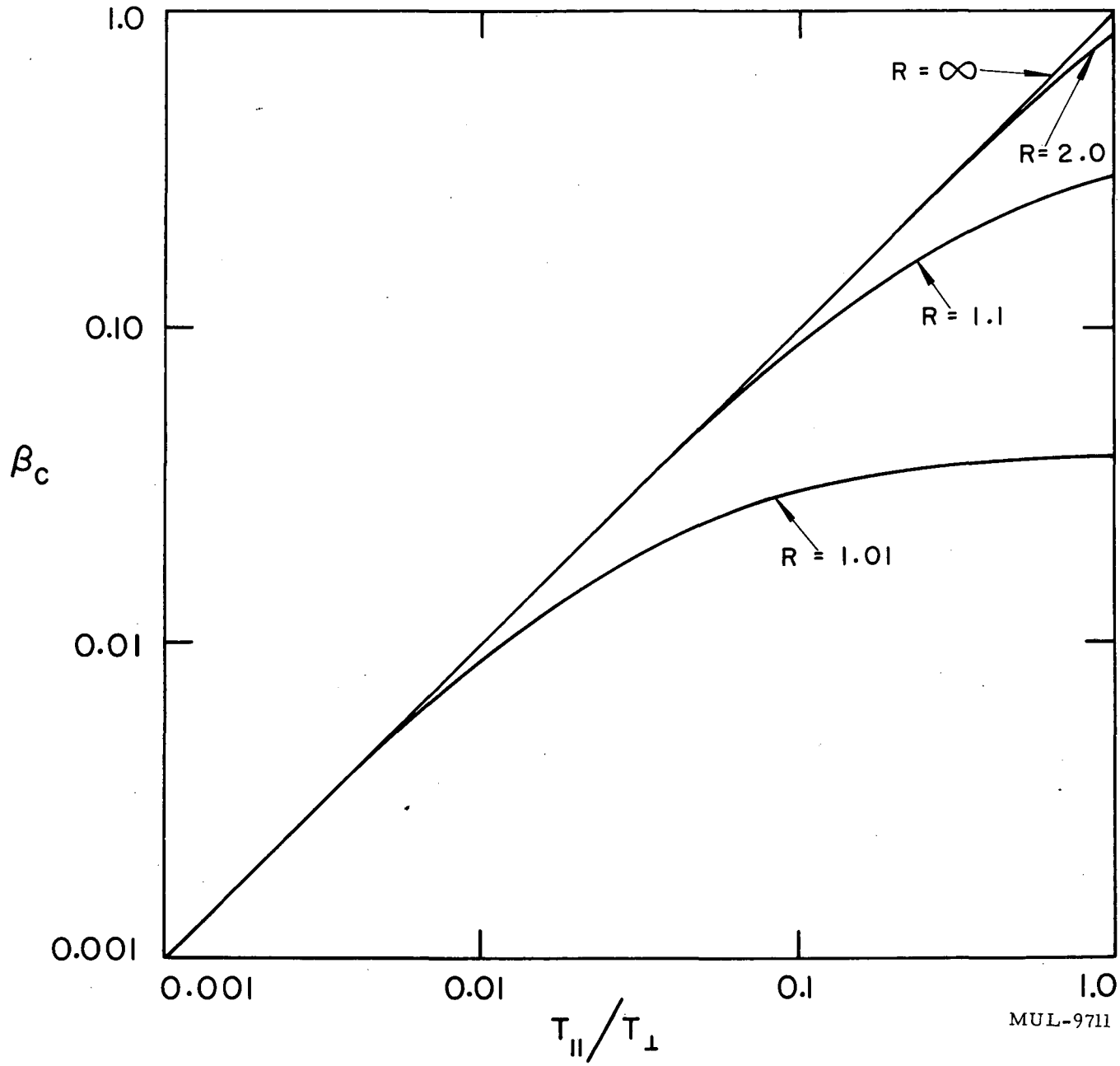

Fig. 1. Critical β curves.

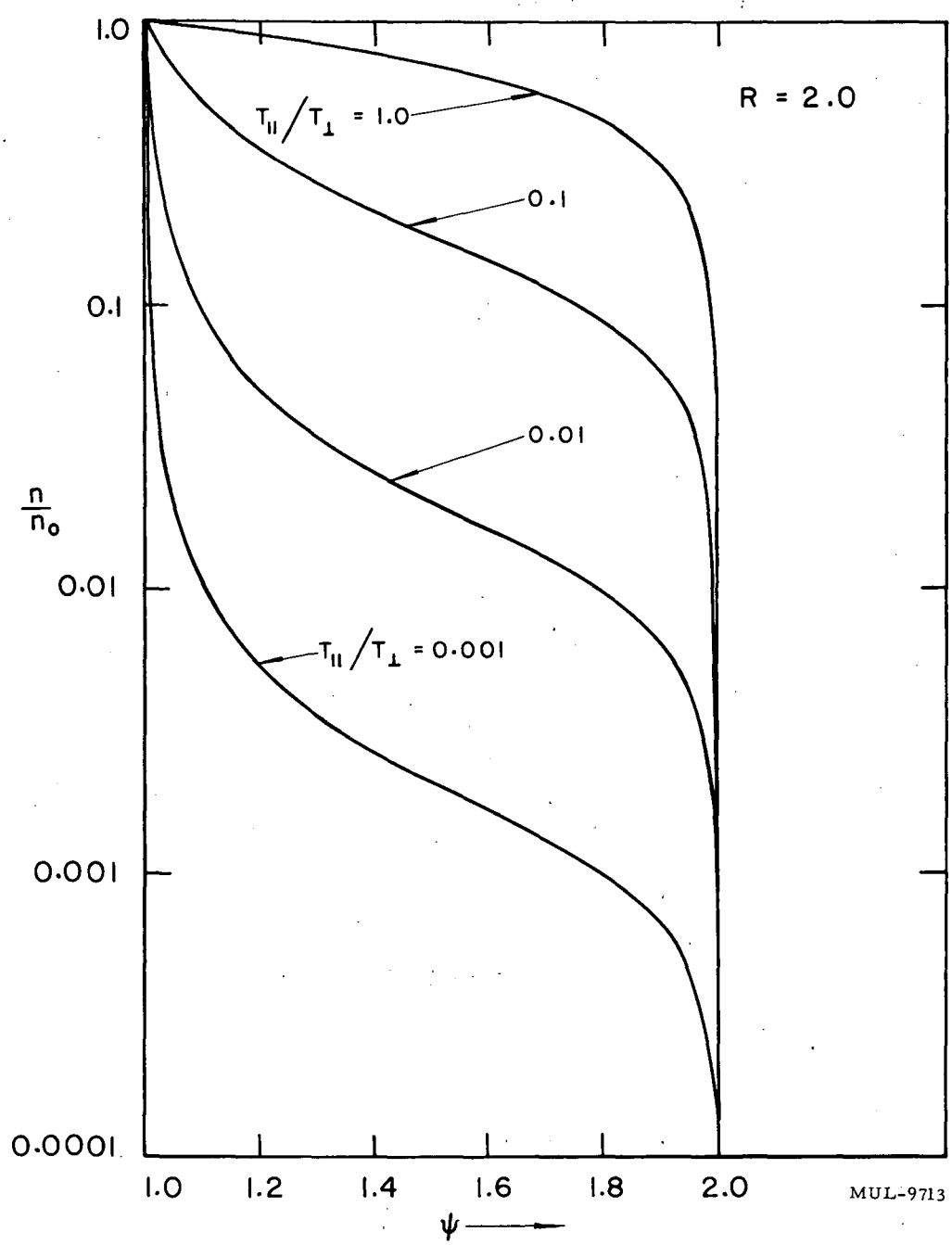

Fig. 2. "Universal" density curves.

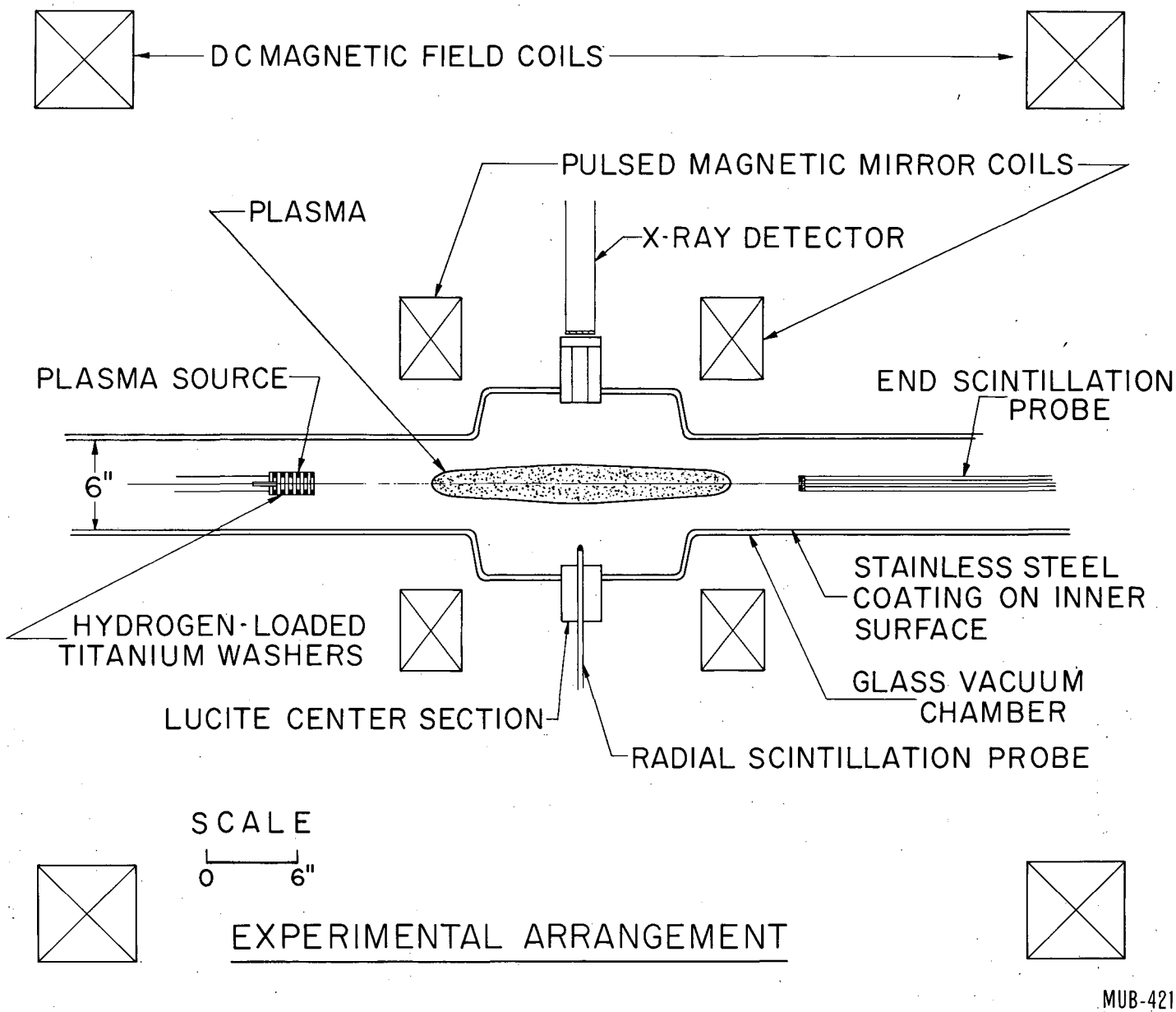

Fig. 3. Diagram of Table Top II.

In the first exploratory experiments, no initial magnetic field was used (i.e., zero dc magnetic field) with a peak pulsed field of 10 kilogauss at the midplane between the mirrors. The position of the radial probe was then varied between the wall of the vacuum chamber and the axis. The end probe recorded a monotonically decreasing signal as the radial probe was moved toward the axis. (This illustrates the effect of an obstacle absorbing the plasma during the magnetic compression). Although strong signals were observed by the radial scintillator even when several inches from the axis, there was no detectable signal from the probe until it was nearer the axis than a fixed protruding obstacle at a diametrically opposite position. This shows that the plasma proceeds across the magnetic field by diffusion, rather than as a jet. A plot of the ratio of radial to end signals as a function of the radial probe's position is shown in Fig. 4. Although the signals from both monitors decrease by a factor of 100 between the 5-1/8-in. position and the 1-1/8-in. position, it can be seen from Fig. 4 that their ratio is constant within the experimental accuracy. From this it can be deduced that the effect of moving in the scintillator probe was only to affect the total number of trapped heated electrons.

Since the radius of the central plasma core has been measured[1] under roughly similar conditions, and found to be less than 3/4-in. at half maximum with a Gaussian shape, the question immediately arises: How are the electrons reaching the radial scintillator with a constant flux at all distances from the axis? We believe that this observed transport of energetic electrons can be explained by the action of velocity-space instabilities, the theory of which is described above.

To study this radial diffusion, other machine parameters were varied. Figure 5 shows a graph of the ratio of radial energy flux to end energy flux as a function of the initial magnetic field. First, one should note that the radial diffusion vanishes as the initial field is increased; this occurs at a relatively small initial field. This is in qualitative agreement with the theory, which shows that β_c increases as $T_\perp/T_\parallel$ decreases, i.e., as the magnetic compression ratio is decreased. On the other hand, an antiparallel initial field tends to increase the radial diffusion. It is clear, however, that both zero and antiparallel initial fields lead to very large effective magnetic-compression ratios.

By varying the voltage across the washers in the plasma source, we were able to vary the density of "trapped" plasma. The effect of this is shown in Fig. 6. In all cases, the end-probe signal increased with increasing density, as expected. The radial-probe signal also increased at low density, but subsequently decreased greatly at high densities. This apparently paradoxical result was already predicted theoretically from the following considerations: At high plasma densities collisions become important during the compression. This greatly lowers the ratio $T_\perp/T_\parallel$ by diffusion in velocity space, so that the plasma again becomes stable.

---

[1] R. F. Post, R. E. Ellis, F. C. Ford, and M. N. Rosenbluth, Phys. Rev. Letters 4, 166 (1960).

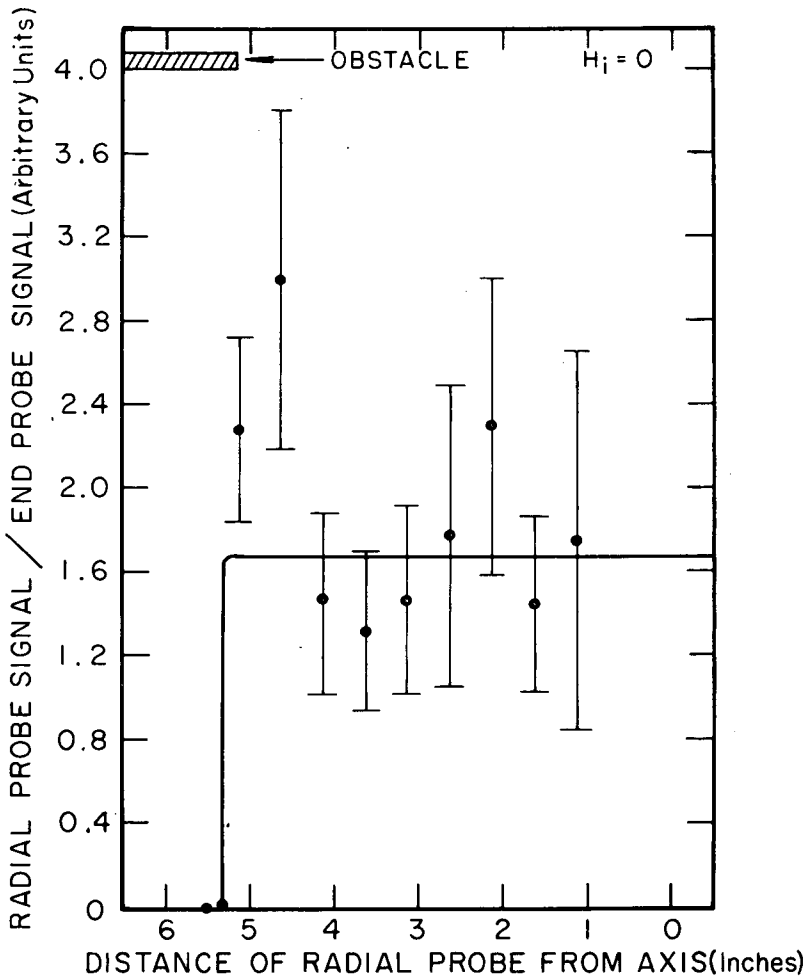

MU-20765

Fig. 4. Ratio of radial-probe signal to end-probe signal as a function of the distance of the radial probe from the axis. Pulsed magnetic field of 10 kilogauss in the midplane, no initial field, and source voltage of 8 kv.

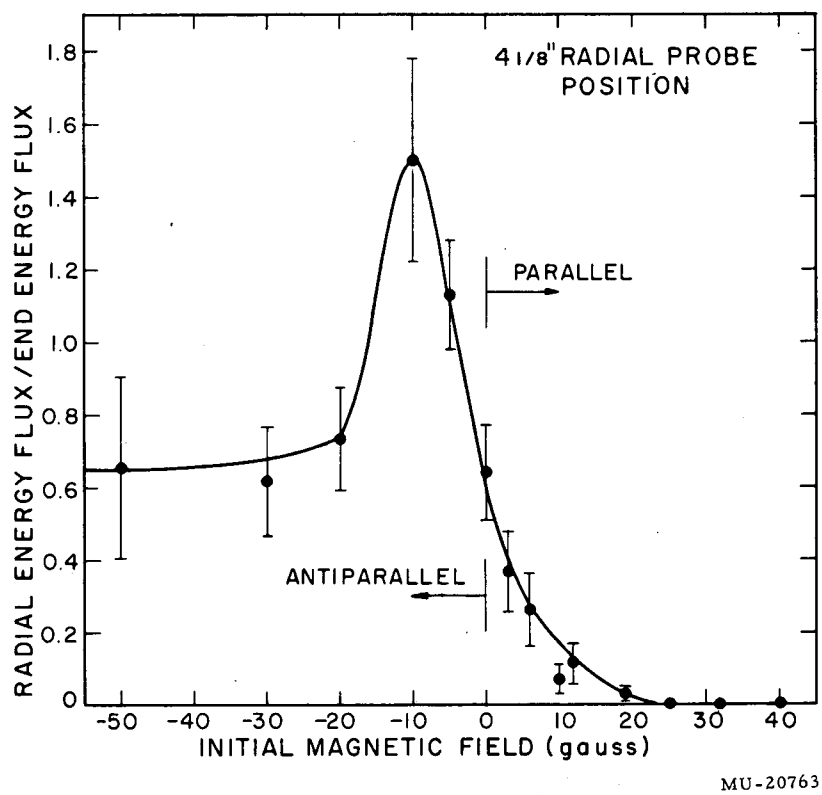

Fig. 5. Ratio of escaping radial-energy flux to end-energy flux as a function of the initial magnetic field. Pulsed magnetic field of 10 kilogauss in the midplane, source voltage of 8 kv.

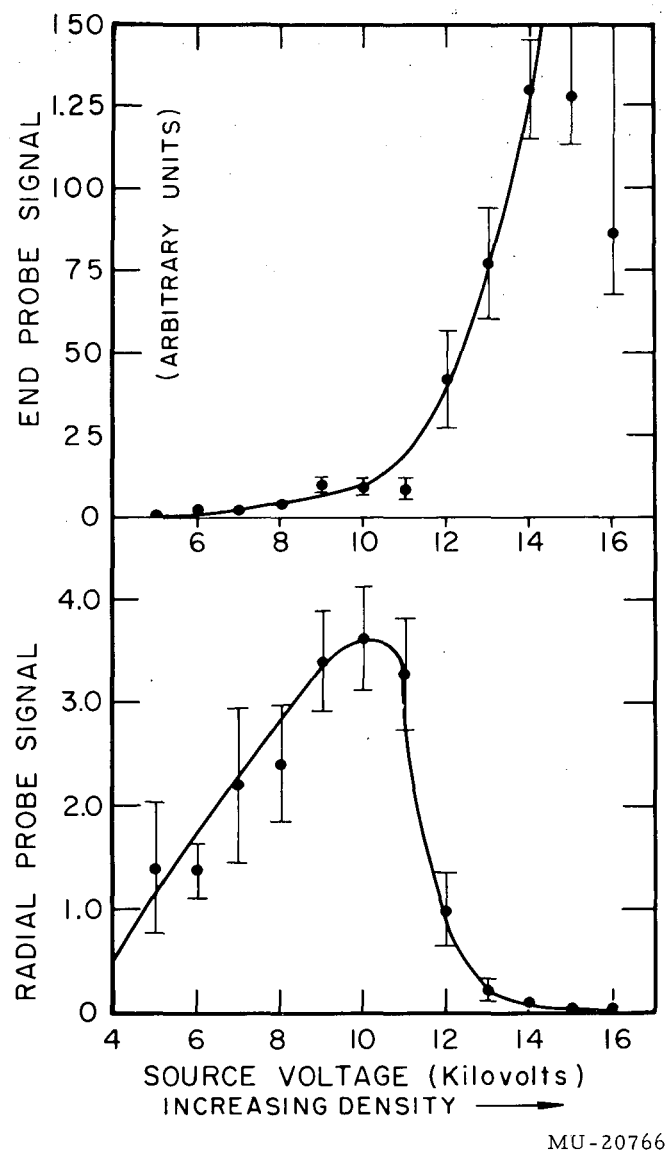

Fig. 6. End- and radial-probe signals as a function of the source voltage. The 15- and 16-kv experimental points for the end probe give only a lower limit because the photomultiplier pulses were saturated. Pulsed magnetic field of 10 kilogauss in the mid-plane, no initial field, and 4-1/8-in. radial-probe position.

In these experiments, in those cases in which instabilities are clearly present it has been determined that the ratio of $T_{\perp}/T_{\parallel}$ is of order 10^3. This leads to theoretical β_c values of about 10^{-3}. Since the electron temperature is about 25 kev, this means that the plasma electron density at which the instability can develop is very low, i.e., of order $10^{11}/cm^3$. At this density and temperature, collision effects are unimportant during the confinement time.

Further analysis of the data to determine rates of diffusion and other important aspects of this new instability are in progress.

4. PLASMA CALORIMETRY AND ELECTRIC FIELD MEASUREMENTS ON TABLE TOP

Thomas O. Passell*

Calorimetric measurement of the plasma escaping Table Top during each compression pulse has been accomplished for the following conditions: (a) nonconducting vacuum system walls; (b) titanium hydride source voltages from 6 to 14 kv; (c) delay time of -600 to + 600 μsec between pulsed magnetic field and source firing time; (d) pulsed compression magnetic fields (at the median plane between mirrors) of 0, 6.6, and 10.6 kilogauss, and (e) dc magnetic fields from 0 to 100 gauss, both parallel and antiparallel to the pulsed field.

In the experiment a titanium hydride source was used, oriented axially, 0.32 meter west of the west mirror. Three calorimeters were used, one 11.4-cm-diameter disc axially oriented 25 cm east of the east mirror, a second annular disc mounted on the source itself 35.6 cm west of the west mirror, and a third disc probe, 1.0 cm in diameter by 0.075 cm thick, in the median plane between the mirrors, 8.9 to 11.5 cm south of the east-west magnetic axis.

These calorimeters were calibrated by using electric heating to simulate the pulsed heating due to escaping plasma. Manganin wire (0.08 mm diameter) was woven throughout the larger axial discs in noninductive spirals, and simply wound as a noninductive coil around the smaller disc probe in the median plane. Thus the heat was added from a distributed source and at or very near the outer surface of the calorimeters. All calibration heating was in 5- to 10-second heating periods, a time short with respect to both the thermal time constants of the calorimeters and the recorder response time.

Thermistors were used to sense the temperature rises, 0.005 to 1.0°C. The probe calorimeter in the median plane was a bare disc thermistor wound with the manganin heater wire. The axial disc calorimeters were made of two layers of graphite cloth, vacuum-evaporation-coated with gold or silver to decrease the radiant-energy loss rate.

Data from an extended run on Table Top are now being reduced. From the sizes and positions of the calorimeters, and assuming the plasma spindle is 6 cm diameter in the median plane, we conclude that some 86% of the total energy escaping Table Top in the form of charged particles was recorded for each pulse. Generally speaking, the total energy in the escaping charged particles was less than 0.3 joule per pulse. Marked effects were noted on the off-axis median-plane probe calorimeter as the dc magnetic field was varied. That is, for conditions expected to excite instabilities and hence enhance diffusion across field lines, larger signals were obtained on this probe than under stable conditions, showing that particles had diffused out to the probe. These data appear to corroborate the measurements by Perkins and Post reported on p. 11 of this report.

---

*Stanford Research Institute, Menlo Park, California.

Development continued of a lithium ion gun to provide a beam for measurement of electric fields during a compression pulse in Table Top. Several attempts to heat indirectly the lithium-mineral-coated anode failed to achieve the required temperature of 1100°C. An anode is now being made in which the lithium mineral is directly applied to a tungsten filament.

Several glass-fiber flexible light guides, 3.6 meters in length by 0.3 cm diameter, are being ordered to bring the lithium ion beam-deflection information from inside the Table Top vacuum system to the outside of the shielded room. A phosphor coating on the machine end of each light guide gives light which is to be sensed by a phototube of the opposite end. Since the fiber light guides transmit best in the green region of the spectrum, a green-emitting phosphor must be used.

5. TABLE TOP DIAGNOSTICS

James T. Mattingly

Electron-Multiplier Studies

The total gain of an electron multiplier is the output current from the structure divided by the input current to the first dynode, where the average gain per stage is the nth root (n being the total number of secondary multiplication stages) of the total gain. The secondary-electron multiplication is a surface and a subsurface effect. Therefore the state of the surface of the dynode has a large part in determining the number of secondary electrons emitted for each incident electron. A change of the state of the surface affects the average gain per stage and also the total gain.

Since the total gain of the RCA 6810 electron-multiplier structure (Rappaport 10 activated) under test had dropped from 10^6 to $\approx 10^{+4}$ or lower (function of voltage on dynodes) a try at rejuvenation was planned. The experimental arrangement was easily adapted to try a gaseous discharge for this purpose.

From a study of Paschen curves, the minimum sparking potential and maintenance voltage was estimated as a function of gas, gas pressure, and plate material. Hydrogen (a natural contaminant of vacuum systems) and argon were the gases used.

The dynodes were discharged in pairs, with the dynode pair acting as one plate, and the acceleration plate in front of the electron multiplier used as the ground plate. The gas pressure was 100 mm of Hg as read on an Auto-vac gauge.

A ratio of the average gain per stage (a function of the voltage per stage) after and before gaseous discharge was determined. Only short-time discharges resulted in a ratio greater than one. The ratio for the 30-sec hydrogen gaseous discharge was 1.12, while the ratio was 1.18 for argon flashing.

For discharges of longer duration, the "improvement" ratios were less than one. A 3-min H_2 discharge destroyed the electron-multiplier structure by ruining the dynode surfaces and plating the insulators.

The leakage current from the electron multiplier increased with the duration of the H_2 discharge. Argon discharges showed evidence of some cleaning, but the surfaces were gradually recontaminated by the vacuum.

The next series of tests will include gaseous discharge (argon only), electron bombardment, and heating. To make better use of the equipment, more than one electron multiplier will be exposed at the same time, one being used as a control.

6. MAGNETIC HIGH-COMPRESSION EXPERIMENTS

Frederic H. Coensgen

In the past quarter, the construction and testing of the facilities for the multistage experiment continued to be the major occupation of the Toy Top group. As indicated in the preceding report, the plasma behavior in the first two stages of the experiment will be studied before the final compression magnets are installed.

Injection of the plasma into the 18-in. chamber and its diffusion along the magnetic field into the 9-in. chamber are fairly well understood from previous work. We are therefore concerned first with the trapping in the 9-in. chamber and the transfer from the 9-in. to the 4-in. chamber. Purity, density, and ion energy of the trapped and transferred plasma will be determined.

The dc fields have been constructed so that it will be possible to determine the angular distribution and hence the rotational energy distribution of the trapped ions. This information together with the ion energy distribution after transfer should yield a quantitative determination of the ion heating in the compression and transfer processes.

If the gating field blocks the late plasma for a sufficient time it may be possible to make a significant measurement of the stability of the plasma in the 9-in. chamber. As the mean ion energy is expected to exceed that of the electrons, the plasma conditions should be such that a measurement of the confinement may help elucidate the results obtained by Ioffe, Sobolyer, Telkovsky, and Yushmanov in the USSR. In their experiment the confinement of even a very-low-density plasma in a Mirror Machine seemed to be subject to some abnormal loss process.

Construction of Multistage Experiment

The dc magnet assembly has been completed and the current distributions determined for the dc fields necessary for the measurements described above. All the power and plumbing associated with these magnets have been installed.

Capacitor Banks 1 and 4, which supply the gating and transfer coils, have been constructed and tested. It has been necessary to install additional bracing for some of the transmission lines in Bank 4, and less resistive line from Bank 4 to the transfer coil is being designed (see Electrical Engineering Progress Reports for February 1960 and May 1960 by David R. Branum). During the full-scale tests the first set of transfer magnets was destroyed. The failures were mechanical in nature and occurred in the current leads at the magnet and in the bussing between turns of the magnet. Both the electrical and mechanical stresses are greatest at these positions, but the space available for insulation and mechanical bracing is restricted.

The first magnet was insulated by a nylon coating independent of the bracing. A second set of transfer magnets has been constructed using glass cloth and roving impregnated with epon. In these magnets the mechanical and electrical stresses are retained by the same material. These magnet sections have been separately tested at full load (50 pulses) outside the dc system and are now in place. It is still necessary to determine the pulsed field shape and possibly to adjust the transfer-magnet position before the vacuum chamber can be installed.

All the vacuum chamber parts for the experiments discussed above have been fabricated and leak-checked. The assembly should be completed within 1 to 2 weeks after the transfer magnet has been positioned.

Vacuum Techniques

During this quarter a major effort has been made to improve the vacuum in the Toy Top systems without sacrificing accessibility or flexibility. A lower base vacuum should allow us to operate the plasma generators at a slower repetition rate, which in turn reduces the pumping load. It also simplifies the controls for experiments using pulsed magnetic fields. An improved vacuum is also important for the stability experiments.

Robert Jopson has given us considerable assistance in improving both the base pressure of the mercury diffusion pumps and the over-all pumping speed of the pump and baffle system. This speed is now 900 liters per second compared with the previous speed of 300 to 400 l/sec. It now appears that the system may operate at a base pressure of 10^{-7} mm of Hg, compared with the former 5×10^{-6} mm of Hg. The trapped base pressure of the pump and baffle is 10^{-8} mm of Hg.

Plasma Generators

Recently we have succeeded in limiting the current through the plasma generators to a single half cycle. It is now also possible to short-circuit the generator after the first quarter cycle (crowbar operation).

The ion output for half-cycle operation is only half that of the ringing operation. The angular distribution in zero field appears unchanged. Probe signals appear much shorter in duration. Measurements are in progress to determine the ion energy distribution. It is believed that the high-energy end of the distribution will be unchanged and that the number of low-energy and late ions will be decreased. These results would simplify the operation and the pumping requirements in the Toy Top experiment.

7. ADIABATIC LOW-ENERGY INJECTION AND CAPTURE EXPERIMENT (ALICE)

Preliminary Build-Up Experiment ("Baby Alice")

James F. Steinhaus and Charles C. Damm

The ion beam can now be deflected before neutralization so that the neutral beam traversing the chamber can be switched on or off in a few microseconds. In this way one can observe the plasma growth and decay. A preliminary measurement of plasma decay at one pressure indicates agreement with the predicted charge-exchange time, but a quantitative comparison will require some refinement of the diagnostic electronics. The measurement of the local neutral density in the plasma region during the magnetic field pulse remains, however, a problem. On the other hand, if one accepts simple charge exchange as the dominant loss mechanism, the plasma decay time can be used as a measure of the local gas density.

Photographs have been obtained of the beam traversing the mirror region. With the magnetic field present, the precession of the trapped particles is shown by a region of light, progressing farther around the magnetic axis as the pressure is lowered and the charge-exchange time lengthened. The direction of precession reverses with the magnetic field direction, as expected.

Several equipment modifications have been made in order to obtain lower operating pressures in the confinement chamber. The hydrogen gas cell neutralizer was simplified and rebuilt to eliminate vacuum leaks. A water-cooled beam collimator was installed at the beam entrance to the mirror region. Two leaking titanium evaporator pump tanks were replaced with tight units. All in all, the base pressure was improved by a factor of ten, and the lowest operating pressure is now in the 10^{-6} mm Hg range. Vacuum ionization gauge calibration curves were made for hydrogen, helium, and air against a McLeod gauge, with results comparable to those Dushman and others.

A palladium leak has been installed for the introduction of all hydrogen used in this system, in order to eliminate inert components (particularly argon) for which our pumping speeds are low. Such gases could seriously alter the gas composition in the confinement region, confusing the diagnostic signals.

Theoretical Considerations

Archer H. Futch and Charles C. Damm

The spatially dependent build-up equations for ALICE discussed in previous progress reports have been recoded to improve the numerical accuracy. The results, although somewhat different numerically, are in general agreement with previously reported solutions.

Theory indicates that the trapped ion density will increase exponentially if the ratio of neutral beam current density, J_0, to background gas density, n_0, exceeds a certain value termed the critical ratio. For the geometry and parameters being considered for ALICE, the critical ratio is approximately 4.5×10^8 atoms-cm/msec. In order to investigate the relative value of increased beam vs better vacuum, four machine solutions were obtained for a constant value of the ratio J_0/n_0. The value of J_0/n_0 used was 9.7×10^8 cm/sec, or about twice the critical ratio. Numerical results are shown in Fig. 7 and the appropriate parameters are listed in Table I. Curves 2 and 4 omit the effect of charge exchange of the trapped fast ions with the beam, while Curves 1 and 3 include it. Comparison of Curve 1 with 3 (or 2 with 4) shows that a larger beam current is clearly preferable to improved vacuum, as to both final ion density and build-up time. This result is in qualitative agreement with the simple theory[1] which predicts a limiting ion density proportional to beam current, and an e-folding time inversely proportional to the same quantity when the ratio J_0/n_0 is held constant. The numerical results, however, indicate a somewhat stronger dependence of these two parameters on the current.

To determine the optimum neutral beam width, calculations of the ion density as a function of time were made for various beam widths. The results are shown in Fig. 8, where t is the beam width and the other parameters for these curves are given in Table I. It appears from this that a beam slightly smaller than the 2.54 cm contemplated may be advantageous, especially since this also aids in achievement of the necessary vacuum condition (an effect, however, not included in the computations for Fig. 8).

---

[1] R. F. Post, IV International Conference on Ionization Phenomena in Gases, Uppsala, 1959 (North-Holland Publishing Company), and Richard F. Post, Some Aspects of High-Temperature Plasma Research with the Mirror Machine, UCRL-5604-T, Jan. 1960.

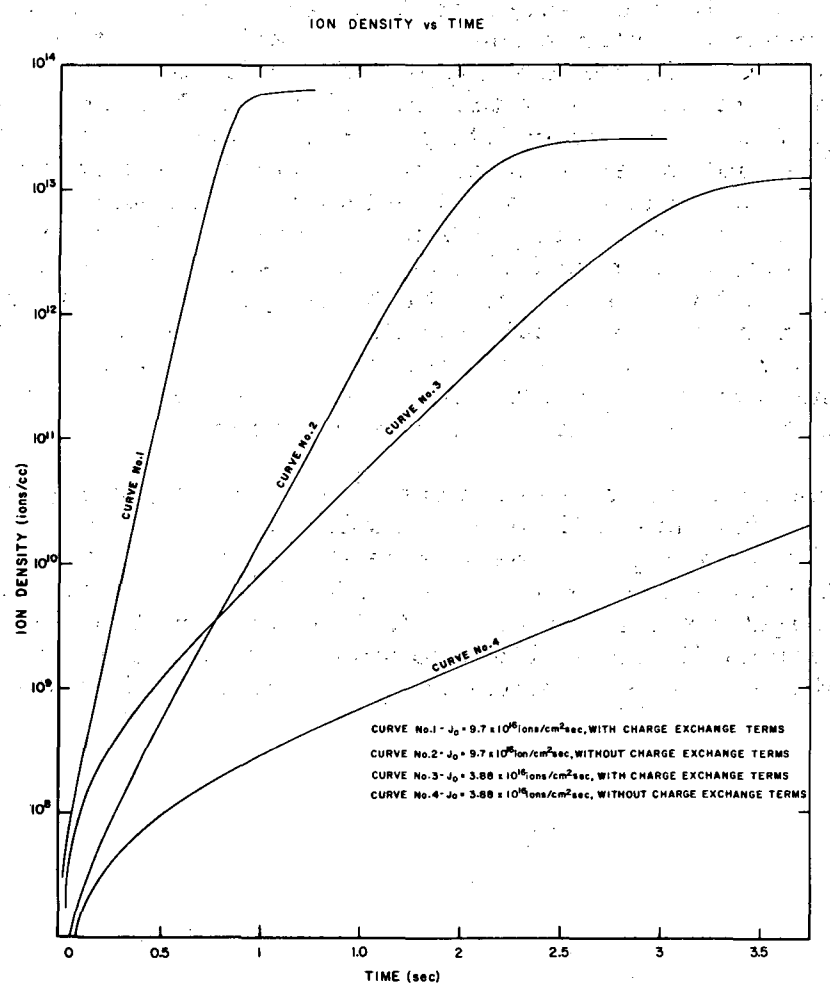

MU-20761

Fig. 7. Ion density vs time.

Table I

Parameters for build-up equations

Parameter	Fig. 7		Fig. 8
	Curves 1 and 2	Curves 3 and 4	
Deuterium neutral gas density (molecules/cc)	1×10^{8}	4×10^{7}	1×10^{8}
Injected neutral atom current (atoms/cm^2-sec)	9.7×10^{16}	3.88×10^{16}	9.7×10^{16}
Energy of injected deuterium atoms (kev)	20	20	20
Magnetic field (gauss)	50,000	50,000	50,000
Beam width (cm)	2.54	2.54	(see Fig. 2)
Distance of beam center above the magnetic axis (cm)	0.575	0.575	0.575
Direction of magnetic field if viewing the plasma from the direction of the source	From left to right	From left to right	From left to right

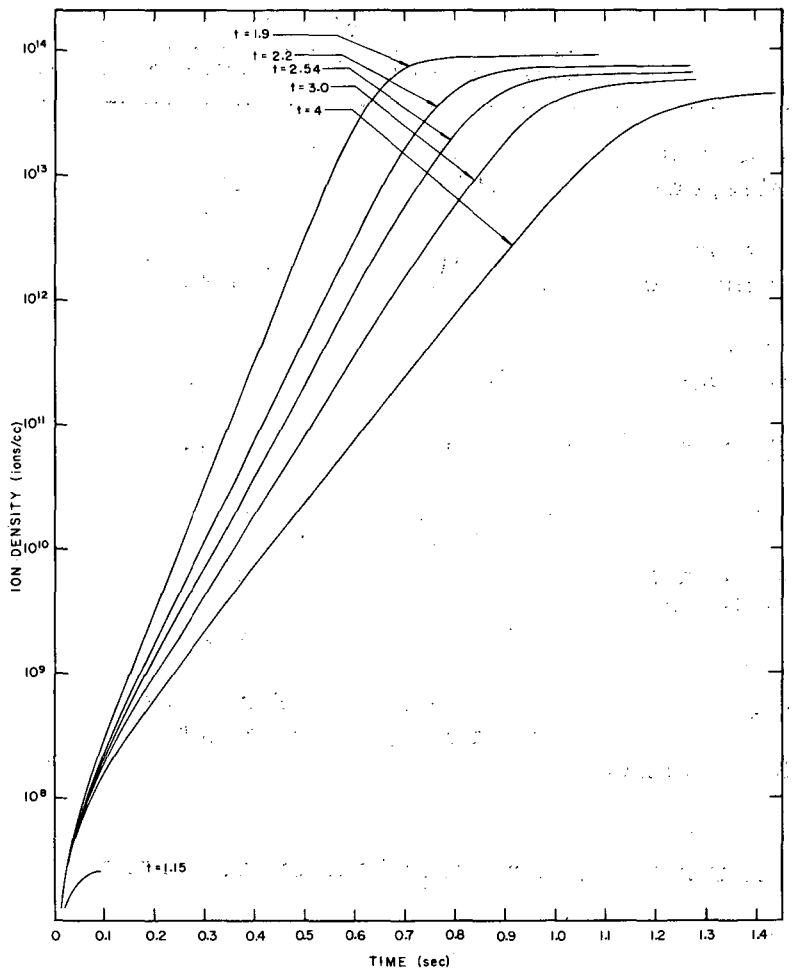

MU-20762

Fig. 8. Ion density vs time for various beam widths.

8. MOLECULAR-BEAM EXPERIMENT

Archer H. Futch

One of the difficulties associated with achieving necessary vacuum in ALICE is the small component of thermal gas from the neutralizer that is scattered straight down the beam tube. Since this gas does not strike the walls of the beam tube, it cannot be "pumped." It therefore results in a lower limit to the local density that can be attained in the trapping region of the Mirror Machine. It is necessary to determine this gas density, and, if it is too great, to reduce or eliminate the thermal beam.

A molecular-beam experiment has been undertaken to study the problem. Two types of information can be obtained from this work. The first is that cross sections for small-angle scattering of a D_2 molecule by H_2 or H_2O molecules can be measured. These cross sections are needed for calculation of the molecular density in the beam entering the Mirror Machine.*

It has been suggested that either a PIG or arc-type discharge could be operated across the beam tube. It is hoped that a discharge can be found which can shield the thermal gas of the neutralizer from the trapped plasma, allowing the energetic atoms to pass through as a result of their much greater velocity. The decrease in intensity of a molecular beam after traversing a discharge is a direct measurement of the shielding ability of the discharge for thermal gas. This is the second type of information desired from the molecular-beam experiment.

Apparatus and Preliminary Results

A thermal beam of deuterium molecules has been formed by collimating the gas streaming out of a small hole in the deuterium reservoir. The D_2 pressure in the reservoir is approximately 10^{-3} mm Hg. The deuterium beam is then passed through either the scattering gas or the electrical discharge and the decrease in beam intensity measured. The detector consists of a small hole 0.125 in. in diameter through which the beam passes into a helium leak detector. Since the charge-to-mass ratio for D_2 is the same as for He, this readily available equipment provides a sensitive measurement of the molecular-beam intensity.

---

*A preliminary calculation by Charles C. Damm indicates that the molecular density from the neutralizer is approximately 10^8 molecules/cc along the beam axis. This calculation is based on somewhat uncertain cross sections measured by earlier workers with molecular beams.

Preliminary cross-section measurements have been made for scattering of D_2 by H_2 and by H_2O. The results are:

Scattering gas	Cross section for scattering greater than 0.75 degree
Hydrogen	5.1×10^{-15} cm^2
Water vapor	$16. \times 10^{-15}$ cm^2

No decrease in beam intensity was observed when the beam was passed through a PIG discharge approximately 1 in. in diameter and in length, operating at 0.1 ampere drain from the high-voltage supply. This would indicate that the electron density in the discharge is less than 10^{12} electrons/cc. Measurements on an arc-type discharge produced by an electron source designed by Frank Gordon will be tried within the next few weeks.

9. VACUUM AND SURFACE STUDIES

Angus L. Hunt, Charles C. Damm, and Earl C. Popp

Getters and Getter Pump Development

The evaporative deposition of molybdenum has been extended to a baked stainless steel vacuum system. Moderate heating (150°C for 12 hr) reduced the initial pressure readings to 5×10^{-9} mm Hg, before evaporation of any molybdenum. Deposition of molybdenum resulted in gauge readings no lower than 4×10^{-10} mm Hg. In this moderately baked system no lower ultimate pressure was obtained than in the unbaked system when molybdenum was deposited on the walls of the vessel.

It was possible to isolate this particular system from the liquid nitrogen trap and diffusion pump by an all-metal ultra-high-vacuum valve, and to measure the pressure increase as a function of time after valve closure. Figure 9 shows the pressure rise with time after the system is isolated from the trap and diffusion pump. The upper curve is the pressure rise observed for the cold system after baking and before any molybdenum was evaporated. The remaining curves indicate the decrease in both the rate of rise and the maximum pressure attained as molybdenum is deposited. That the components responsible for the pressure rise in the molybdenum system are inactive with respect to molybdenum is conclusively shown in Fig. 10, where two molybdenum depositions were completed with the system isolated from the liquid nitrogen trap and the diffusion pump. After closure of the valve at time zero, the usual pressure rise occurs. Two 1-minute vaporizations of molybdenum did not reduce this pressure. Opening the valve to the diffusion pump and trap rapidly reduced the pressure below the initial value. These pressure variations are consistent with the hypothesis that part of the function of a molybdenum deposit is to reduce the degassing rate of inactive gases, allowing the relatively small pumping speed of the diffusion pump and trap to reduce the inactive gas pressure within the system. The molybdenum deposit might reduce the conductance between the contaminated walls and the system and thereby reduce the rate at which ungetterable components reach the system. The ungettered components must have a sufficiently low vapor pressure to remain on the walls of the vessel during the low-temperature baking cycle. Thus it appears that the reduction in pressure produced in unbaked or moderately baked systems by the vaporization of molybdenum is probably related to the proportion of surface covered by the molybdenum as well as the adsorptive properties of the molybdenum deposit.

In a different system, which was not baked, the pumping speed for a molybdenum deposit on a substrate of 8×10^{3} cm^2 area has been determined for pure H_2 and D_2. The H_2 or D_2 was introduced directly into the system through a Pd diffusion thimble. The initial pumping speed for our geometry is much higher than that previously reported. This is almost certainly due to the improved purity of the H_2 or D_2 used. The initial speed at room temperature is about 8×10^{4} liters per sec for D_2 and 10^5 per sec for H_2. A sufficiently small H_2 or D_2 loading rate, approximately 2×10^{10} molecules per cm^2, provided a long monolayer time, about 10^4 sec. Gauge readings indicated a pressure of less than 10^{-9} mm Hg over the molybdenum deposit during the measurements. The effective sticking probability for D_2

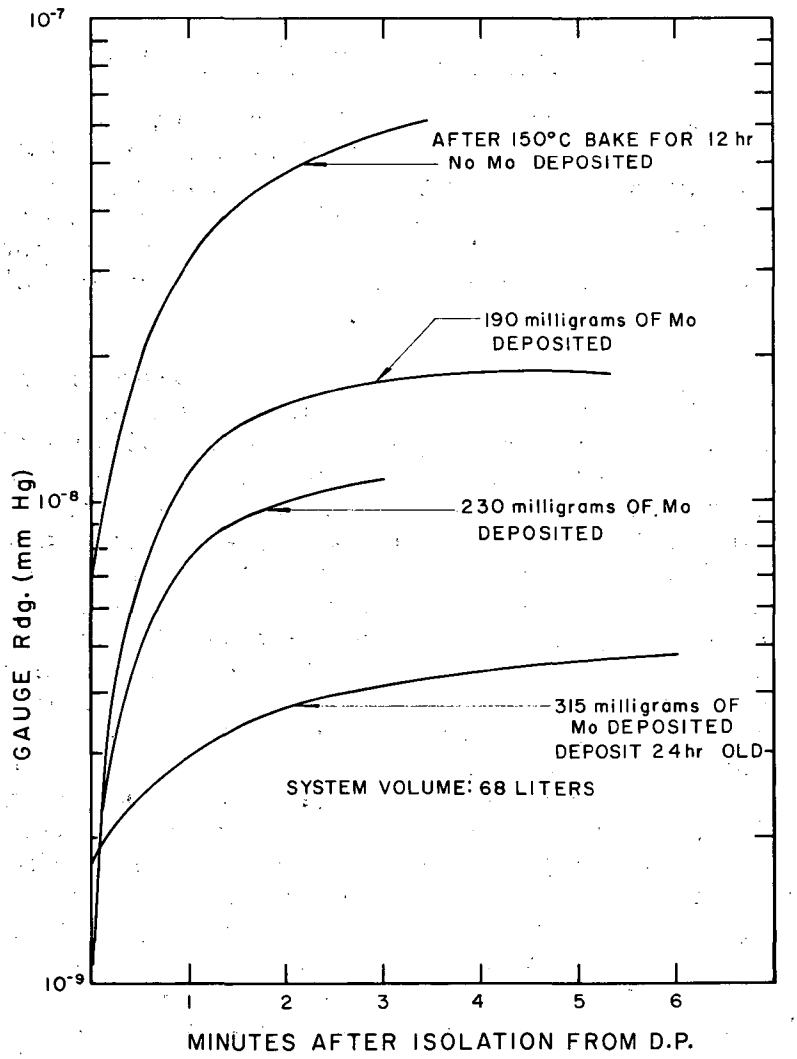

MU-20768

Fig. 9. Pressure rise after isolation from the diffusion pump, as a function of the amount of molybdenum deposited.

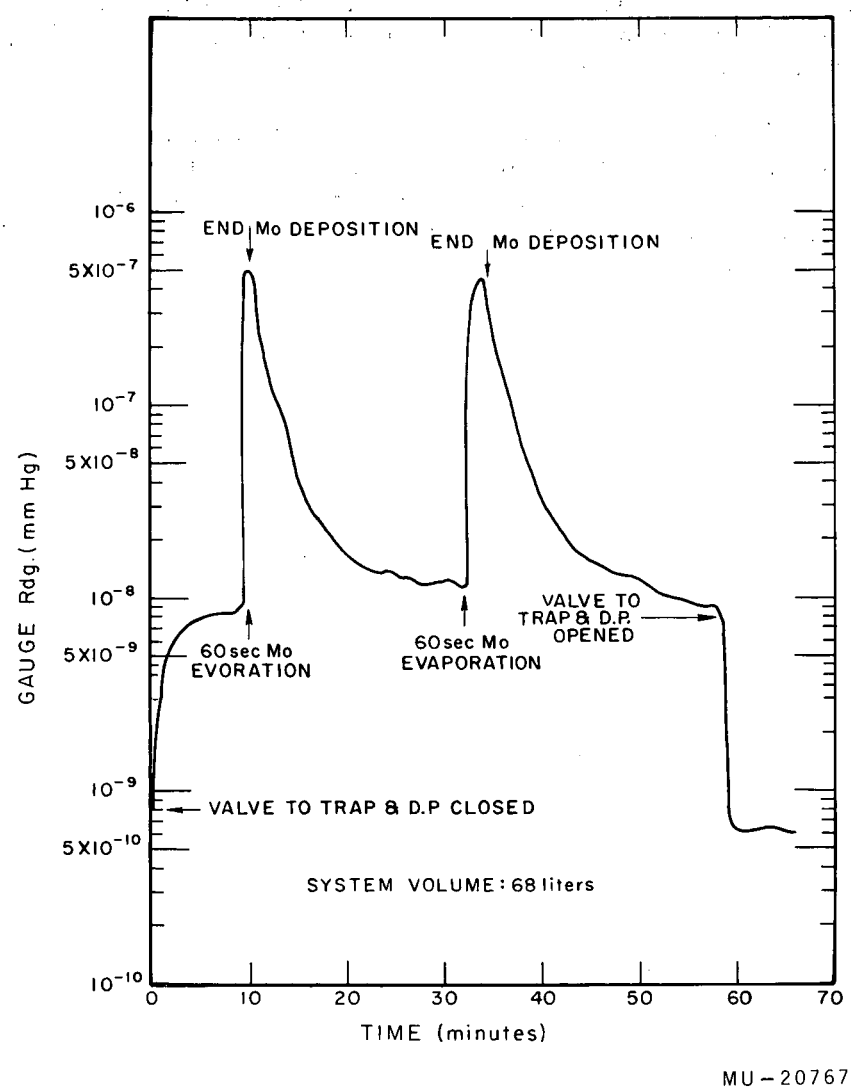

Fig. 10. Molybdenum depositions in a system isolated from the diffusion pump, indicating components not adsorbed by molybdenum, but rapidly pumped by the diffusion pump.

on a fresh molybdenum deposit appears to be about 0.3. The measured pumping speed decreased with the age of the molybdenum deposit as well as with the H_2 or D_2 coverage. It is assumed that the reduced speed for the older deposits is due to contamination by residual gas.

Although the sticking probabilities or pumping speeds might be higher than those reported, more exact work seems to require the use of molecular beams, since the large chance that a H_2 or D_2 molecule will not survive a single encounter with a "clean" molybdenum surface makes the measurement of pressure a function of the relative positions of the gas source, gauge, and adsorbing surfaces.

10. P-4 (STEADY-STATE PLASMA) SYSTEM

William L. Barr, Daune M. Gall,* Andrew L. Gardner, Laurence S. Hall, Raymond L. Kelly,** and Norman L. Oleson*

Report

A report has been prepared by these authors describing the P-4 system and various measurements of the characteristics of its plasma (Probe Measurements on the P-4 System in Single-Cathode Operation, UCRL-5904, May 1960).

Operation with a Single Cathode

In analyzing the P-4 system it appeared likely that reflection of electrons by the second cathode was not an important factor in the operation of the discharge. Furthermore, measurements in the plasma column downstream from the PIG discharge indicated that in the present configuration the hole in the second cathode, through which the plasma effuses into the differentially pumped region, is not the limiting aperture that determines the diameter of the dense portion of the plasma column.

Recent operation confirms the view that the role of the second cathode in the present system is indeed a minor one. Tests show that once the discharge is in operation it is feasible to disconnect the second cathode and allow it to float electrically or to connect it to the anode without any appreciable effect upon the operation of the system. This substantiates the assumption that the anode aperture is determining the present diameter of the dense plasma column.

A comparison of probe measurements of the system with single-cathode operation (i.e., with the second cathode floating) and with the usual two-cathode operation is made in a separate report (Daune M. Gall, Probe Measurements on the P-4 System in Single-Cathode Operation, UCRL-5998, May 1960).

Excitation Cross Sections of Lithium-Like Ions

Preliminary measurements were made of the radial distribution of carbon IV emitters (λ 1550) in the P-4 plasma using the Seya monochromator and a horizontal slit operating in the vacuum system near the plasma beam. With a low-pass filter ($<$ 10 cps) on the output of a photomultiplier detector, the signal diminished to a level comparable to noise when the beam was viewed about 1 cm off axis. At such distances a modulated beam from an electron gun should not have prohibitively large interaction with the electrons of the plasma. The feasibility of the cross-section experiment with such an arrangement will thus depend on (a) the extent to which a lock-in amplifier system can discriminate against the background noise and (b) the degree of success with which an electron gun may operate to introduce a modulated beam of electrons into the plasma.

---

*U. S. Naval Postgraduate School, Monterey, California.

**Stanford Research Institute, Menlo Park, California.

Testing and further design are proceeding on a thin electron gun (about 1/8 in. thick) for use in this experiment. The slender structure will minimize the interaction of the gun itself with the plasma beam.

Tests show that the introduction of a moderate flow of acetylene into the predominantly helium plasma increases the C IV emission by several times. The nitrogen V resonance line, with extra nitrogen added, gave substantially less response than the "enhanced" C IV line. Some advantages may be expected in the study of the boron III resonance line. Tests are planned in which boron will be introduced into the plasma.

Identification of Spectra

Films exposed in the grazing-incidence spectrograph have been printed onto plates, and the plates rather than the films have been measured. Ten plates of the P-4 spectrum have been measured and the lines identified with the help of some computer work. Some of the spectra included deliberately added elements besides the He, C, N, and O always found in P-4. Some of the lines observed, e.g., in tungsten and titanium, have been previously tabulated while others have not. Identification of the spectra is continuing.

II. ASTRON PROGRAM

1. INTRODUCTION

Nicholas Christofilos

During this quarter the activity of the Astron group was mostly in developing and designing components for the Astron model. However, some work was done in the theoretical field as well as in the dry-run experiment.

In the theoretical field Dr. Tonks started formulating the problem of self-consistent distribution of an E layer of finite length. He also did some calculations on radiation losses of the E layer. The ratio of Coulomb collision loss, which is a useful loss providing the means of heating the plasma, to the radiation loss has been computed as a function of the plasma density and the E-layer electron energy. For example, at a plasma density of 10^{12} these two losses are equal for an electron energy of 18 Mev. Actually in the Astron model a plasma density of 10^{12} is expected, while the electron energy is 4.5 Mev. Consequently the radiation loss is negligible. At a plasma density of 3×10^{14} and with 50-Mev electrons, the proper parameters for a power reactor, the radiation loss is only 25% of the Coulomb collision loss. Therefore it appears that the radiation loss of the E-layer electrons does not create any problem. In the second theoretical paper in this report, prepared by the writer, the plasma parameters of the Astron model are calculated. It appears that, assuming no instabilities, a $\beta = 0.5$ is feasible in this model, i.e., a high enough value to probe the feasibility of the Astron scheme. If instabilities should set in at lower plasma density, a comprehensive study of the conditions under which an instability develops would be possible. Since the machine operates at a steady state it will be possible to increase β very slowly so that the growth time will be very long initially as the critical β is approached. Thus the critical β, if it exists, can be determined as a function of the temperature and the E-layer parameters. By varying the rate of injection of the relativistic electrons and the neutral gas it is possible to adjust the plasma density and temperature. Thus the diffusion rate under a variety of conditions can be measured experimentally and the values compared with the theoretical predictions. The Astron model is being built with a high degree of flexibility so that a variety of conditions can be studied as required to prove the Astron principle.

Some experimental investigation was carried out on the shock excitation of rf cavity modes upon injection of the electrons in the dry-run E-layer tank. It turned out that adherence to the prescribed requirements on beam quality and energy spread as well as proper geometry are sufficient to control the amplitude of the fields of these modes. This experiment is described by Ross Hester.

Finally some measurements were started to evaluate the 10-inch cathode required for the 200-amp electron gun. This work is reported by Daryl D. Reagan and Robert E. Wright.

2. ASTRON E-LAYER CALCULATIONS

Lewi Tonks*

A. Electron Retardation in the E Layer

The dynamical friction of the plasma on the relativistic E-layer electrons was investigated theoretically by attempting a modification of Cherenkov radiation theory, but without success. To avoid an investigation which might be unwarrantedly extensive in view of the over-all E-layer problem, I have used the result of J. Neufeld and R. H. Ritchie,[1] although I have not found (in the time I spent on it) that their treatment was clear, and it may be subject to serious question. Their result, confined to the relativistic range ($\beta \approx 1$), simply changes the time constant ν of the slowing-down equation

$$d\gamma/dt = -\nu/\beta \tag{1}$$

(γ being the relativistic mass ratio and $\beta = v/c$) by substituting $\ell n\Lambda_{NR}$ for $\ell n\Lambda_D$ as a factor in ν, where

$$\Lambda_D = \frac{3}{2e^3}\left(\frac{k^3T^3}{\pi n_e}\right)^{1/2} = 1.24\times10^4 \frac{T^{3/2}}{n_e^{1/2}}, \tag{2}$$

$$\Lambda_{NR} = \frac{2.246\, m_0c^2}{(4\pi n_e/m_0)^{1/2}\, eh} = 4.9\times10^{15}\, n_e^{-1/2}. \tag{3}$$

Contrary to my expectation[2] there is little difference between the ν's in the range of plasma temperature that is of interest, for the two Λ's are equal at $T = 54\times10^6\,^{\circ}K$. In the build-up of plasma energy the drag will be slightly greater than that calculated from the nonrelativistic theory.

The slowing down due to radiation arising from the acceleration of the electrons in the magnetic field can be important relative to the dynamic friction. This relative importance increases with increase of electron energy and decrease of plasma density. The radiative drag leaves the axial component of velocity unchanged and reduces only the electron's transverse motion. In this it differs markedly from dynamical friction, so that in order to make an accurate estimate of relative effects the changes contributed to both energy and canonical angular momentum would have to be calculated.

*Consultant to Lawrence Radiation Laboratory from General Electric Vallecitos Atomic Laboratory, Pleasanton, California.

[1] Phys. Rev. 98, 1632 (1955), Eq. (87).

[2] L. Tonks, Controlled Thermonuclear Research Quarterly Report, December 1959, January, February 1960, UCRL-9106, p. 40.

Since the changes in angular momentum were the more complicated I have confined attention to the energy losses. The ratio of the instantaneous rates of energy loss is

$$\frac{\text{Radiative}}{\text{Friction}} \approx \frac{5.6\times10^{-3}\,\lambda^4\gamma^4}{\nu a^2}\,, \tag{4}$$

where $\lambda = v_\perp/v$ and $1/a$ is the local curvature of the projection of the trajectory on the plane perpendicular to the magnetic field. A reasonable value for λ is 0.5. The results of the self-consistent field calculations indicate that the mean-square curvature of the virgin electrons--noting the curvature reversal due to field reversal--is about equal to the reciprocal of the injection radius, that is, to $1/r_2$. Since r_2 is 30, it follows that for equality of radiative and friction loss we have

$$\gamma = 40\ \nu^{1/4}\,. \tag{5}$$

The evaluation of ν for different plasma densities by using the relativistic formula, Eq. (3) above, leads to the following table for the electron energies E above which radiation is the more effective in slowing down the electrons.

Electron energy at which radiation drag equals dynamical friction drag, as related to plasma density n_e (cm^{-3})

	10^8	10^{10}	10^{12}	10^{14}	10^{16}
$\nu(sec^{-1})$	7.9(-5)[a]	7.2(-3)	6.6(-1)	5.9(1)	5.2(3)
γ	3.8	11.7	36	111	340
E (Mev)	1.8	5.8	18	55	170

[a] $7.9(-5) = 7.9\times10^{-5}$, etc.

B. Injection Problem and End Effects

This is an area of the Astron problem that may be far more crucial than has been realized, and its challenge to analysis is greater than that of turbulent motion in a fluid. No satisfying approach has been developed yet, but the importance of the problem is such as to justify an outline of the lines of thought that its consideration has developed so far.

An important parameter governing the field modification that the E layer accomplishes is the ratio of the radius of the injection circle (the locus of apocenters of the virgin electrons) to the radius of gyration that each of these electrons would have in a vacuum field--that is, if the others were not present and modifying it. This ratio has been denoted by G. The greater the value of G the greater the degree of reversal that is theoretically possible, as can be seen in Fig. 13, p. 39, the preceding Quarterly Report (UCRL-9106). Probably G = 1.3 is the lowest "practical" value. It leads to reversed fields of relative magnitude 0.1 to 0.2 of the vacuum field.

The problem that arises is that as the electrons are being conducted toward the E layer for injection into it they are moving in a circular helical pattern, and for this we have $G = 1$. On any adiabatic basis for the transition into the E layer their G would remain unity and no reversal would be possible. But then one sees that not only apocentral injection but also epicentral injection is theoretically possible, in which the electrons would be injected at the epicenters of their first radial excursions. This would place the E layer generally outside, instead of inside, the injection radius. (Such solutions are already included in the array of apocentral ones. They simply require a change in interpretation of some of the parameters.) An enlarged E layer would require a bigger container. Also, if a field configuration at all similar to conventional mirrors were used there would be a further increase in size relative to the injection system.

These earlier threads of reasoning are completely overshadowed by the actual nonadiabaticity of the transition into the E layer. That this will almost certainly be the condition can be seen by looking upon a semi-infinite coil carrying a current as an E-layer analogue. One-half the field change between free space and the deep interior occurs within little more than one radial distance, centered at the open end.

There are two consequences--an effect on injection, already mentioned, and the effect on the electrons already in the E layer which are reflected from its ends. It is seen that quite aside from an impressed magnetic field, the termination of the E layer in itself sets up a reflecting configuration of the magnetic field. (The magnetic field of a current-carrying coil pushes in on its ends.) How powerful a mirror this is has not been analyzed. Such a termination, supposed to exist in a uniform impressed field, would certainly be unstable, for there is nothing to fix its axial position. The existence of the other end within a finite distance might serve. On the other hand, a small step in the impressed field might fix the termination.

The failure of adiabaticity means that when an E-layer electron is reflected back from the end of the E layer only its canonical angular momentum will be preserved and there will have been an exchange between axial and trasverse energies. Here is something akin to scattering which may, however, possess some ordering. Somehow, concepts of the nature of the self-consistent solution under these conditions need to be developed. This is the most important next step in the development of Astron theory.

3. ASTRON-MODEL PLASMA PARAMETERS

Nicholas Christofilos

A. Calculation of Allowed Plasma Density and Temperature

The possible density and temperature of the plasma in the Astron model depend on the electron energy and the radius of the E layer. The theory of the energy balance of the plasma was described two years ago.[1] The numerical example, however, cited in that paper was for a power reactor employing 50-Mev electrons. We shall calculate, hereafter, the plasma parameters for the Astron model. The E-layer parameters in the Astron model are:

Electron energy at injection	$E = 5$ Mev
Electron energy at the E-layer region	$E = 4.5$ Mev
or	$\gamma = 10$
E-layer radius	$r_i = 27$ cm
E-layer length	$L = 600$ cm
Number of electrons/cm in the E layer at the moment of field reversal	$N_0 = 3.5 \times 10^{13}$
Total number of electrons in the E layer	2.1×10^{16}
Average electron injection current (where T_e is the electron lifetime in seconds)	$j_e = 3.5/T_e$ ma
Maximum average injection current	$j_a = 2.4$ ma
Peak injection current	$I = 200$ amp
Duration of injection	0.2 μsec
Maximum injected pulses per second	60

Following the definitions of the reference,[1] B_w and B_i are the magnetic field just outside and inside the E layer respectively, where B_i is assumed in the opposite direction in respect to B_w. The required number of electrons (N) per cm length of the E layer is

$$N = s\, N_0 \tag{1}$$

where

$$s = \frac{B_w + B_i}{B_w - B_i} \quad . \tag{2}$$

---

[1] N. Christofilos, in Proceedings of the Second International Conference on Peaceful Uses of Atomic Energy, Vol. 32, Geneva, 1958 (United Nations, Geneva, 1958), P/2446, p. 279.

Then the other quantities are

$s = 1.66,$

$N = 3.5 \times 10^{13}/\text{cm},$

$\cos \delta^* = 0.44,$

$B_w = 700$ gauss,

$B_i = 175$ gauss.

The self-consistent solution for the plasma pressure, density, etc., is assumed as described in the reference.[1] Hence the diffusion velocity is

$$v = \frac{\lambda r_0}{4\pi r_e \tau n_0} \tanh[\lambda(r_0^2 - r_i^2)] \text{ cm/sec}, \tag{3}$$

where

$$\tau = \left(\frac{u}{V_0}\right)^{3/2} \frac{1}{n_0 \sigma_0 c}, \tag{3a}$$

$$\sigma_0 = 2.10^{-23} \text{ cm}^2, \tag{3b}$$

r_0, n_0 are the plasma radius and density respectively, u is the plasma temperature, V_0 is 1700 esu (the electron rest energy), and τ is the effective mean time between electron-ion collisions in the plasma. The value of τ has been selected one order of magnitude smaller than the actual value, in order to take into account enhancement of diffusion due to micro-turbulence, contaminations, etc.

The diffusion loss under these assumptions is

$$W_d = \frac{\sigma_0 c}{r_e} (16 \pi n_0 e V_0)^{1/2} \frac{e V_0 n_0}{B_w} F\, 10^{-7} \text{ watts/cm}, \tag{4}$$

where

$$F = \frac{\sinh^{-1} y + \sinh^{-1}[(B_w/B_i)y]}{\sqrt{1 + y^2}}, \tag{4a}$$

$$y = \sqrt{8\pi p_0}\sqrt{B_w}, \tag{4b}$$

where p_0 is the maximum plasma pressure. The energy transferred to the plasma by Coulomb scattering with the E-layer electrons is

---

*$\cos \delta$ is the ratio p_θ/p, where p_θ is the azimuthal mechanical momentum and p is the total momentum of the electrons.

$$W_e = eV_0 \, N\sigma_0 \, cn_0 \, 10^{-7} \text{ watts/cm} . \tag{5}$$

Assuming n_0 fixed we observe that F, hence the diffusion loss, too, goes through a maximum value at a certain plasma pressure or temperature. The plasma temperature can rise to any desired value as long as we have

$$W_e > W_d . \tag{6}$$

From the above equations and Inequality (6) we derive the condition

$$n_c = \frac{1}{r_e} \frac{s^2(s+1)^2}{F^2_{max}} \gamma^4 \frac{\cos^2\delta}{16\pi r_i^2} . \tag{7}$$

The critical temperature, where $W_e = W_d$ and $n_0 = n_c$, is

$$u_c = V_0 \left(\frac{F_{max}}{s\gamma} \right)^2 . \tag{8}$$

Upon substitution of the E-layer parameters the above equations yield

$$r_0 = 32.4 \text{ cm},$$
$$n_c = 8.5 \times 10^{11}/\text{cm}^3,$$
$$u_c = 8300 \text{ ev},$$
$$F_{max} = 2.12 .$$

The maximum occurs at $y = 1.1$.

The rate of the temperature rise is

$$\frac{du}{dt} = \frac{u_c}{T_c} \left(1 - \frac{F}{F_{max}} \right), \tag{9}$$

where T_c is the average lifetime of a particle in the plasma at the temperature and density u_c and n_e respectively. The value of T_c is

$$T_c = \frac{r_0}{2v_c} . \tag{10}$$

The values of v_c and T_c are 6.5 cm/sec and 2.5 sec respectively, where v_c is the diffusion velocity at the critical temperature and density. By integrating Eq. (9) we obtain

$$\frac{t}{T} = \int_0^x \frac{2.12\sqrt{1+1.2x}\, ds}{2.12\sqrt{1+1.2x} - \sinh^{-1}(1.1\sqrt{x}) - \sinh^{-1}(4.4\sqrt{x})} , \tag{11}$$

where

$$x = u/u_c .$$

The integral has been evaluated numerically. The values of the pertinent quantities as a function of the time are cited in the following table.

t (sec)	u (ev)	v (cm/sec)	S_μ (lit/sec)	$(B_0 - B_w)$ (gauss)	$\beta = \frac{B_0^2 - B_w^2}{B_0^2}$
0.0021	8.3	616	1170		
0.024	83	195	370		0.012
0.1	300	95	180		0.041
0.9	1000	36	68	45	0.125
4	3000	17	32	135	0.300
17	5000	11	21	200	0.417
32	6000	9	17	240	0.462
60	6900	7.9	15	270	0.500

At low temperature, below 100 ev, the calculations are not correct, as the assumption of plasma of constant density is then not valid, for the temperature rises up to 100 ev in less than 30 msec. However, more than 10 msec are required to ionize enough particles to form a plasma of 10^{12} density. Consequently at this low-temperature region a more accurate solution is required where the plasma density (which grows from zero up to 10^{12}), would be considered a time-varying quantity. This calculation will be carried out in a separate paper.

B. Experiments with the Astron Plasma

In Section A the allowed plasma parameters on the Astron model were derived. This derivation, though, was obtained by assuming that the plasma leaks out according to classical diffusion theory. Quantitatively, we assumed a diffusion rate 10 times as high as the classical diffusion theory yields. The actual value of the diffusion rate, in the absence of instabilities but with the possible presence of microturbulence, will be measured experimentally. The measurement of the diffusion rate as a function of the plasma pressure, density, and the degree of field reversal (i.e., the ratio B_w/B_i) is one of the main goals of the Astron plasma experiment.

The values in the table (in Section A) indicate that a β up to 0.5 is possible. However, how large the actual value would be before instabilities set in is another question. Since in other machines β up to 10% has been observed, it is quite probable, provided that the E layer is stable, that below a critical β value the plasma will be stable. Since the machine operates at steady state it will be possible in increase β very slowly, thus the onset of instabilities, if they do exist, will be gradual so that the growth time will be rather long initially as the critical β is approached. The evaluation of the critical β as a function of the temperature is of extreme importance for all the Sherwood schemes. The slow onset of instability shall allow the

study of the behavior of the plasma, to find the mode of instability and possible correction. During the heating-up process it is possible to stop at any desired temperature by increasing the neutral-gas flow. By injecting more neutrals than the diffused ions one makes the plasma density higher. Consequently the E-layer electron lifetime is reduced, resulting in reduction of the reversed field (B_i). Therefore, the diffusion rate is enhanced and the temperature will not rise any further.

The same result can be accomplished by reducing the E-layer injection rate. The E layer provides a very elegant way of controlling the rate of diffusion. By varying B_i from zero to 0.25 B_w it is possible to obtain any equilibrium temperature desired from a few ev up to a few kev.

The plasma density depends on the rate of E-layer electron injection. If the density rises the reverse field drops and the excess plasma is discharged. If the density drops, the reverse field rises and the diffusion rate is reduced, resulting in a rise in the density. Thus this self-control feature stabilizes the plasma density within a wide margin of variation of the neutral-gas flow. The plasma temperature is controlled by the rate of neutral-gas flow. The amount (S) of injected gas (in microliters per second) as a function of the temperature is shown in the table. Of course since the diffusion rate is not known within an order of magnitude, the exact value of S will be determined experimentally.

There will be provided in the Astron facility three basic controls:

(a) The rate of injection of fast electrons. This control determines the plasma density.

(b) The rate of injection of neutral gas, allowing the control of the plasma temperature.

(c) The intensity of the externally applied field B_0. This control will be operated by observing the radial position of the E layer. If the radius of the E layer expands the external field should be increased, and vice versa.

The time constants are of the order of a second, so that all three controls can be operated manually.

The power input by Coulomb collisions with the E-layer electrons is given by Eq. (5). Substituting the selected parameters, we find

E-layer energy loss per cm,	W_0 = 2.4 watts/cm;
Total E-layer energy loss,	W_e = 1440 watts;
The average accelerator beam power is	W_i = 12,000 watts.

Consequently there is a safety margin of a factor of 8 to take care of any electron losses either in the injection region or in the E layer; for example, if the E-layer electrons are lost to the system, after losing only 30% of their energy, we would have a margin of a factor of 2, and so on.

C. Neutral-Beam Injection

It is quite possible to use neutral atomic (D^0) beams of 20 kev with total current of 1 to 2 amp to enhance the energy input to the plasma. Since a safety margin of 8 is provided in the required rate of electron injection, it is possible, if the electron losses are not excessive, to increase the plasma density by a factor of 5 (approximately), provided that an additional energy input comparable with the E-layer Coulomb scattering losses can be made available.

The ionization cross section of 20-kev neutrals is 8×10^{-17}, approximately. The ionization probability for a neutral traveling once through the 600-cm length of the Astron plasma, of 10^{12} density, is approximately 5%. Hence the energy input to the plasma is 1000 watts per ampere of neutral beam. This is comparable to the energy input from the E layer. Consequently it appears of interest to try neutral injection in the Astron at a later phase of the experiments.

4. ASTRON DRY RUN EXPERIMENT

Ross E. Hester

In some of the beam-trapping experiments reported earlier,[1] the groove coil structure was removed and the beam was trapped in the cylindrical aluminum cavity. When large amounts of beam (10 to 20 amp) were injected under these conditions, large rf signals could be picked up in the cavity. Under some conditions signals of 600 to 700 volts were observed on 1/4×1-in. pickup loops. The signals were observed to be of approximately equal amplitude on loops whose planes were oriented either perpendicular or parallel to the axis of the aluminum tank. The frequencies observed varied from pulse to pulse, and indeed more than one frequency could be identified in a given pulse. The frequencies involved ranged from 180 to 800 Mc. The amplitude of the signals observed was too high to be accounted for by simple "shock excitation" of the cavity by a beam pulse. The signal level strongly suggested some regenerative coupling between the beam and the rf field. It would appear from the experiments performed in the last several months that these oscillations can be controlled by adherence to the prescribed beam quality, and through the use of appropriate suppressors.

One type of phenomenon that appeared likely was a two-stream effect. Haeff and Pierce[2] have shown that amplification can occur when two streams of drifting electrons having nearly equal velocities, $U \pm v$ (for $U \gg v$), are modulated by a constant rf source. The sinusoidal voltage pulse that appears across the accelerating column of the Astron electron accelerator makes it possible to inject beam into the solenoid in such a manner that the leading part of the beam pulse is overtaken by the higher-energy electrons that follow, forming the two-peak velocity distribution that is necessary for two-stream amplification.

A two-slit collimator was installed in the machine. The first and last slits were located at focal points for the beam and were 180 deg apart in azimuth (see Fig. 11). The first slit was enclosed in a copper tank which isolated the accelerator from the tank except for communication through the slit. This enclosure in itself reduced the rf level for a given set of conditions.

An experiment was run in which the total charge and energy of the beam injected into the tank were maintained constant as the slit widths of the collimator were varied from 1/4 to 1-1/2 in., changing the momentum spread in the beam from 4 to 20%. Under these conditions the rf level in the tank remained constant.

Another experiment was performed in which the solenoidal magnetic field was maintained at a low value, preventing the high-energy peak from passing through the collimator but allowing two lower-energy beam pulses to

---

[1] W. A. S. Lamb, in Controlled Thermonuclear Research Quarterly Report, UCRL-8887, Sept. 1959, p. 67.

[2] A. V. Haeff, Proc. Inst. Radio Engineers 37, 4 (1959); J. R. Pierce, Proc. Inst. Radio Engineers 37, 980 (1949).

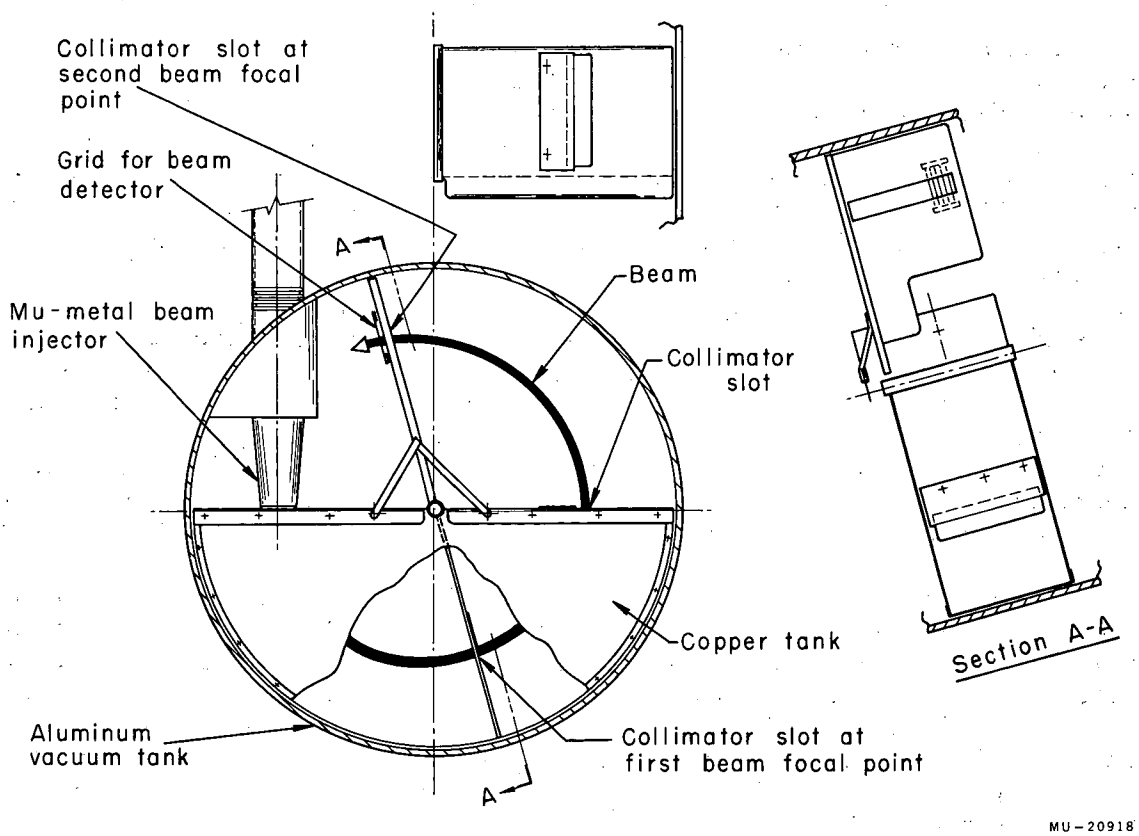

Fig. 11. Collimating apparatus.

enter the tank. The beam was allowed to traverse the full length of the tank where it was collected. The width of the beam pulses was 0.06 μsec. Under the conditions of the experiment, the first current pulse was collected about 0.3 μsec before the second current pulse entered the tank. No rf was observed before the second pulse entered the tank, but with the entry of the second pulse, the rf built up rapidly. The interesting thing about this experiment was that the second pulse produced the rf at a detectable level, and in this current pulse the high-energy particles enter the tank first, preventing any possibility of meeting the conditions for two-stream amplification. As a corollary of this experiment the accelerating voltage was lowered until the collimating system admitted a single pulse into the tank. The time base for this pulse was about 0.2 μsec. It was observed under these conditions that about three times as much charge was required to produce the rf as was required in the sum of the two pulses. It was inferred from this experiment that the high-frequency components in the shorter beam pulses enhanced the "shock excitation" of the tank, providing an rf field for interaction with the beam.

It was observed that sparking in the accelerator greatly enhanced the production of rf. An investigation of the accelerator revealed that considerable sparking occurred near the wires that connected the secondary of the pulse transformer with the accelerating column. These wires were replaced with 1-in.-wide annealed copper strips, which reduced the sparking probability and reduced the inductance between the accelerating column and secondary of the transformer, thus lessening the probability of "ringing" in the accelerator column. An immediate improvement in operation resulted. The remaining rf in the tank appeared to be mostly connected with TE modes and oscillated at a frequency of 170 Mc. The rf signal on the horizontal loops was about one-fifth that in the TE mode, and was at a frequency of 330 Mc. Four mode suppressors were installed in the tanks. These suppressors were copper strips extending 6 in. radially inward from the circumference of the tank and running laterally the full length of the tanks. With these suppressors installed the frequency observed on the vertical loop increased to 330 Mc and the voltage on the loop dropped to the level observed on the horizontal loop, namely about 40 volts when 15 to 20 amperes were injected.

It would appear from these results that elimination of "ringing" in the electron gun and proper geometry in the tank will prevent the rf from becoming a problem. The absence of rf in the experiments with the groove coil in the tank can probably be attributed to the low "Q" of the tank with the "lossy" groove coil assembly installed.

5. 10-INCH CATHODE DEVELOPMENT

Daryl D. Reagan and Robert E. Wright

An improved heater design (Fig. 12) has resulted in a marked decrease in gas evolution during activation. Typical power required for this heater assembly is given below.

Cathode temp (C)	Power (watts)	
1000	3600	Activation temperature
920	3500	Activation temperature
830	2280	Operating temperature

The maximum temperature difference across the 10-in.-diameter face is $\pm 10^{\circ}C$.

Figure 13 is a view of the cable Marx generator designed to test the pulsed-emission characteristics of the cathode, and the output is 148 kv into a 125Ω load. The pulse is square-topped, with a length of 0.2μsec and a rise time of 4×10^{-8} sec, and with a decay of about the same interval.

The assembly is designed to be operated in an atmosphere of dry nitrogen or Freon-12, and hence it is shaped to fit into a cylindrical tank.

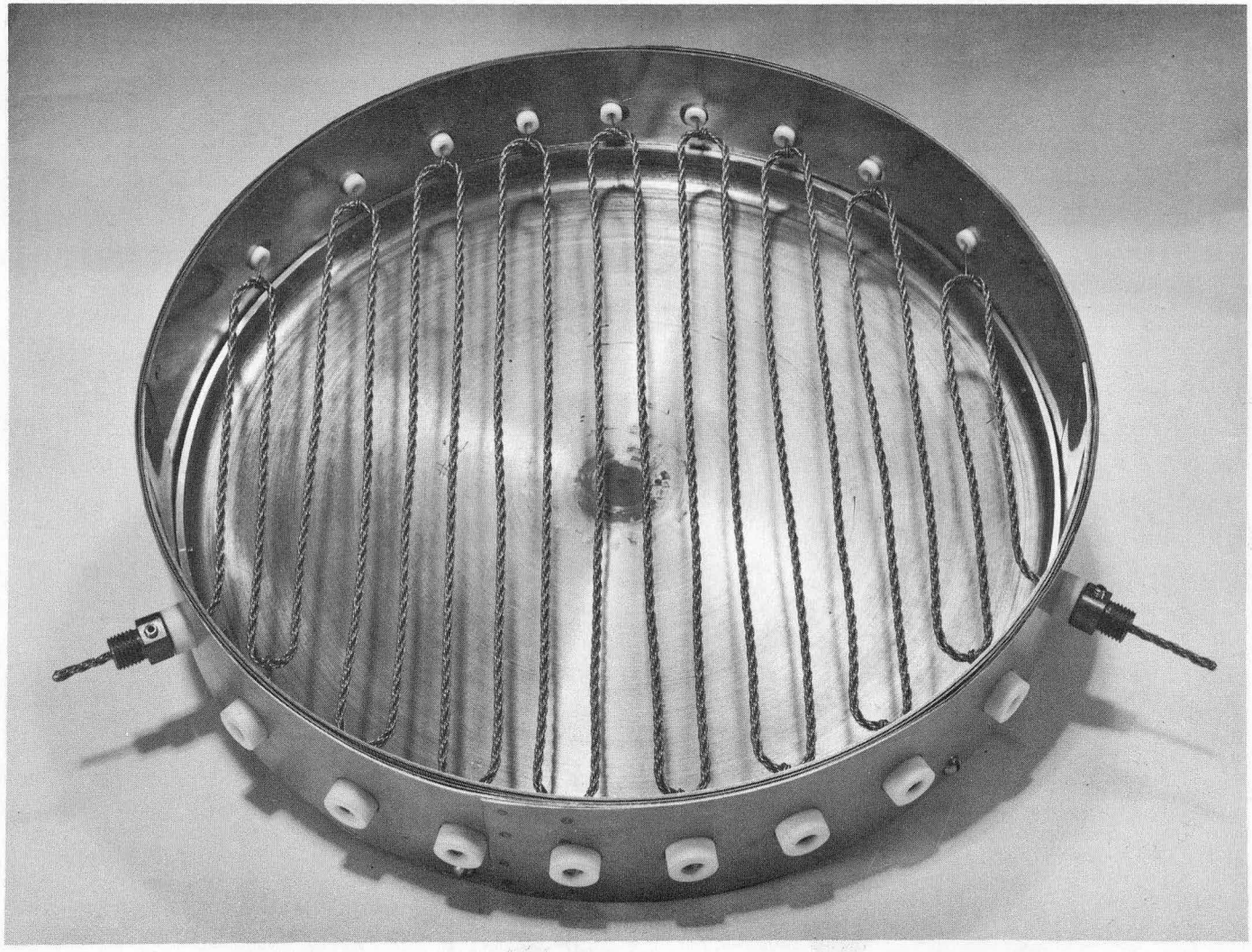

ZN-2556

Fig. 12. Cathode-heater assembly.

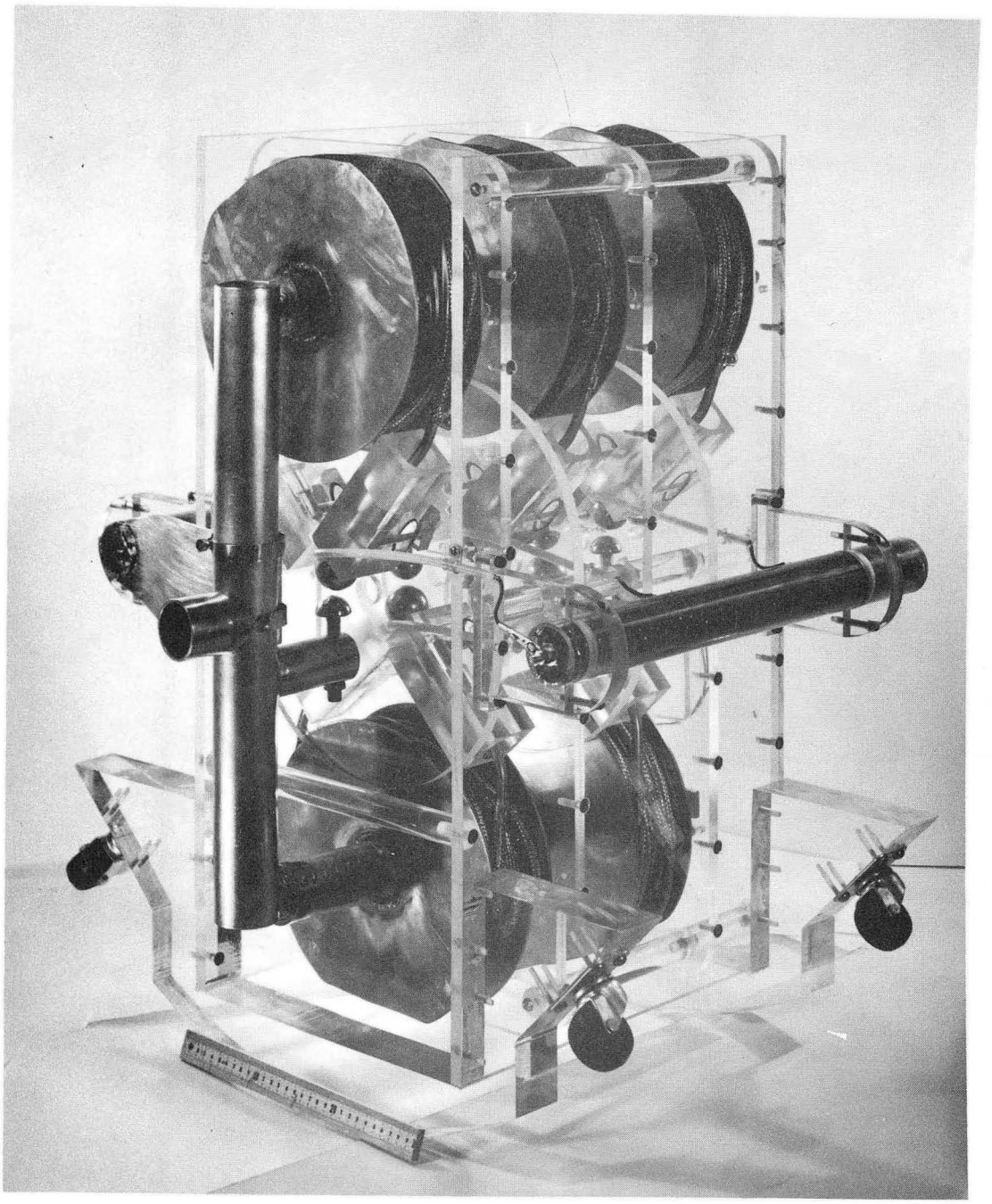

ZN-2557

Fig. 13. Cable Marx generator.

III. LIVERMORE PINCH PROGRAM

Dale H. Birdsall, Edmund S. Chambers, Stirling A. Colgate, Harold P. Furth, Fred O. Halliday, Charles W. Hartman, Edward R. Horton,* and Ross L. Spoerlein

1. SUMMARY

The primary effort of the Pinch Group has still been centered on the construction of the levitron. Although this construction has taken somewhat longer than expected, the various components called for have been developed without serious problems. At this stage the final welding of the core inside the liner and of the liner segments into a single continuous piece is under way. The mass spectrometer, levitators, theta coil, filaments, and diverter are developed. Operation by the end of the next quarter is to be expected.

The electron-beam pinch has been operating reliably, and with the completion of extensive magnetic probe measurements has demonstrated the usefulness of the electron beam as a means of measuring the pinch-field behavior. The large asymmetry introduced by the spark trigger has now been removed by fast-B_z ionization. The erratic path of the beam has been suggestive of instabilities. The density of the conical-pinch accelerated plasma has been established by using a piezoelectric probe. The liquid soidum experiments have confirmed the "tearing" instability to be expected with a dc sheet current. The plasma in the ion-cyclotron heating experiment has demonstrated an anomalously high rf impedance and transmission coefficient. These results can be interpreted in terms of plasma sheaths.

*U. S. Naval Postgraduate School, Monterey, California.

2. ELECTRON-BEAM PINCH

Extensive magnetic-probe measurements have been made,[1] which will serve as basis for the interpretation of the beam trace as a function of time.

Further studies have been made of the anomalous beam decentering,[2] which is found even when no radial beam displacement is programmed (see Fig. 14b). The anomalous behavior has been traced to the centering of the beam-input electrode. This dislocation of the pinch center is strongly affected by the trigger element imbedded in the electrode. With highly symmetrical preionization, the electron beam can be maintained properly centered throughout the pinch discharge. A preionization system using an oscillating B_z field for this purpose is being constructed.

A new electrode diaphragm has been perfected for the camera end of the pinch tube, consisting of a 200-mesh unsupported stainless steel screen. The phosphor disk is covered with 1-mil Al foil, and is set back somewhat. With this arrangement, the electron beam produces a visible trace down to 80 kev.

Variation of beam energy from 80 to 400 kev does not have a substantial effect on the beam trace. Reversal of B_z field reverses the trace in mirror fashion. One concludes that the electron beam tends to follow the field lines in an "adiabatic" manner.

Thus the apparatus is now operating controllably in the desired regime, and can be applied to the study of pinch instability and diffusion. Direct information about magnetic-field fluctuations is given by traces like that of Fig. 14c. (The erratic pattern shown is traced out during the 0.1-μsec beam duration.) At low particle density and high power the beam fluctuation increases. Future studies will be aimed at gathering statistics on the pattern and distribution in time and space of magnetic disturbances in the "stabilized pinch" under various operating conditions. For comparison, an "inverse stabilized pinch" setup is being prepared.

The electron-beam apparatus is also particularly well suited to the study of magnetic field interdiffusion in the pinch. If both the plasma and end electrode had infinite conductivity, the spot produced by the beam at the phosphor should not move during pinching, since the same field line always connects the point of entry of the beam through the input electrode with the spot on the phosphor. Owing to resistive diffusion, however, the field line passing through the point of entry may change its shape, and the spot on the phosphor moves accordingly. Specifically, in the case of the stabilized pinch, an originally straight field line may become helical as B_θ diffuses into the B_z-field region, and a circular trace then appears on the phosphor (see Fig. 14d). This technique gives a more convenient measure of diffusion than the magnetic-probe technique, since a magnetic probe cannot readily distinguish between diffusion and convection.

[1] Edward R. Horton and Ross L. Spoerlein, Electron Beam Pinch, UCRL-6011, May 1960.

[2] Controlled Thermonuclear Research Quarterly Report, UCRL-9106, March 1960.

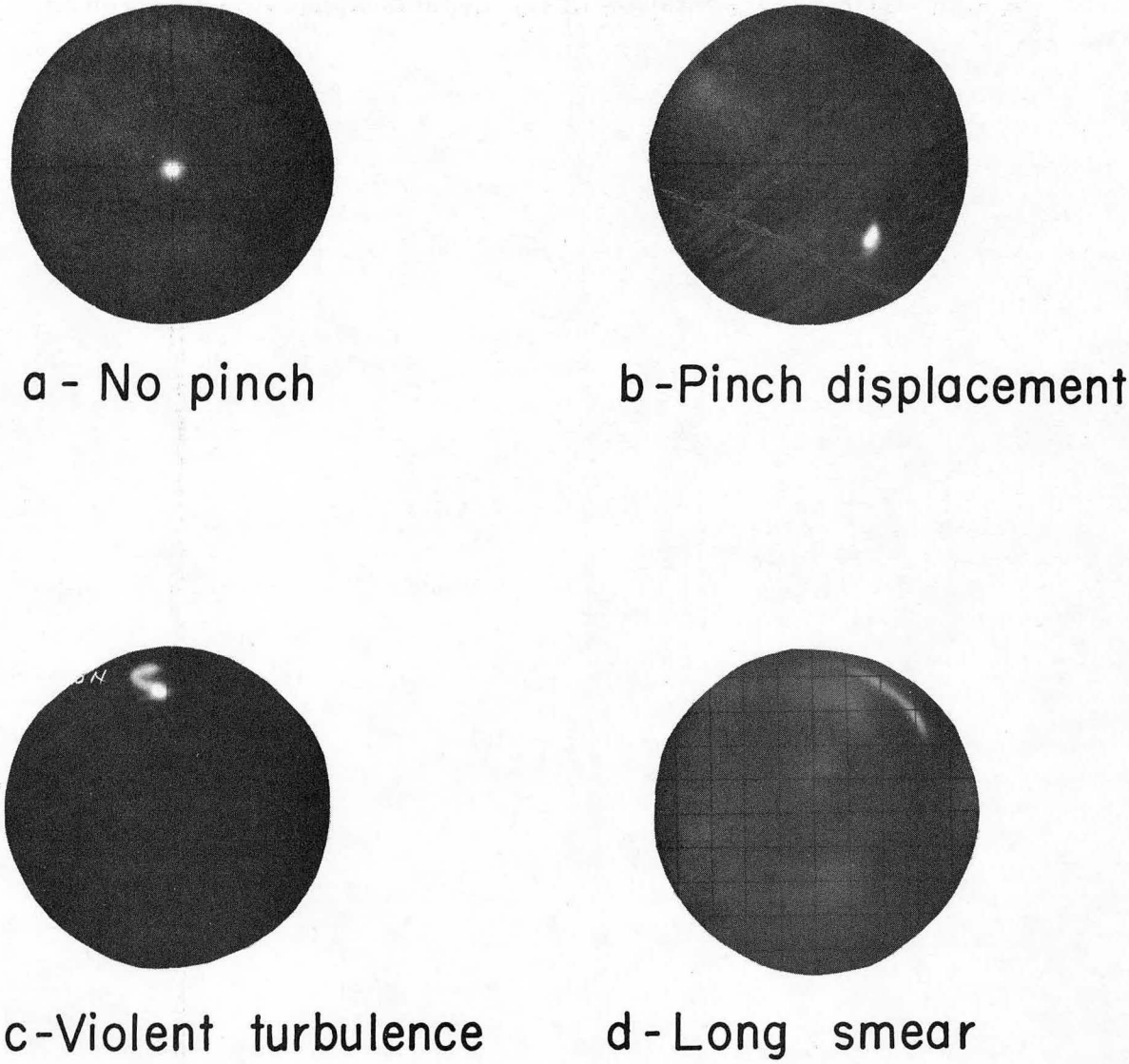

ZN-2558

Fig. 14. Electron-beam spot on phosphor (beam introduced on axis).

To increase the efficiency of gathering information, the beam accelerator is being modified to allow passage of multiple electron pulses during a single pinch.

A schematic representation of the present apparatus is given in Fig. 15.

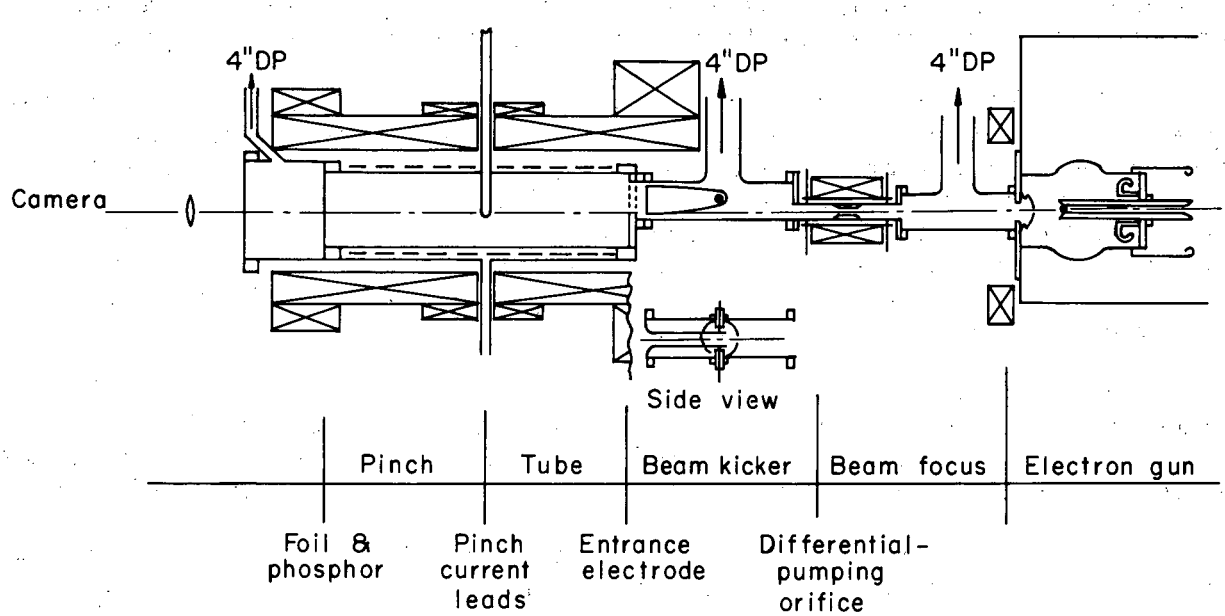

MU-20920

Fig. 15. Electron-beam experiment: cross section of setup.

3. CONICAL PINCH PLASMA ACCELERATOR

The major effort of this quarter has been devoted to density measurements on the accelerated plasma. Various new techniques have been tried, the most successful one being an acoustical transmission-line type of transducer probe similar to that described by DeSilva.[3] The probe is calibrated by applying to the input end a known magnetic pressure impulse of the same duration (1 μsec), magnitude (1 atm), and rise time (1/2 μsec) as the observed plasma pulse. For these conditions the probe sensitivity is 1/5 v/atm.

Time-of-flight data, rechecked with the pressure probe, are in rough agreement with previous observations. Pressure measurements made 5 cm from the exit orifice show the density of accelerated plasma to increase linearly with initial gas pressure from 10^{14} D^+/cm^3 at 100 μ D_2 to 2×10^{15} at 400 μ. The average energy decreases from 3000 ev to 100 ev, for the same range of pressure, with the pinch current held constant at 200 ka peak. Transducer measurements are in rough agreement with previous estimates of density obtained from diamagnetic-probe data.

The total number of deuterium ions accelerated is 10^{17} to 10^{18}, which amounts to 1 to 10°/o of the initial discharge mass. If one attributes the acceleration to a hydromagnetic effect this fraction accelerated corresponds reasonably well to the total axial impulse deliverable by the magnetic field.

There is definite evidence, however, that electrostatic ion acceleration plays a dominant role. Reversal of tube voltage, so that the output electrode becomes the anode, can reduce the mean output velocity by a factor of 2. To discriminate between hydromagnetic and electrostatic phenomena, the effect of voltage reversal on velocity and total output has been studied over a wide range of parameters.

---

[3] A. W. DeSilva, in Controlled Thermonuclear Research Quarterly Report, UCRL-8887, Sept. 1959, p. 81.

4. LIQUID SODIUM EXPERIMENT

A radio-frequency liquid sodium experiment analogous to the hard-core pinch has been shown previously[2] to exhibit complete stability, as predicted by the hydromagnetic stability theory in the limit of infinite conductivity. (Since the rf skin depth in the sodium was very small, the effective conductivity was indeed essentially infinite.) Very little is known theoretically about the effect of finite conductivity on hydromagnetic stability. It was therefore of great interest to repeat the hard-core experiment in liquid sodium, using a dc current. In that case the finite conductivity of the sodium can play an important role.

Various experimental arrangements were tried, using both wide, shallow sodium pools and thin, tall tubes of sodium, as in Fig. 16. In each case, the dc current distribution was such that the hydromagnetic theory in the limit of infinite conductivity would indicate complete stability. No small-scale instabilities were observed, and complete quiescence of the sodium was found possible at currents as high as 2300 amperes (i.e., fields of approx 200 gauss). Asymmetries of 10°/o in the alignment of the electrodes and insulating tubes sufficed, however, to produce radical asymmetries in the liquid sodium surface, as well as large-scale turbulent motion. The observation of a stable equilibrium under conditions of perfect alignment may be due to the restraining effect of the surface tension of the sodium.

To test the effect of a small region of zero conductivity, a micarta disk was inserted into the sodium tube (see Fig. 16), thus creating a "hole" in the tube. This hole became enlarged by a factor of two in the azimuthal direction on application of current. The hole, together with the disk, tended to slide azimuthally toward one side of the tube, where the spacing of the glass cylinders was narrowest (by a few percent).

These results are consistent with a simple theory in which one treats a small, poorly conducting region as a region where a local inverse current is superimposed on the equilibrium current pattern. Since the equilibrium forces vanish, the problem reduces to that of calculating the force exerted by the perturbation current on the unperturbed current pattern. In this way it is easy to show that a small hole in a dc current sheet will grow most rapidly in the direction along field lines. By the usual principle of inductance maximization, one can also show that a region of inverse current tends to move away from where the unperturbed current is strongest. (For example, a longitudinal streamer having poor conductivity would be expelled from a dc pinch toward the wall.)

Experiments using rf in mirror and cusp geometries are about to be resumed, using a newly built 2000-volt 2000-cps ignitron inverter.

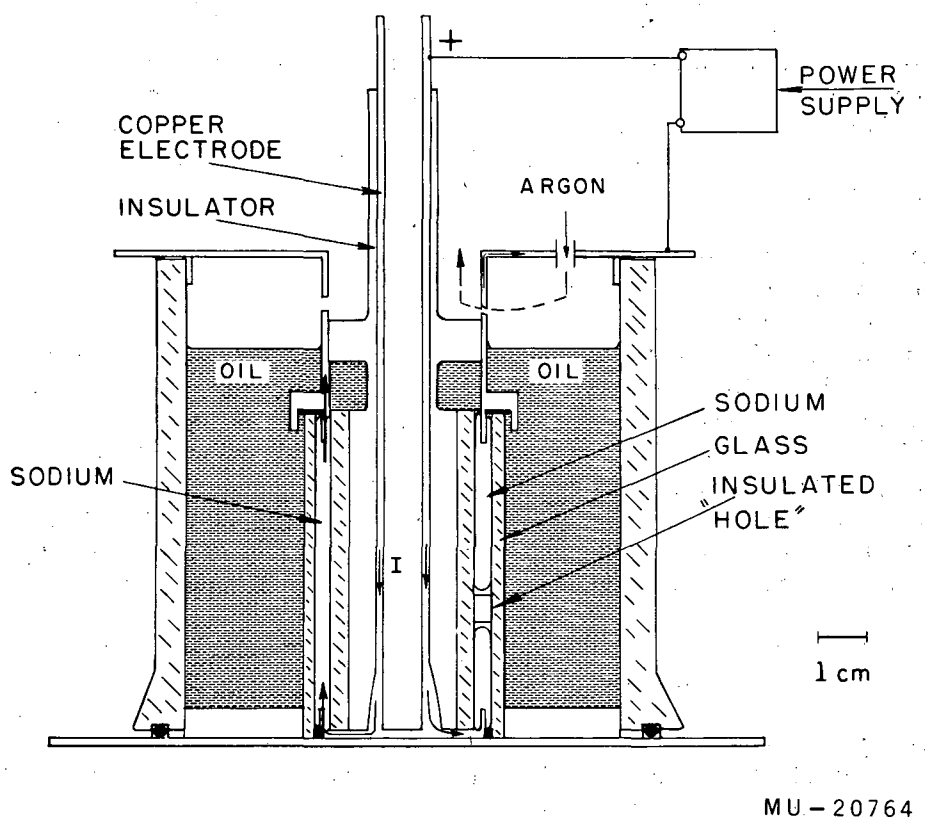

Fig. 16. Liquid sodium constant shut-current apparatus.

5. 12-INCH LEVITRON

Divertor-Injector Theory

The divertor concept, as used in the stellarator, has been generalized. One desires coil geometries in which magnetic flux is diverted from the main chamber without intersecting the material walls (or producing null traces that intersect material walls) anywhere except in places well removed from the main chamber. Such an arrangement is useful for preventing hot plasma from diffusing to the main chamber wall, and conversely, for injecting hot plasma into the main confining field without bombarding the chamber wall. The latter is the feature of principal interest in the levitron.

An extensive study indicates that a perfect divertor can be achieved only if the coil producing the flux diversion is left mechanically unsupported except at those points (removed from the main chamber) where the diverted field lines are actually desired to intersect material.

The stellarator-divertor satisfies this condition. Alternatively, one may locate a floating solenoid concentrically in a pumpout, supporting the solenoid only at the end furthest from the main chamber. The diverted flux then passes through the center of the solenoid, intersects the support, and can be returned between the outside of the solenoid and the pumpout wall. For plasma injection, the source is located inside the solenoid.

Levitron components are in the following stages of construction:

Inconel-X Liner

Two complete liner assemblies have been received and the first one to be used has been modified with two additional ports to provide for plasma injection.

An alternative method of forming the levitron vacuum wall has been tested on a 1-foot linear section and appears satisfactory. It consists of wrapping the thin stainless steel liner in epoxy and fiberglass prior to placing it inside the copper shell. This technique offers a satisfactory backup if difficulties are encountered in sealing the split copper sections.

B_θ Coil Windings

These windings have been completed, insulated, and checked to 25 kv.

Torus Shells

The high-temperature epoxy coating of the shells is complete, and the insulation has been checked to 20 kv.

Mechanical Levitators

Five magnetic-pneumatic levitators have been fabricated and are being assembled. Vacuum seals which provide access for the levitator rods have been designed, fabricated, and tested.

Hard-Core Fabrication

The hard core which was originally to be joined by heliarcing with OFHC copper is now to be joined with silver solder because of possible vacuum weld difficulties in the thick copper wall. Satisfactory solder joints have been made on a similar test section.

Plasma Injection

Pulsed coils for the plasma injector have been tested to 70 kilogauss. Further mechanical details of the injector are being worked out.

Ion Gauges

A small ion gauge has been fabricated, which will slip inside the 5/8-in.-diameter levitron ports so that vacuum inside the baked region can be measured.

Vacuum and Diagnostic Ports

All stainless steel port components are complete and vacuum-seal techniques have been worked out.

Mass Spectrometer

A fast-read-out mass spectrometer is being developed for analyzing the levitron vacuum during bakeout and immediately after a pinch. The system uses a Diatron 20B in conjunction with an ion-accelerating electrode, secondary emitter, and electron multiplier. Well-defined peaks have been obtained in the low-mass ranges in a fraction of a second, using manual voltage sweeping. A 10-msec readout is desired in order that wall-emitted contaminants can be measured before recondensing on the walls. This appears feasible, since the detection scheme has a sensitivity limited by the statistics of individual ions, which is 10^4 times the electrometer sensitivity.

6. ION HEATING BY TORSIONAL WAVES IN A MIRROR MACHINE

Further measurements on the hot ion flux have been made and found consistent with a simple theory,[1] which described ion acceleration in the presence of charge exchange. On an ion accelerator of 1/8-in. aperture, with 300-v bucking voltage, located 1-1/2 in. from the PIG surface, the ion current at 0.2 μ D_2 was 10 μa and at 0.9 μ D_2 was 3 μa (the PIG current being held constant). From measurements of this kind one concludes that larger accelerated-ion currents can be achieved only by supplying more ions through the PIG without supplying more neutrals, i.e., by arrangements similar to P-4. Present ion currents above 300 v extrapolate to some tens of milliamperes per cm of PIG length.

Measurements of plasma density were made by passing 10.2-kMc microwaves diametrically through the PIG at its mid-point. The density was calculated as about $10^{12}/cm^3$ at 20 amp of PIG current. It varied linearly with the current, and did not seem sensitive to gauge pressure or magnetic field. Application of the rf raised both the plasma density and PIG current by as much as 30°/o, the proportionality between the two being preserved.

Further measurements were made on the plasma rf impedance, which is in the range 1 to 10 ohms and increases with increasing rf voltage.[2] The impedance expected from hydromagnetic waves at $10^{12}/cm^3$ plasma density is a few tenths of an ohm.

To study the transmission of waves along the PIG, detector electrodes were placed inside and outside the plasma tube at the receiving end. At sufficiently high magnetic field so that no resonance occurred, a 20-v signal at the driving frequency was observed, when the driving voltage was 100 v. At lower fields, where a resonance occurred, the signal was 50°/o attenuated, had a strong second-harmonic component, and was generally blurred. Further experiments with movable detector electrodes are in progress. The rf impedance presented by the heated cathode as a termination of the PIG transmission line is being evaluated.

In order to explain the anomalously high rf impedance, as well as the continued transmission of rf signal under cutoff conditions, the presence of tubular rf sheaths along the PIG has been suggested.[3] If the rf voltage appears mostly across a thin surface region of the PIG, ions can still be accelerated effectively when their orbits intersect the sheath (as in an ordinary cyclotron, the sheath taking the place of the gap between dees). A resonance is still expected, but the impedance and transmission properties are altered. Also, it is predicted that a closed plasma tube is unnecessary for effective ion acceleration. This point will be tested soon by means of a semitubular PIG.

---

[2] Edmund S. Chambers, The Guppy III (April Status Report), CVL-60-12, May 1960.

[3] Harold P. Furth, A Plasma Cyclotron, UCRL-5911-T, April 1960.

To study the sources of charge-exchange neutrals, a pin-hole camera has been developed, using a plate of MoO_3 (which is reduced to MoO_2 by reaction with impinging deuterium atoms). The tubular PIG has been "photographed" accurately in this way, using the low-energy neutral flux in the absence of rf. To make the high-energy neutral contribution from the rf mechanism distinguishable in spite of its smaller amplitude, thin protective coatings will be tried on the MoO_3, to eliminate the low-energy flux.

IV. BERKELEY PLASMA RESEARCH

1. SHEET PINCH STUDIES

Oscar A. Anderson

Introduction

High-level operation of the large Triax tubes has been delayed by the lack of reliable switchgear and by the poor insulation in the tubes themselves.[1] These two obstacles have now been removed. In the switch, a redesign of the electrode apertures (see Fig. 17) has given completely satisfactory triggering, with jitter less than 10^{-8} sec. Furthermore, the margin of safety against accidental discharge has been improved. In the Triax tubes an insulation system has been designed which stands up under tests at 120 kv. Other work during the quarter included magnetic-probe studies in the 8×10 Triax at low level and the development of a technique for producing stereoscopic streak photographs.

8×10 Tubular Pinch

A streak photograph with some interesting features was shown and discussed in the preceding quarterly report.[1] A magnetic-probe scan under the same conditions has been completed in spite of some difficulty with occasional signal variation. These variations have been traced back to the preheating system, on which more work is evidently needed. Although the magnetic-field data are imperfect, they seem good enough to be useful, and current-density profiles are being computed.

Some streak photographs (such as the one mentioned above) have shown bursts of light near the wall after the pinch current has passed its peak. It was suggested by Dr. John M. Stone that such effects could be conveniently studied by making stereoscopic streak photographs. These would reveal, for example, whether such luminous regions extended over the full length of the tube or were localized blobs. One stereoscopic scheme that has been tested is shown in Fig. 18. Temporary water-filled prisms were constructed of microscope slides and used for the photograph shown in Fig. 19. By chance the light bursts that inspired this work failed to appear, so their nature is still an open question.

High-Current Switch

The switch modifications described in the preceding report had given considerable improvement, but for jitter times of much less than 5×10^{-8} sec it was necessary to operate with pressures dangerously near the point of accidental discharge. The problem seemed to be that while the electrode apertures were efficient in passing the triggering discharge through the switch they were not sufficiently effective in preventing long-path spontaneous

---

[1] Oscar A. Anderson, in Controlled Thermonuclear Research Quarterly Report, UCRL-9106, March 1960, p. 52.

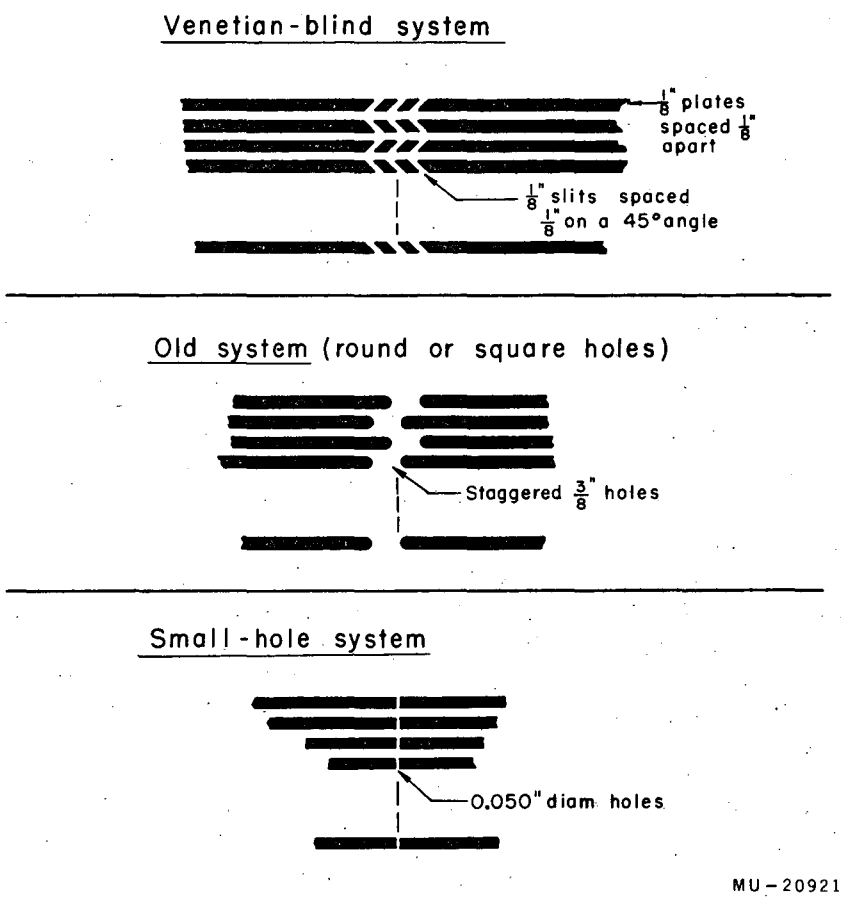

Fig. 17. Various voltage-dividing electrodes tested for use in the high-current switch.

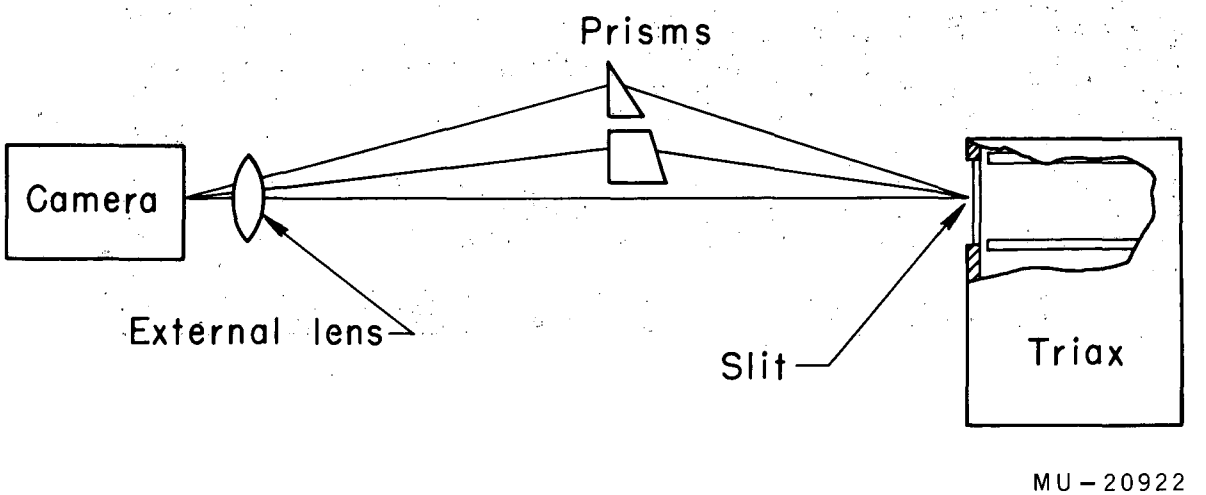

Fig. 18. Scheme for producing stereoscopic streak photographs.

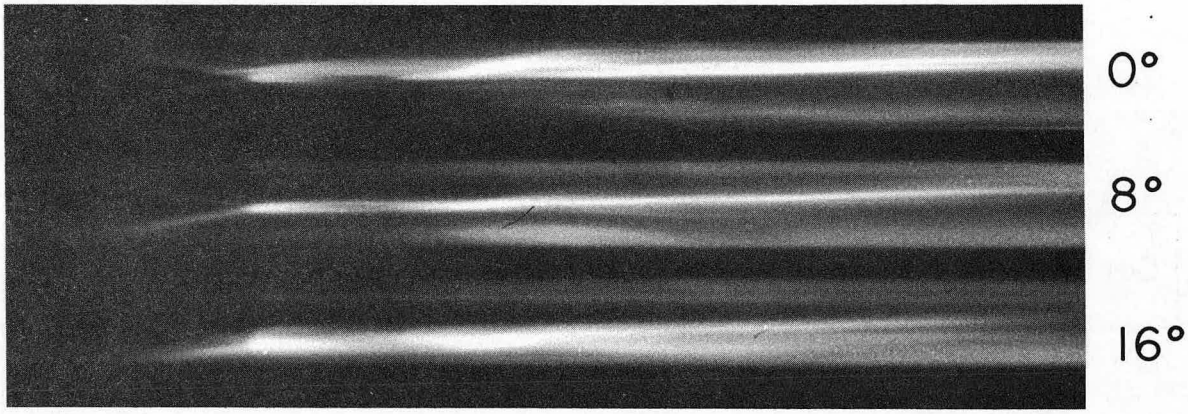

ZN-2559

Fig. 19. Stereoscopic streak photograph.

breakdowns. William Baker suggested that a Venetian-blind type of arrangement (Fig. 17) might answer both requirements, and this proved to be correct. Figure 20 shows the curves for pressure vs breakdown time for the Venetian-blind electrodes and also for four other types that were tested. The curves show that the type with very small holes (0.050 in. in diameter) placed in line also gives good results--the jitter is less than 10^{-8} sec. The small-hole system, which of course is easier to make, was the suggestion of Sejfi Protopapa, who carried out all the measurements.

High-Voltage Insulation

It has always been difficult to insulate adequately the region where voltage is applied to the tubular pinch tubes. Since the condenser banks are intended to run at 30 kv, one must allow for transient voltages of 60 kv, hence a reasonable degree of safety would require a system capable of a 120-kv test. Unfortunately the 8×10 tube has typically tested at 35 kv, and the 4×10 tube is even worse. Silastic rubber insulation was successful in curing this problem in the switches, and was considered for the pinch tubes. However, a new material, silicone gel (Dow-Corning F-1 0042 dielectric gel), offers the advantage over rubber of very low rigidity, allowing uniform pressure to be maintained at all points. This is necessary to prevent voids. During this quarter John Mark has undertaken a program of evaluating silicone gel and designing an insulation system based on it. He has made numerous tests for gelling properties in the presence of other materials. Several fixtures simulating the insulation conditions in the Triax tubes have been built and used for measuring dielectric strength. The last six tests were made on an assembly whose design is shown in Fig. 21. One hundred kv dc was maintained for several minutes in each case. Usually the RG-8/U cable failed before the gel.

At present a Triax tube using silicone gel is being assembled and will be installed on the 200-μf bank together with the four new low-jitter switches.

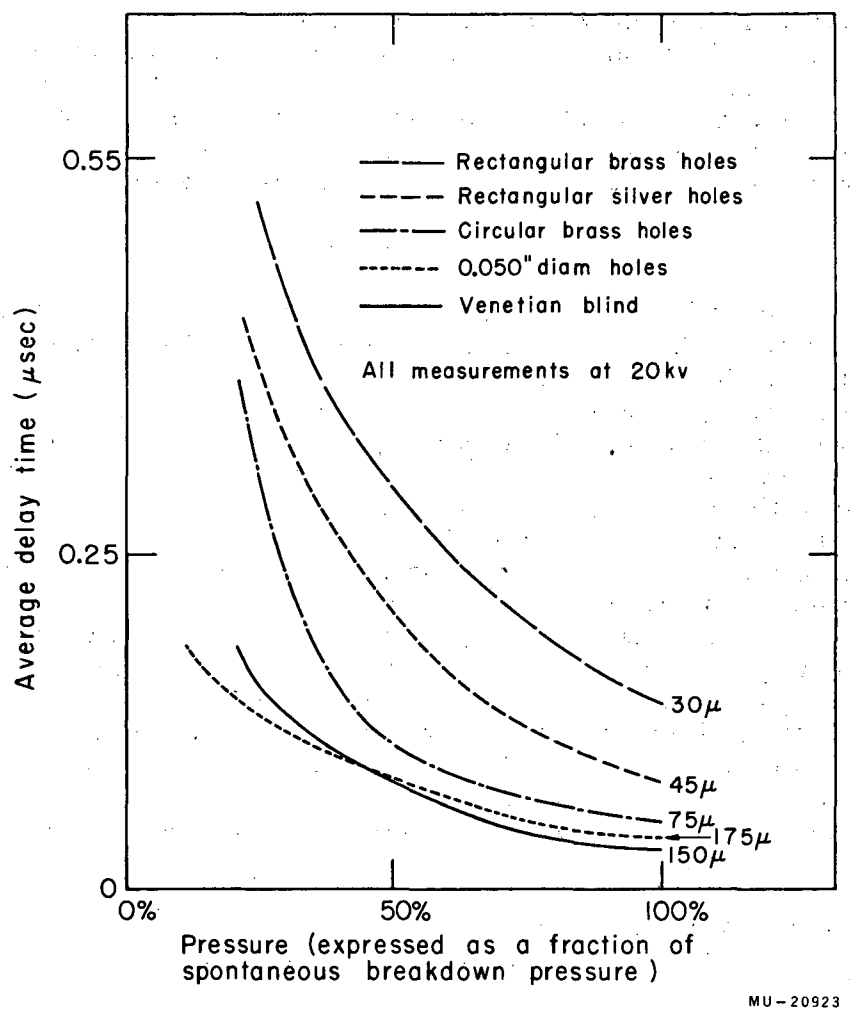

Fig. 20. Switch delay vs. pressure.

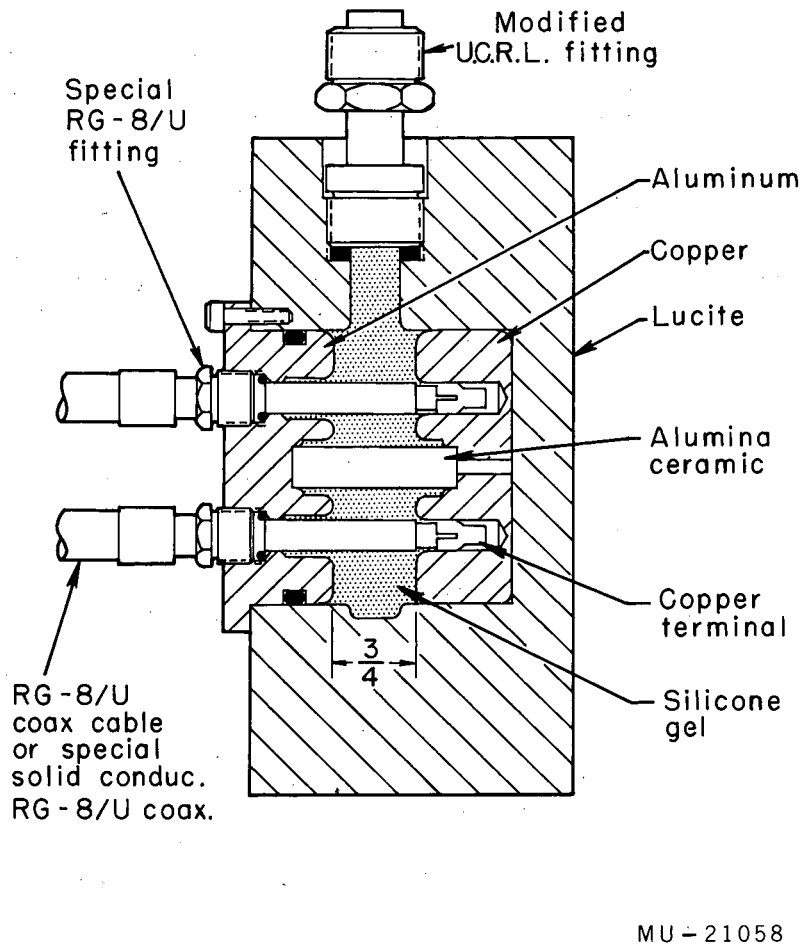

Fig. 21. Test assembly--silicone gel insulation system.

2. HOMOPOLAR PROGRAM

Alexander Bratenahl, Wulf B. Kunkel, William R. Baker,
John W. Blamey,* and Didier Veron†

Introduction

As pointed out in the preceding quarterly report,[1] there is growing evidence in certain types of crossed field plasma devices that the drift velocity of the plasma tends to be limited to several times 10^6 cm/sec by some unknown mechanism. In a homopolar device the velocity is simply proportional to the voltage so that a velocity limit is made evident by a voltage limit. The work by Fahleson and Block in Sweden, as reported by Alfvén,[2] showed that if a series resistance is introduced so that the voltage across a homopolar is permitted to be self-determining then the voltage is indeed fixed. The magnetic field and the nature of the gas alone determine this fixed value, which is otherwise independent of current, gas pressure, or applied voltage.

Homopolar III

Some studies of the voltage-regulating or velocity-limiting characteristics of the homopolar device have been continued. By limiting the current with various series resistances up to 4 ohms, confirmation of the observations by Fahleson and Block were obtained.

The current varied from 1.2 to 120 kiloamperes in these discharges. Below about 15 ka (about 0.25 ohm) the voltage and current are essentially constant in time, and the voltage is proportional to the magnetic field alone, independent of the pressure, current, or applied voltage. Above 15 ka the voltage and current are no longer constant in time; the voltage increases above this fixed self-regulated critical value in a broad bump which becomes narrower and higher as the source impedance is lowered and the current raised.

---

*Visitor from the Research School of Physical Sciences, The Australian National University, Canberra, Australia.

†Visitor from Centre d'Etudes Nucléaires de Fontenay-aux-Roses, France.

[1] Alexander Bratenahl, Wulf B. Kunkel, William R. Baker, John W. Blamey, and Didier Veron, in Controlled Thermonuclear Research Quarterly Report, UCRL-9106, March 1960, p. 57.

[2] H. Alfvén, Ionic Heating and Confinement of a Magnetized Plasma, invited paper, January 1960 meeting of the American Physical Society, New York, N. Y.

The normal "capacity"[3] of the Homopolar is readily calculated upon assumption that all the gas is rotating as a plasma. At low currents, at which the machine exhibits voltage regulation, the capacity is far below this value. At very high currents the capacity is frequently five or more times the normal value.[4] Along with this observation is that when the machine is operated with the vacuum pump sealed off, there is a large increase of permanent gas, the increase being proportional to the energy delivered from the source.

It has also been observed that the radial current starts in the equatorial plane and spreads toward the insulators in times of the order of 5 to 10 μsec.

All these observations can be brought into harmony in a qualitative way by assuming that there are regions of velocity shear in which the velocity gradient is parallel to the field lines. These regions of shear separate the rotating plasma in the equatorial region from neutral gas near the insulator. In these shear regions ionization is continually taking place. If we further assume that Alfvén's postulate,[5]

$$\left(\frac{m v^2}{2} - W_i\right) \frac{dn_i}{dt} = 0$$

(with W_i the ionization potential, n_i the ion density), holds in the ionizing region, then the velocity (and hence the voltage) is regulated at the value

$$v = \sqrt{\frac{2 W_i}{m}} \quad .$$

If, by supplying sufficient power, one can push this ionization region all the way to the insulators, the ionization process evidently continues just as before, for the insulator seems somehow quite capable of supplying practically unlimited quantities of material to ionize. But the velocity gradient near the insulators is dominated by a nonslip condition, resulting in Hartmann boundary-layer flow.[6] Therefore if the ionization is taking place in this boundary layer, it is possible that the Alfvén regulation can no longer restrict the flow in the main body of the plasma to the critical value.

---

[3] O. A. Anderson, W. R. Baker, A. Bratenahl, H. P. Furth, and W. B. Kunkel, J. Appl. Phys. 30, 188 (1959).

[4] A. Bratenahl and W. B. Kunkel, Some Studies of Current Flow and Boundary Effects in Homopolar III, UCRL-8962 Abstract, Oct. 1959. (Meeting of the Division of Plasma Physics of the American Physical Society, Monterey, Calif., Dec. 3-5, 1959.)

[5] Although not stated in this form, this is the essential implication of Alfvén's explanation of the experiment by Fahleson and Block reported in Reference 2. We are indebted to Harry E. Petschek, Avco-Everett Research Laboratory, to this expression.

[6] W. R. Baker, A. Bratenahl, and W. B. Kunkel, Viscous Effects in Highly Ionized Rotating Plasmas, IV International Conference on Ionization Phenomena in Gases, Uppsala, Sweden, Aug. 17-21, 1959. (UCRL-8861, Aug. 1959).

Higher velocities are possible under these conditions, but the enormous power required quickly exhausts the source condenser bank. If the applied voltage is raised still higher, actual breakdown across the insulator is observed.

Since there is considerable hope of avoiding all these difficulties in Homopolar IV, all further work on Homopolar III has been discontinued in favor of this new device.

Homopolar IV

Homopolar IV, the Puffatron,[1] has been assembled except for installation of the fast valve. The device is undergoing high-voltage tests and the valve is being tested under vacuum conditions.

The machine will hold ±120 kv at pressures of 4×10^{-7} mm Hg without magnetic field. It has been found, however, that in the presence of the magnetic field a breakdown occurs in a time that varies inversely with voltage. At 70 kv, for instance, the breakdown time is 120μsec. The breakdown is preceded by a current buildup requiring some 30 μsec. This discovery, which is probably related to high-power magnetron misbehavior, requires that the condenser bank be pulse-charged immediately before the valve is opened. For this purpose, a suitable 100-kv Marx generator has been constructed and tested, and is presently being used for further study of the high-vacuum breakdown problem.

So far there is little reason to believe that the breakdown problem is going to thwart our efforts to put the machine into operation.

The fast valve has proved satisfactory under high-vacuum conditions, except that the valve stem made of Lexan (a material produced by General Electric Co., with somewhat higher impact strength than nylon) cracked after about 100 operations. A minor redesign is in process.

3. CROSSED-FIELD BREAKDOWN STUDIES

Melvin J. Bernstein and Wulf B. Kunkel

During this quarter an experiment has been set up to study the build-up of ionization and the electrical breakdown in crossed electric and magnetic fields. The geometry is coaxial. An aluminum cylinder 15.5 cm in diameter and 10 cm in length serves as a cathode. The anode is made of copper and is divided up into three identical cylindrical sections which are insulated from one another and which have an inside diameter of 16.5 cm, so that the gap is 0.5 cm. Other anodes may be inserted if different gap spacings are desired. The electric field can be varied up to 1000 V/cm. The entire electrode structure is inside a pyrex vacuum system which is mounted between the pole faces of the magnet that was formerly used for the Homopolar II experiment. The magnetic field, which can be varied from 400 to 12,000 gauss, is parallel to the cylinder axis.

The cathode can be irradiated in a certain region with ultraviolet light from a mercury lamp to provide a small emission current. In the initial phase of the experiments currents will be measured with Keithley electrometers. It is planned that the first part of the study will be concerned with a conventional measurement of gas amplification of currents as a function of electric field strength, gas pressure, and magnetic field intensity under well-controlled steady-state conditions. It is hoped that in this way ultimately some light can be shed on the conditions existing in the space between the electrodes when nonsteady discharges set in and when the transition to a self-sustaining discharge (breakdown) occurs. A good understanding of these phenomena is of extreme importance for work with rotating plasma, PIG discharges, ion magnetrons, and all other crossed-field plasma devices as well as for dealing with some types of breakdown in accelerators.

4. PLASMA PHYSICS AND MICROWAVE DIAGNOSTICS

Donald B. Hopkins, M. C. Horton, George A. Paulikas,* Robert V. Pyle, Henry F. Rugge, and J. Warren Stearns

Microwaves

The microwave effort has been directed chiefly to diagnostic support for Hothouse II, the Puffatron(which requires 100-kv isolation), and the thermally ionized Cs plasma. Dielectric waveguides have been designed for the Puffatron, and the cavity-frequency-shift technique (which has not been used previously at this Laboratory) has been developed for Cs plasma-density measurements.

Enhanced-Diffusion Experiment

A report has been prepared summarizing all measurements directly relating to the loss of azimuthal symmetry in the positive column. (T. K. Allen, George A. Paulikas, and Robert V. Pyle, Instability of a Positive Column in a Magnetic Field, UCRL-9110, March 1960.) Experimental and theoretical studies relating to the determination of the radial potential distribution are continuing.

Cs Plasma Experiment

A rod of thermally ionized Cs, 1 cm in diameter and up to 2 meters long, has been produced. The present arrangement is such that Cs vapor from a small oven is ejected as a hollow cone and strikes some part of a structure consisting of a tungsten filament at about 2300° and a concentric molybdenum cylinder at 1200°. The filament structure is in the diverging field of the magnet and the plasma is guided by magnetic fields of up to 3 kG through the 4-in.-i.d. glass vacuum chamber. If the plasma is collected with a negatively biased probe at the far end of the vacuum system, a current is observed for all voltages more negative than the filament structure. The collected current increases approximately as the square root of the applied voltage, with all of the potential drop except a fraction of a volt occurring at the negative electrode. The collected current varies with the filament temperature and the distance of the collector from the source, and charged-particle densities in the range from 10^{10} to 10^{11} are obtained under typical conditions. Pressures in the vacuum vessel are not well known at present, but are somewhat higher than 10^{-6} mm Hg. Experiments are in progress using Langmuir probes and a microwave cavity for density measurements and with hot electrodes at both ends of the magnet.

---

*National Science Foundation Fellow.

5. HYDROMAGNETIC WAVE AND CYCLOTRON HEATING

William S. Cooper, Alan W. DeSilva, and John M. Wilcox

Propagation of torsional hydromagnetic (Alfvén) waves in a cylindrical plasma has been reported.[1] These experiments have been extended to include measurements of the radial distribution of the oscillating magnetic field which is associated with the wave, and of reflections of the wave from the end of the cylindrical plasma. These observations make possible a quantitative comparison between predictions of hydromagnetic theory and experimental results.

A new method of plasma preparation has been developed which produces a quiescent, fairly highly ionized plasma which is relatively free of impurities. The ionizing current pulse is supplied from a lumped-constant pulse line connected by means of an ignitron switch between the copper outer wall of the tube and a coaxial electrode at one end. Ionization is initiated by a spark plug on the electrode, following which a well-defined front travels down the tube. Ahead of this front the gas is composed of cold neutrals. Behind the front we have a well-ionized spinning plasma which has been shown spectroscopically to be quite free of contaminants. When the front reaches the far insulator, impurity lines begin to appear. If, however, the bank is short-circuited just as the front reaches the receiving end, the plasma is rapidly braked to a halt, and the impurity lines do not appear. We have attempted to measure the ion density by means of the Stark broadening of the hydrogen lines. Preliminary results indicate an ion density of at least 20% of the initial neutral density.

We have measured the radial distribution of the oscillating magnetic field which is associated with the wave, and find a good agreement with the results of an analysis of the modes of propagation to be expected. We have observed reflections of the hydromagnetic waves from the end of the cylindrical plasma[2] and have used this effect to measure the radial magnetic field distribution of a wave which has made three transits of the hydromagnetic waveguide. Since the lowest-order mode has the least attenuation, the wave which has made three transits of the tube would be expected to consist almost entirely of the lowest-order mode. This is verified experimentally.

Using Maxwell's equations, Ohm's law, and Newton's second law of motion, one can show[3] that the radial distribution of azimuthal magnetic field b_θ associated with the wave is described by a first-order Bessel function $J_1(k_{cn} r)$, where $n = 1, 2, 3 \cdots$ designates the various principal modes, and the k_{cn} are evaluated from a boundary condition which was determined experimentally in the following manner. Radial current probes

---

[1] Allen, Baker, Pyle, and Wilcox, Phys. Rev. Letters 2, 383 (1959); Wilcox, Boley, and DeSilva, Phys. Fluids 3, 15 (1960).

[2] Reflection of plasma Alfvén waves has independently been observed by Shigeo Nagao and Teruyuki Sato, Tohoku University, Sendai, Japan (private communication).

[3] W. A. Newcomb in Magnetohydrodynamics (Stanford University Press, Stanford, California, 1957), p. 109.

inserted into the wall of the waveguide failed to detect a current associated with the propagating wave. Therefore the radial current density, which is also proportional to $J_1(k_{cn} r)$, is zero at the wall, and the boundary condition is $J_1(k_{cn} a) = 0$, where a is the waveguide radius. The attenuation length for ohmic losses is proportional to $(k_{cn}^2 + k^2)^{-1}$, where k is the wave number of the wave. Since $k_{c1} < k_{c2} < k_{c3} \cdots$, the attenuation of the lowest-order mode is considerably less than the attenuation of the higher modes. Thus although an arbitrary disturbance at the driving end can excite many modes, only the lowest-order modes survive for an appreciable distance.

The radial variation of b_θ has been measured with six magnetic probes inserted into the plasma at six radial positions near the receiving end of the tube. Results for the wave which has made one transit of the tube are shown in Fig. 22. The solid line represents the lowest mode of propagation plus 30% of the second mode. The amount of second mode present was determined by a best fit to the experimental data. The effective plasma radius for wave propagation appears to be about 4 mm less than the radius of the copper cylinder. This may be a measure of the thickness of the sheath or layer of neutral particles, which isolates the wave currents from the conducting boundary.

When the wave reaches the receiving end it undergoes a reflection which corresponds to that of an open-ended transmission line. A similar reflection occurs at the driving end, and we can then observe a wave that has made three transits of the waveguide, as shown in Fig. 23. According to the theory a second mode, which was present to the extent of 30% after one transit, would be present after three transits to the extent of only 0.4%, i.e., negligible. Thus the solid line in Fig. 23 represents the lowest mode only.

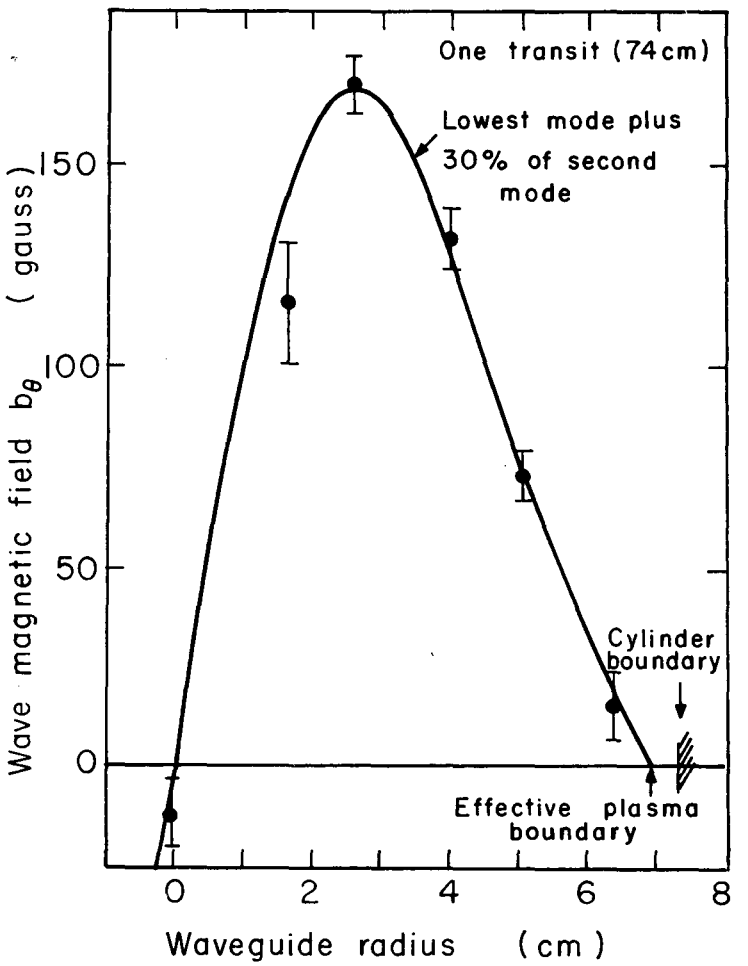

MU-20360

Fig. 22. Measured radial distribution of wave magnetic field after one transit of waveguide (74 cm). Solid line is proportional to $J_1(k_{c1} r) + 0.3 J_1(k_{c2} r)$, i.e., first mode plus 30% second mode. Vertical bars indicate standard deviation of mean of eight measurements plus estimate of calibration uncertainties.

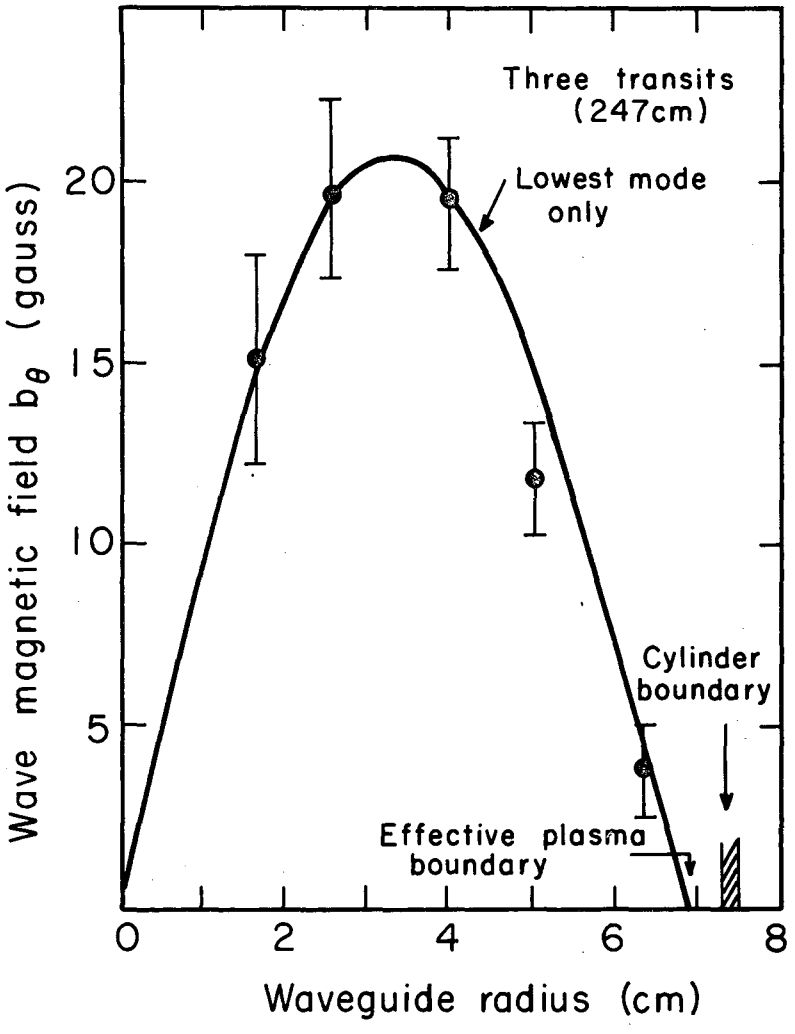

MU-20361

Fig. 23. Measured radial distribution of wave magnetic field after two reflections, i.e., three transits of waveguide (247 cm). Solid line is proportional to $J_1(k_{c1} r)$, i.e., first mode only.

6. ION MAGNETRON

Robert W. Layman

Described briefly in the preceding quarterly report (UCRL-9106) was an experiment designed to test the possibility of reducing the loss of circulating ions due to charge exchange. The following is a report on the continuation of this experiment.

Since the charge-exchange rate is a function of the density of the neutral gas molecules in the circulating-ion region, this experiment was designed to prevent neutrals from the liner wall from entering the discharge region. Figure 24 shows the experimental setup installed in the liner. The ring filament emits electrons, which are accelerated along magnetic field lines to the opposite end of the liner, where they are reflected back. A thin-walled hollow cylindrical plasma concentric with the anode and extending longitudinally from the filament to the reflector is thus formed. With sufficiently high filament emission (a milliampere is more than ample) thermal neutrals entering this region have a high probability of being ionized and consequently radially trapped. The trapped ions migrate to the ends of the liner, where many are removed from the system by either cathode pumping or the diffusion pumps. Thus the neutral-gas flux into the circulating-ion region is reduced.

The filament, filament channel, and reflector were to be run at the same potential with the accelerator biased positive to get the desired electron emission. However, the positive voltage on the accelerator affected the operation of the main discharge, therefore the filament channel and accelerator were run at liner potential, and the filament was biased negatively. The high drain from the filament to the filament channel limited the filament bias to 40 volts with the power supply available. The electron emission outward was sufficient, however, to give the experiment a fair trial.

To test the effectiveness of the setup, neutron counting rates with the filament on and off were compared while other parameters were left undisturbed. Increases of 30% to factors of 10 were observed with the filament on. Figure 25 shows neutron rates with increasing voltage for the filament on and off. Variations in other parameters, such as magnetic field or pressure, showed the same results, a net gain in neutral output but no significant change in response to variations in these parameters. Although the filament was biased with only 40 volts, variations in neutron output could be observed with changes in bias voltage. The assembly was then removed to be modified to allow for much higher filament bias voltages.

So far this experiment has demonstrated that some control of charge exchange is possible. To what extent is not yet known; this experiment was only to investigate the possibilities of this method. With proper design of this type of apparatus (not possible with the present liner), and increased sheath efficiency through higher voltages and magnetic fields, it would not be unreasonable to expect burnout in a machine of this type.

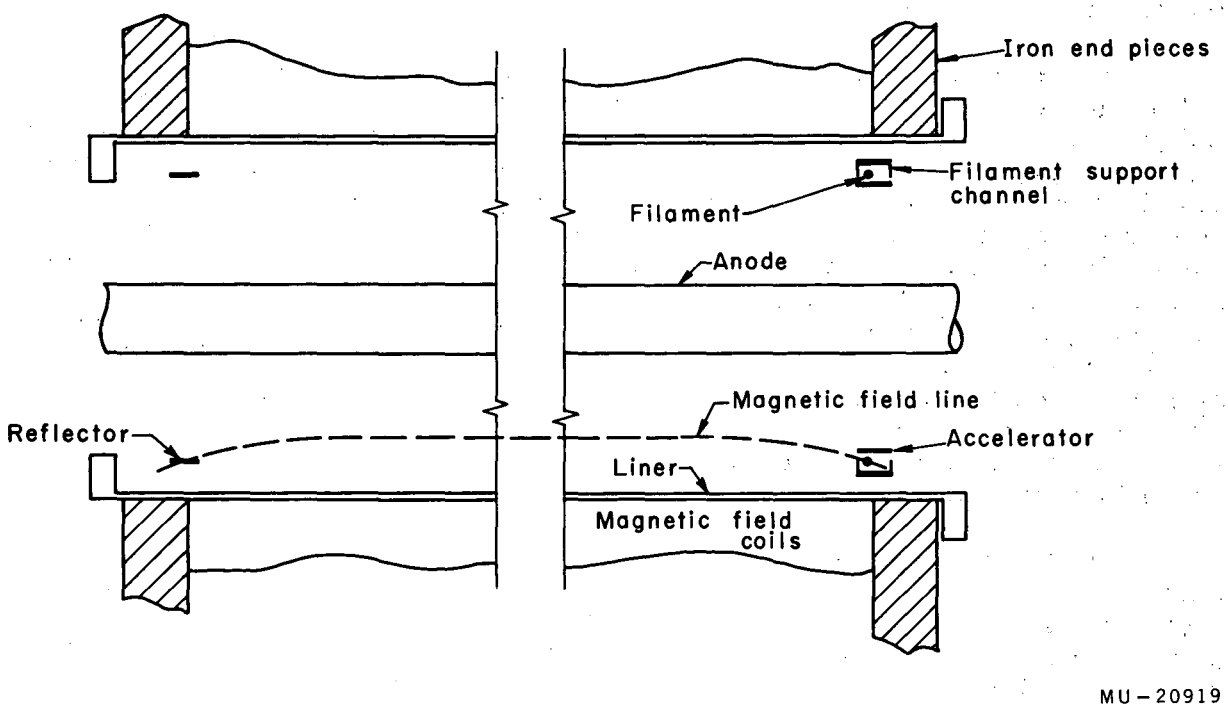

Fig. 24. Ion magnetron.

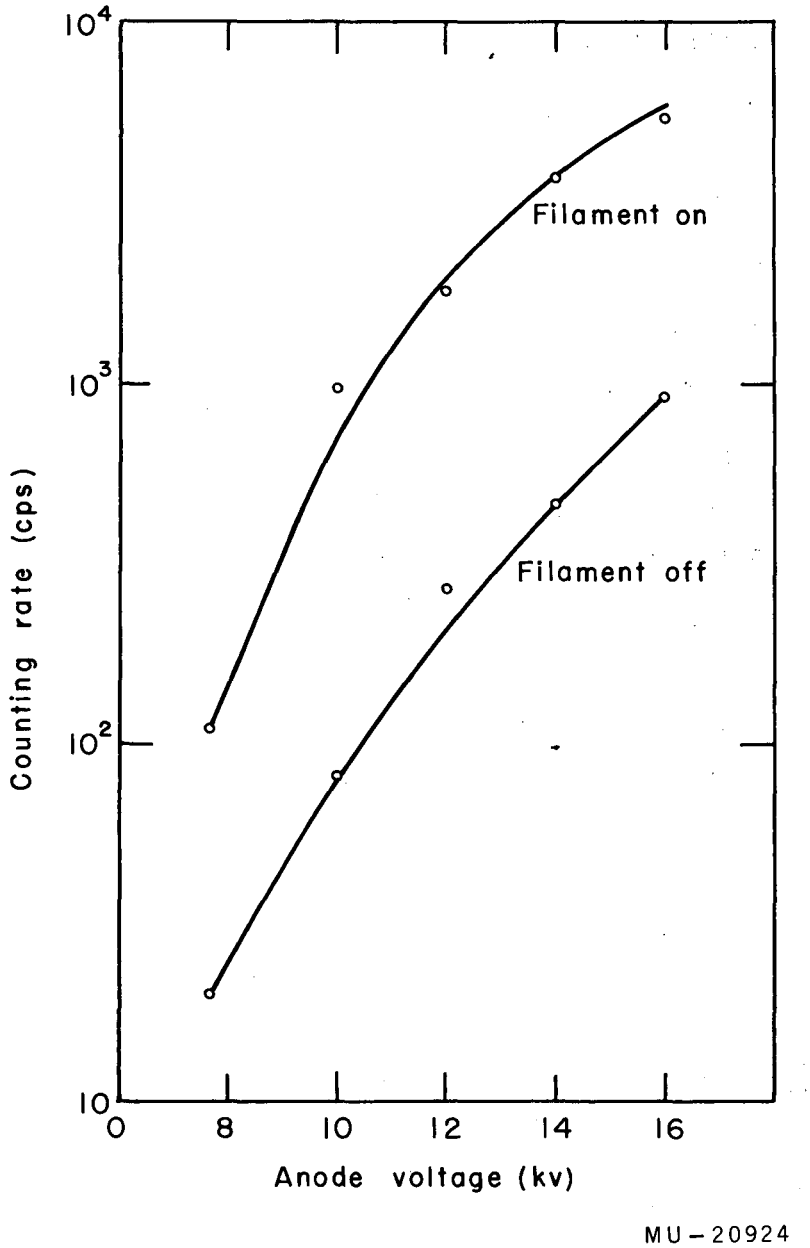

Fig. 25. Counting rate vs. voltage with filament on and off.

7. EXPERIMENTS WITH PULSED MAGNETIC CUSPS

William R. Baker and Jean-Paul H. Watteau†

INTRODUCTION

Confinement of a plasma by magnetic fields in cusp-shaped configurations was proposed several years ago.[1] Stability and particle loss rate for such geometries have been the subject of considerable analysis.[2] Experimental work with these schemes, however, has been very disappointing, as may be judged from the dearth of published results. Recently, interest in cusped-geometry containment has been revived,[3] largely because it is feared that the radiation losses from a plasma will be excessive if the latter is permeated by a strong magnetic field.[4] Accordingly, a fair number of experiments are now under way at various laboratories. Many of these[5] deal with the problem of injection of plasma from an external source into, and trapping by, an already existing cusp-shaped magnetic field configuration. In this paper experiments are described in which the plasma is generated inside the region to be enclosed by a rapidly rising cusp-forming magnetic field. In the initial phases of the study the ionization was produced by the rapidly rising magnetic field itself. This case was somewhat similar to the experiment called "CHALICE" which is being performed at Stevens Institute of Technology.[6] In later work power discharges have been used to

---

† Visitor under the sponsorship of the Ministère des Affaires Etrangères, Relations Culturelles, France, 1959-1960.

[1] e.g. J. L. Tuck, Conference on Thermonuclear Reactions, Princeton University, Oct. 1954, U. S. AEC Tech. Inf. Service WASH-184, 1955, p. 77.

[2] J. Berkowitz, K. O. Friedrichs, H. Goertzel, H. Grad, J. Killeen, and E. Rubin, Proceedings of the Second United Nations International Conference on the Peaceful Uses of Atomic Energy, Geneva, 1958 (United Nations, Geneva, 1958), Vol. 31, p. 171.

[3] J. L. Tuck, Phys. Rev. Letters 3, 313 (1959).

[4] B. A. Trubnikov and V. S. Kudryavtsev, Proceedings of the Second United Nations International Conference on the Peaceful Uses of Atomic Energy, Geneva, 1958 (United Nations, Geneva, 1958), Vol. 31, p. 93.

[5] F. R. Scott, R. E. Wenzel, W. R. Snow, and J. A. Rutherford, Bull. Am. Phys. Soc. 5, Series II, 327 (1960); F. H. Coensgen, W. E. Nexsen, W. F. Cummins, and A. E. Sherman, Bull. Am. Phys. Soc. 5, Series II, 327 (1960); also D. C. Hagerman and J. E. Osher, Bull. Am. Phys. Soc. 5, Series II, 350 (1960).

[6] David Finkelstein, Samuel Koslov, Kenneth C. Rogers, and George Schmidt, ibid., 310 (1960).

generate the plasma before the confining field is pulsed on. In general, therefore, these experiments may be divided into three distinct steps:

(a) creation of a plasma,

(b) creation of the magnetic cusp field resulting in isolation and compression of this plasma,

(c) sustainment of this magnetic field for extended containment.

Before the experiments themselves are described, it is necessary to discuss, in a little more detail, the specific magnetic-field configurations used.

THE MAGNETIC FIELD

A two-dimentional cusped geometry is shown in its cross section in Fig. 26a. It has the essential features of the so-called "Picket Fence" configuration.[1] By rotation about the x'x axis a three-dimensional bicuspid geometry is obtained, as indicated in Fig. 26b. This is the simplest magnetic cusp field, and the following study was done in such a configuration. The field is produced by passing the same current in opposite directions through two identical Helmholtz coils, as shown in Figs. 26b and 27. The geometry may be characterized by the ratio $\alpha = d/2R$, where d is the distance between the coils and R is their radius. The vacuum field due to such coils may be computed.

Let

B_0 = the magnetic field created by one coil alone at its center,

B_A = the magnetic field at this point when the coils are associated,

B_P = the magnetic field in plane P at distance R from the axis.

It can be shown that the maximum magnetic field in the plane P occurs very nearly at distance R from the axis for the range of α considered. It is found that for $\alpha = 1$ we have $B_A/B_0 = 0.9$ and $B_P/B_0 = 0.4$, i.e., at the ring cusp the field intensity is only about half of that at the point cusps. Equal field strength $B_A = B_P$ is found for $\alpha = 0.7$, where then we have $B_A/B_0 = B_P/B_0 = 0.8$.

The variation of the magnetic field in time ideally would consist of a compression phase followed by a containment phase, as indicated in curve 1 of Fig. 28. In practice, however, it is much simpler to produce an oscillating field shown in curve 2 of Fig. 28 and use only the first half-period for the experiment. This is the case in the present investigation. It is planned to add the necessary circuit components at a later date to produce a prolonged containment time of a character shown in curve 3.

In this work typical values used are: R = 5.5 cm, capacitive energy stored for the magnetic field $W = 10^4$ joules, ringing period 10 μsec, peak current $I_{max} = 4.5 \times 10^5$ amperes, peak magnetic field (calculated) $B_{0_{max}} = 2.5 \times 10^4$ gauss. The aspect ratios used were first $\alpha = 1$, later $\alpha = 0.7$.

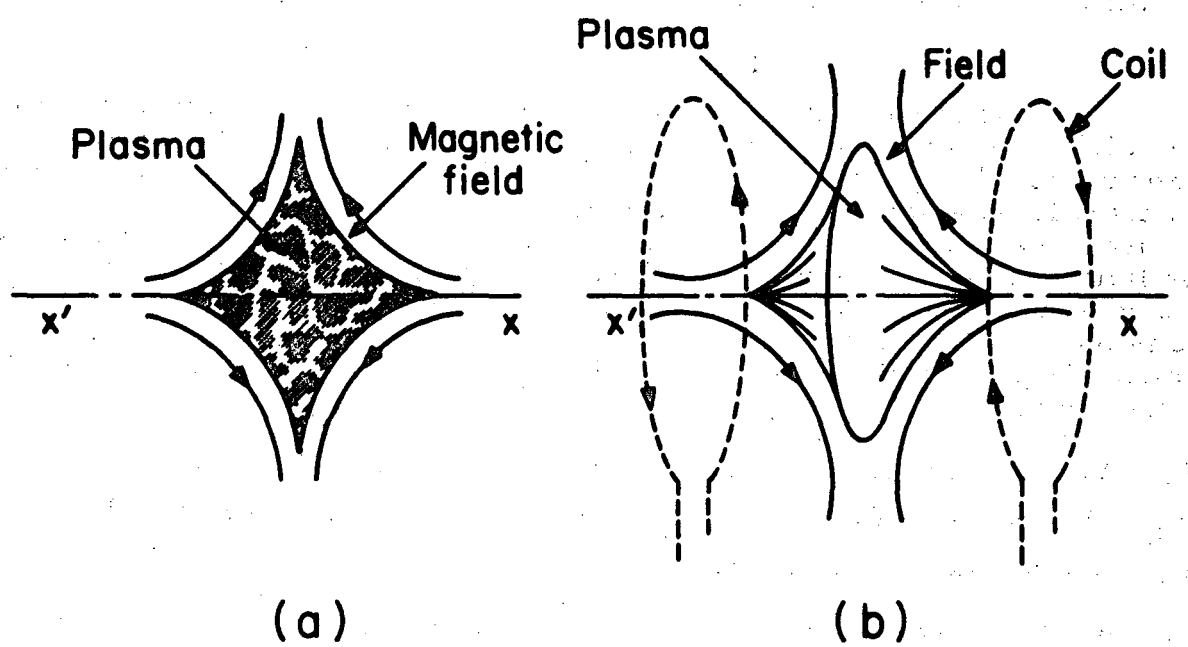

MU-20539

Fig. 26. (a) Two-dimensional cusped geometry.
26 (b) Three-dimensional cusped geometry (bicuspid).

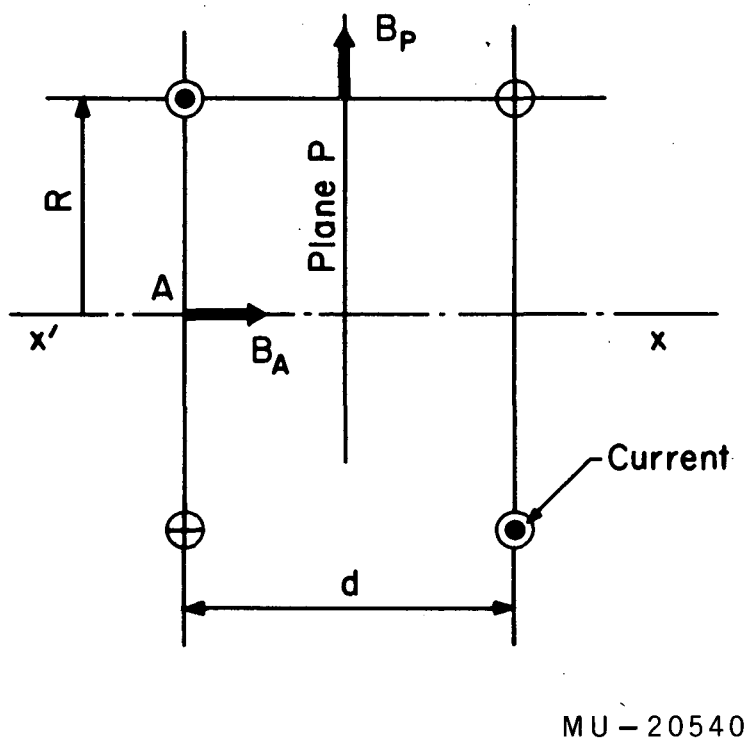

Fig. 27. Cross section of Helmholtz coils showing definition of pertinent quantities.

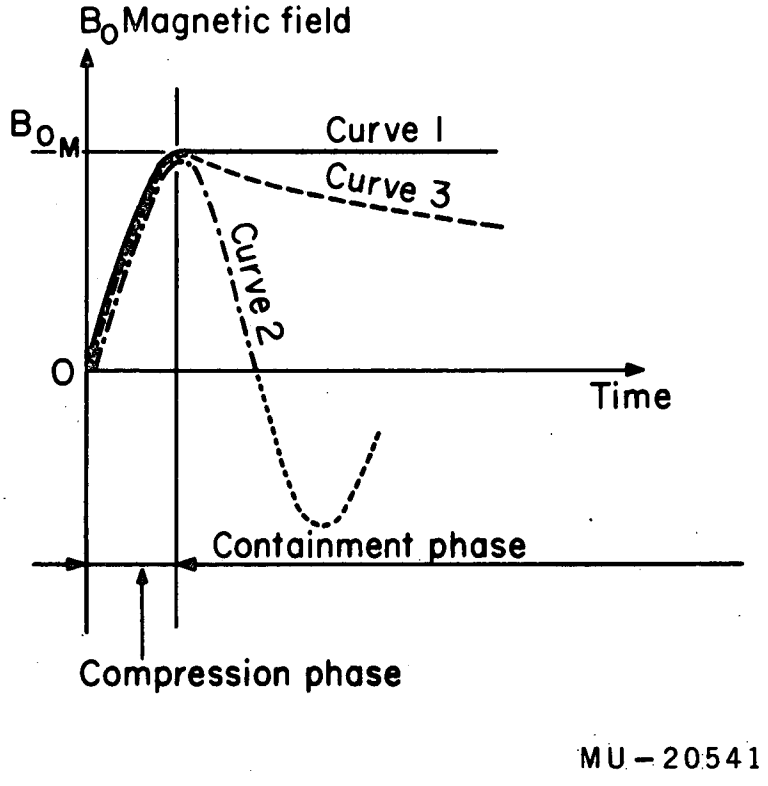

Fig. 28. Variation of the magnetic field with time.

THE EXPERIMENTS

The first experiments were performed in a quartz tube with straight cylindrical walls. Time-resolved visual observations were made by using a Kerr cell with 0.2 μsec exposure.

Model A (Fig. 29)

The rapidly rising magnetic field generates a high electric field, and this was expected to provide a sufficient degree of ionization. A small steady current was applied through the gas to provide an initial source of electrons and make the main discharge reproducible.

The working conditions were: air 100 μ, $B_{0_{max}} = 1 \times 10^4$ gauss, $\alpha = 1$.

When $B_0 = 0$, the electric field is maximum, and we observed the formation of two plasma rings near the coils (electric field maximum in space). These are squeezed toward the axis as the magnetic field rises. The observation of a persistent hole in each ring shows the trapping of a portion of the main field by the increasing conductivity of the plasma with time. The ionization process by this method in regions outside these plasma rings seems to be strongly inhibited by the cross magnetic field.

Model B (Fig. 30)

From the foregoing study we found that it is better to form the plasma first, with a minimum of included magnetic field. This was attempted by using a very fast current pulse through an auxiliary coil between the two main cusp coils. After the ionization, the magnetic field was applied. The conditions for this second model were: $H_2 = 100$ μ, $B_{0_{max}} = 2 \times 10^4$ gauss, $\alpha = 1$.

The behavior of the ionized gas is similar to that in Model A and the phenomenon is stronger. There not only is a radial compression, but also parts of the plasma rings are shot into the central region of the cusp as a result of the shape of the magnetic field lines. Roughly speaking, it acts like two weak plasma guns shooting into the cusped geometry. A well-defined cuspate plasma body was observed. The presence of a band of light, approximately 1 centimeter wide, on the glass circling the region between the cusp coils indicated that a great deal of plasma was "leaking" out.

Pinch-Cusp Experiment

To reduce this leakage, α was decreased to a value of 0.7 for which $B_A = B_P$. Also the quartz tube was modified as shown by Fig. 31. This placed the field B_P inside the glass.

Because of the apparent inefficiency of the preceding coil method for ionizing the gas, a direct discharge through the tube was tried. With sufficient current a pinch is formed. The advantages of a pinch are:

(a) The gas is ionized with a minimum of included magnetic field, gathered near the axis, and heated. Wall contamination is minimized.

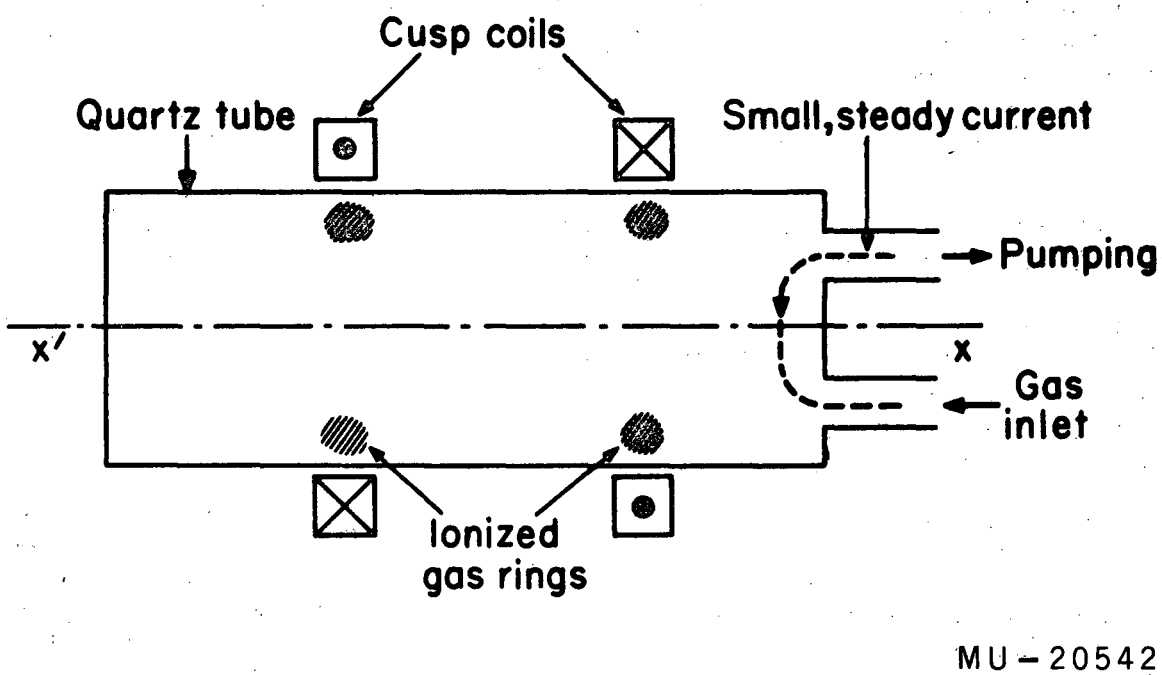

Fig. 29. Cross-section view of Model A.

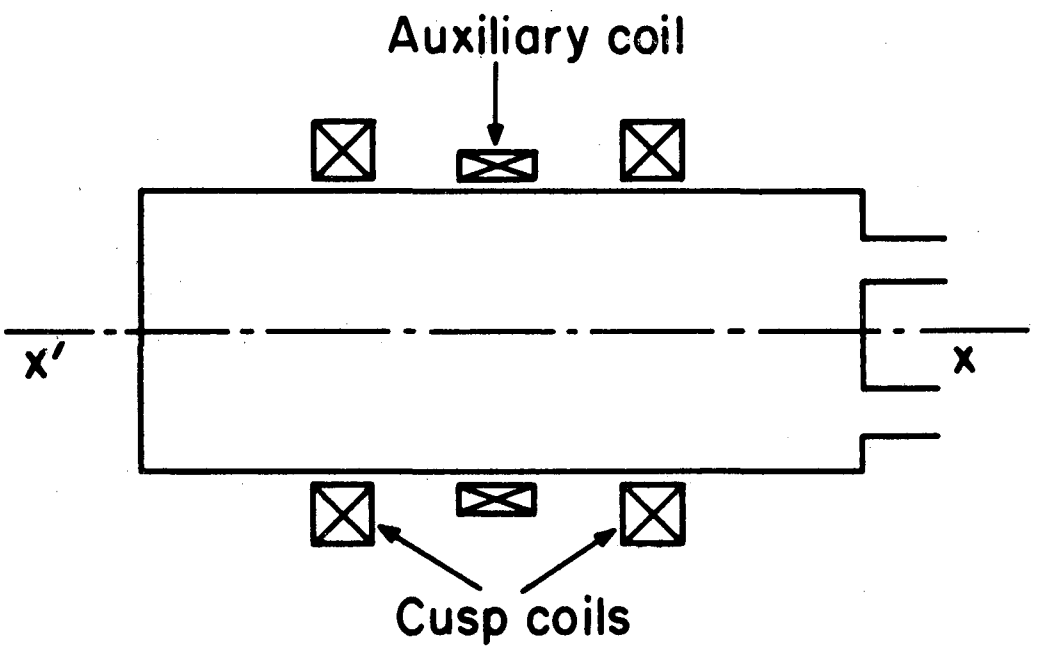

MU-20543

Fig. 30. Cross-section view of Model B.

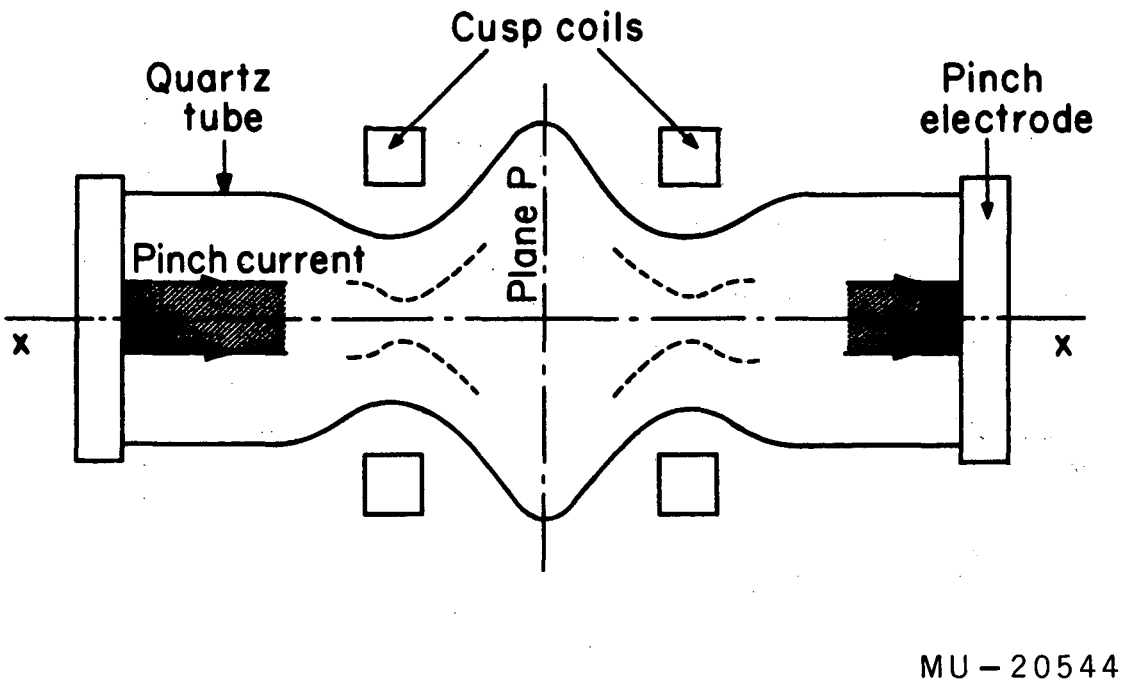

Fig. 31. Cross-section view of the pinch-cusp model.

(b) After the maximum compression of the pinch, instabilities grow; however, if the cusp is started at this time one can hope for the formation of a hot plasma body inside. Better than that, we can start the cusp later and add more heat to the plasma by magnetic compression.

By reducing the radius of the glass in the region of the cusp coils, the pinch can be made to occur here first. This gives a spatially controlled $m = 0$ instability such that the plasma on each side of the cusp is accelerated into the central region.

The working conditions were: $D_2 = 100\ \mu$, $B_{0_{max}} = 2.5 \times 10^4$ gauss, $\alpha = 0.7$, pinch peak current 1.5×10^4 amperes, with a rise time of 4.5 μsec.

The following results were obtained:

(a) A silicon line at 4552.50 Å appears only after the first half-cycle of the cusp current, which means that the gas was not previously contaminated by wall materials.

(b) The pictures of the pinch-cusp discharge taken at different times are mainly without light, except for a thin bright line in plane P (Fig. 32a). Clearly the leakage is reduced. On the assumption that the central region was occupied by a fully ionized deuterium plasma and therefore invisible, a small amount of argon gas was added. The results are shown in Fig. 32b. The appearance of an extremely narrow band of erosion of the quartz (see arrow in Fig. 32c) also indicates the great improvement in the control of leakage of plasma in this region over the previous geometries.

(c) Pictures were taken at different times during the first half-cycle. These never showed instability, but the orderly formation, containment, and expansion of the hot gas.

(d) According to Harold Grad,[2] better containment in the cusp is obtained with a sharp boundary between the plasma and the magnetic field. Such a boundary condition seems to be favored experimentally by higher gas densities, as shown by comparison between Figs. 32b and 32d.

Though the mechanism of such a device is not understood in detail, and the measurements to date are mainly qualitative, the combination of linear pinch and cusp geometry investigated here seems sufficiently interesting to warrant further study.

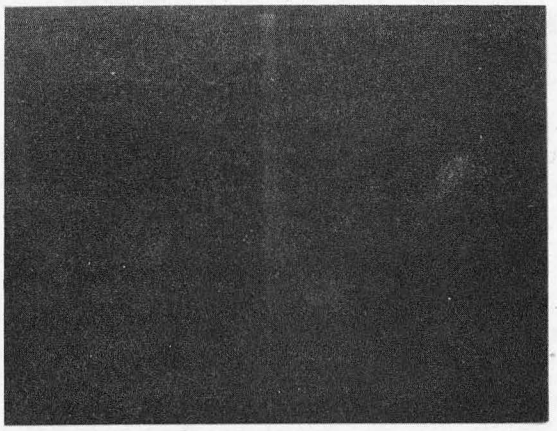

(a)

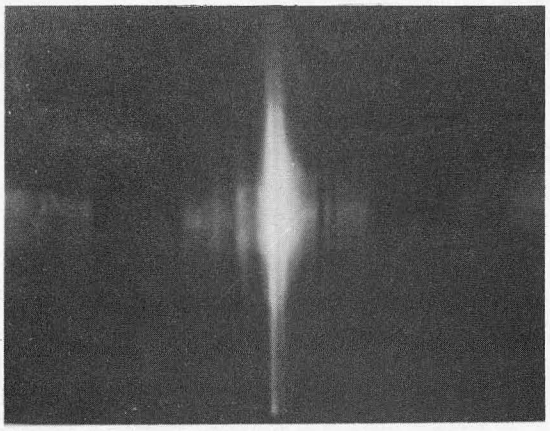

(b)

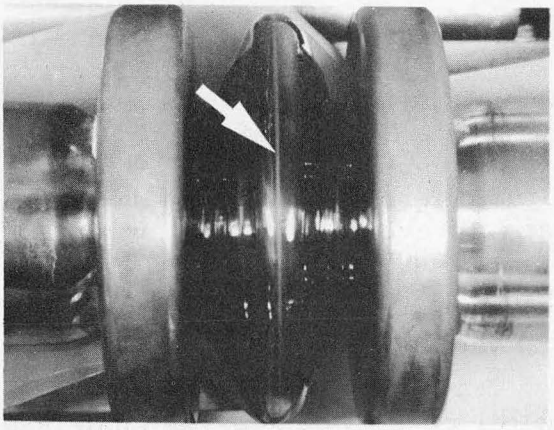

(c)

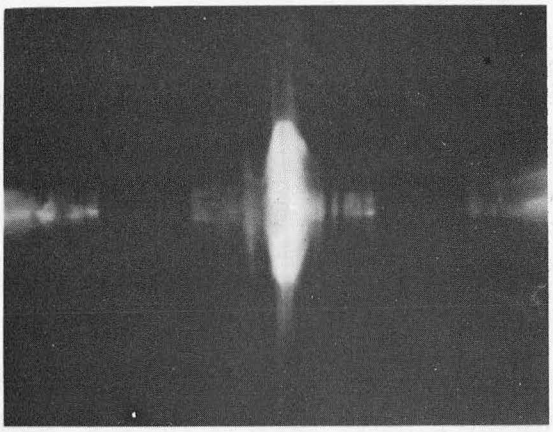

(d)

ZN-2567

Fig. 32. Photographs of the quartz plasma-discharge tube. Photographs (a), (b), and (d) were taken when the magnetic field was at the maximum value. The location of the quartz tube in 32(a), 32(b), and 32(d) can be seen by using 32(c) as a reference. (a) Photograph of the discharge of fully ionized gas (D_2 pressure 100 μ). A thin, bright line is left by the plasma striking the glass. (b) Same conditions as shown in (a). A small amount of argon was added in order to detect the fully ionized deuterium plasma in the central region of the cusp. (c) The quartz tube. The white arrow indicates the trace left by the hot gas on the quartz. (d) Photograph of the discharge with 500 μ of deuterium. A sharp boundary between hot gas and magnetic field is in evidence far from the glass.

V. THEORETICAL AND BASIC EXPERIMENTAL PLASMA PHYSICS

1. ENERGY TRANSFER FROM HOT IONS TO COLD ELECTRONS IN A PLASMA

Warren Heckrotte and John Killeen

The study of the energy transfer from hot ions to cold electrons by means of the numerical solution of the Fokker-Planck equation described in earlier reports[1-3] has been continued. We present here the results of an additional case. The case presented is for deuterons at approximately 20 kev, and the electrons are initially at 10 ev and heat up to 1 kev.

The mean electron energy is given by

$$E_- = \frac{3}{2} k T_- = \frac{1}{2} m v_0^2 \frac{I^-_4}{I^-_2} , \qquad (1)$$

where

$$I^-_2 = \int_0^\infty x^2 F_-(x,t)\, dx ,$$

$$I^-_4 = \int_0^\infty x^4 F_-(x,t)\, dx .$$

The quantity $F_-(x,t)$ is the electron-distribution function. The Fokker-Planck equation for F_- is given in the preceding report.[3] The integral I^-_2 is proportional to the number of particles and is a constant, so $I^-_4(t)$ is then proportional to the mean electron energy. In the case presented the initial electron distribution function was Maxwellian with mean energy 10 ev. This determines v_0 by Eq. (1). The ions are assumed to be all at the same speed, taken to be v_0. This corresponds to a deuteron energy of about 20 kev, given by

---

[1] Warren Heckrotte and John Killeen, The Slowing Down of Fast Ions in a Plasma, in Controlled Thermonuclear Research Quarterly Report, UCRL-8887, Sept. 1959, p. 86.

[2] Warren Heckrotte and John Killeen, The Heating Up of Electrons in a Plasma, in Controlled Thermonuclear Research Quarterly Report, UCRL-9002, Dec. 1959, p. 80.

[3] Warren Heckrotte and John Killeen, Energy Transfer from Hot Ions to Cold Electrons in a Plasma, in Controlled Thermonuclear Research Quarterly Report, UCRL-9106, March 1960, p. 68.

$$E_+ = \frac{1}{2} M v_0^2 . \tag{2}$$

We can compare the energy gain $I^-_4(\tau)$ from the numerical solution to the gain calculated by using the energy-transfer rates given by Lyman Spitzer.[4] From Spitzer we have

$$\frac{dE_-}{dt} = \frac{1}{\sqrt{2M E_+}} \; 4 \pi e^4 n_- \ln \Lambda \left[1 + \frac{M}{m} \right] \left[\phi(x) - x\phi'(x) \right] ,$$

where

$$x = \frac{3}{2} \sqrt{\frac{m}{M} \frac{E_+}{E_-}}$$

and

$$\phi(x) = \frac{2}{\sqrt{\pi}} \int_0^x e^{-y^2} dy .$$

Let

$$\tau = \frac{\Gamma_e}{2} \frac{n_-}{I^-_2 V_0^3} t , \tag{3}$$

where

$$\Gamma_e = \frac{4 \pi e^4 \ln \Lambda}{m^2} .$$

Now, using Eqs. (1), (2), (3), we find the energy gain given by Spitzer is

$$\frac{dI^-_4}{d\tau} = 4 (I^-_2)^2 \left[\frac{m}{M} + 1 \right] \left[\phi(x) - x\phi'(x) \right] ,$$

and

$$x = \sqrt{\frac{3}{2} \frac{I^-_2}{I^-_4}} .$$

---

[4] Lyman Spitzer, Physics of Fully Ionized Gases (Interscience Publishers Inc., New York, 1956), p. 79.

We can then calculate

$$\tau(I^-_4) = \int_{I^-_4(0)}^{I^-_4} \frac{dI_4}{\left(\frac{dI_4}{d\tau}\right)}$$

The $I^-_4(\tau)$ calculated, as above, is compared to the $I^-_4(\tau)$ from the numerical solution in Fig. 26.

As in the case presented previously,[3] the time required for the electrons to reach 1 kev differs considerably for the two calculations. (An electron energy of 1 kev corresponds to an I^-_4 that has increased by a factor of 10^2 over its initial value.)

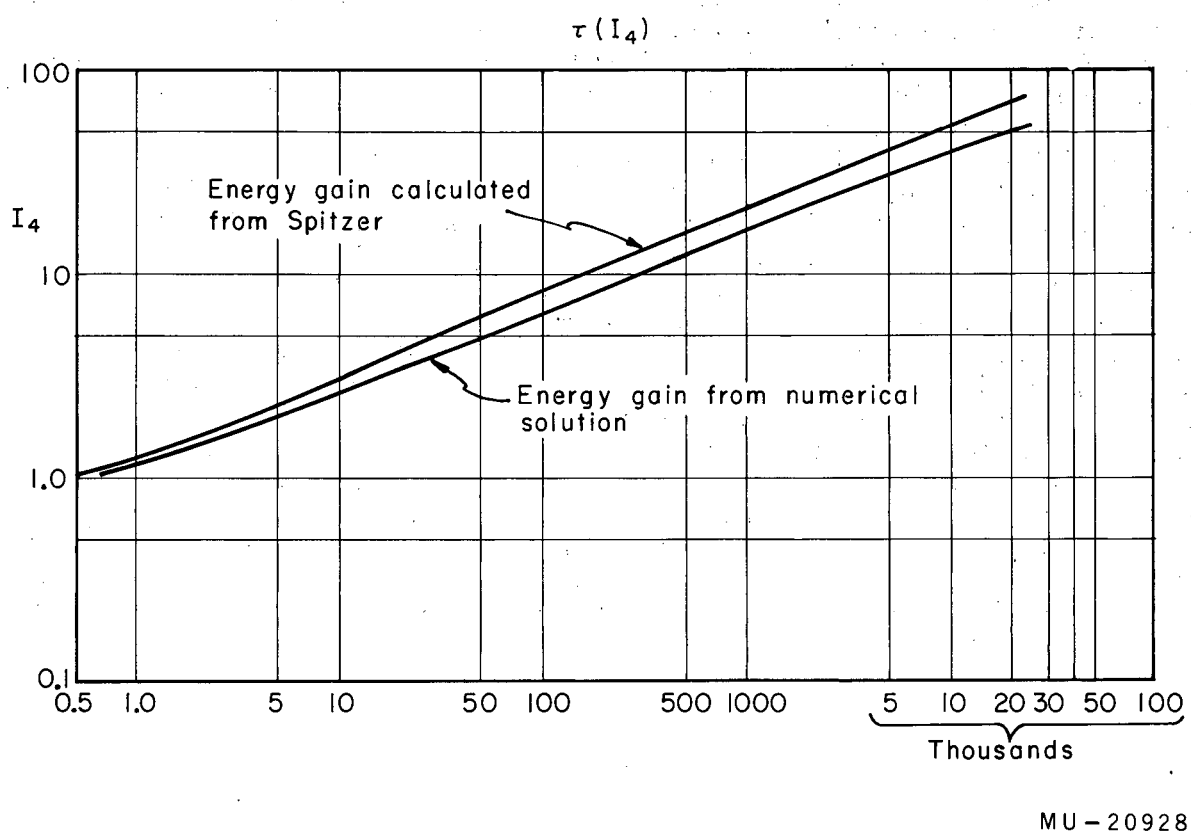

Fig. 33. Average electron energy as a function of time.

2. DENSITIES OF ELECTRONS TRAPPED BY THE GEOMAGNETIC FIELD

John Killeen

Given an arbitrary source distribution n_0 (r, θ, ϕ) in particles/cm^3/sec, it is desirable to know the trapped-particle density along the earth's field lines. An IBM 709 code called APPLE has been completed which calculates the trapped-particle density and also the density of turning points. The earth's magnetic field is taken to be a dipole, so that the coordinates for n_0 are the distance from the dipole center, the geomagnetic colatitude, and the geomagnetic longitude. From the given source distribution a source density along field lines n_0 (θ_0, θ, ϕ) is calculated, where θ_0 specifies the field line. The density of mirror points along field lines resulting from the source n_0 is then calculated, with the assumptions that the injected electron velocities are isotropically distributed, and that the magnetic moment is a constant of the motion. From this injection mirror-point density an equilibrium mirror-point density is calculated by including losses due to atmospheric scattering. From this density the trapped-particle density along a field line is calculated. The code has been used to compute the contribution to the Van Allen radiation belt of electrons resulting from decay of neutrons leaking out of the earth's atmosphere. The neutrons come from cosmic rays entering the atmosphere. The neutron decay source is known[1] at all points in space, and from this source the electron source $n_0(\theta_0, \theta, \phi)$ has been computed. The details of these calculations will be published in the Physical Review.

[1] W. N. Hess, E. H. Canfield, and R. E. Lingenfelter, Cosmic-Ray Neutron Demography, UCRL-5899, March 1960.

3. END LOSSES IN MIRROR MACHINES

John E. Roberts and Marlene Carr

A report of this title by these authors has been issued (UCRL-5651, April 1960). This report collects, summarizes, and extends previously reported work[1] on this subject. This work utilizes the method of the Fokker-Planck equation to treat ion-ion collisions which lead to the scattering of ions into the loss cone of the mirror machine. This report discusses in detail the theoretical aspects of the method and the numerical techniques used to obtain solutions. An extensive collection of numerical results is presented. These include speed and angular distributions of ions as a function of time, starting from assumed initial distributions; loss rates of ions in a mirror geometry; equilibrium distributions for the steady-state injection of ions into the mirror geometry; and d-d, d-t, and charge-exchange reaction rates for the resulting velocity distributions.

---

[1] A. Garren, R. Riddell, L. Smith, G. Bing, J. E. Roberts, T. G. Northrop, and L. Henrich, Individual Particle Motion and the Effect of Scattering in an Axially Symmetric Magnetic Field, in Proceedings of the Second International Conference on the Peaceful Uses of Atomic Energy, Geneva, 1958 (United Nations, Geneva, 1958). (Other references will be found in this report).

4. THE MAGNETIC MIRROR INSTABILITY

William A. Newcomb

I am now preparing a series of papers on the transverse adiabatic (TA) stability theory. This theory deals with the stability of a collisionless plasma in a strong magnetic field, allowing for the possibility of a nonisotropic pressure tensor. It is based on the Boltzmann equation and leads to an energy principle analogous to, but more complicated than, the well-known hydromagnetic energy principle.[1]

I have applied the TA energy principle to a number of special cases, including the linear pinch and the Taylor instability of a plasma supported against gravity by a magnetic field. An especially interesting application is the "magnetic mirror" instability of a plasma with its particle velocity distribution concentrated in the direction perpendicular to the field. This instability comes about as follows: Suppose that a magnetic flux tube is perturbed by the formation of a constriction somewhere along its length. The constriction will act as a magnetic mirror, tending to exclude the particles with velocities directed at large angles to the field. The result, since the velocity distribution is peaked for such particles, will be a decrease in the plasma pressure at the constriction, which under the proper conditions will be greater than the increase in magnetic pressure. Thus the perturbation produces a negative restoring force, which in turn causes the perturbation to grow. In other words, the field and the plasma together form a medium in which compression gives rise to a drop in pressure; such a medium is necessarily unstable.

The conditions under which the magnetic mirror instability appears have been given by Rosenbluth for the special case of a double Maxwellian velocity distribution,[2] and I, using the TA energy principle, have derived the corresponding conditions for a completely general distribution. Qualitatively, we can see from the physical argument given above what these conditions must be. First, the angular distribution of particle velocities must be peaked in the direction perpendicular to the field, and second, for any given angular distribution there is a critical value of P/B^2 above which the instability sets in. This imposes an upper limit on the plasma pressure attainable in a mirror machine.

Now consider a wavelike perturbation consisting of a series of constrictions and bulges along the flux tube. The stability condition is independent of the distance between constrictions, and the TA theory is valid for distances down to the ion Larmor radius. We can therefore expect a small-scale turbulence to develop in any region of the plasma where the stability condition is violated. This turbulence will give rise to enhanced diffusion, which can easily be observed. Post has made use of our stability condition to calculate the critical value of P/B^2 in a mirror machine,[3] and he has conducted an experimental investigation of the enhanced diffusion, obtaining results in agreement with the theory.

---

[1] I. B. Bernstein, E. A. Frieman, M. D. Kruskal, and R. M. Kulsrud, Proc. Roy. Soc. A 244, 17 (1958).

[2] M. N. Rosenbluth, in Proceedings of the Second United Nations International Conference on the Peaceful Uses of Atomic Energy, Geneva, 1958 (United Nations, Geneva, 1958), Vol. 31, p. 89.

[3] R. F. Post, Pyrotron (Mirror Machine) Program, this report, p. 11.

5. STABILITY CALCULATION FOR A DIFFUSE LINEAR PINCH

Don G. Geesaman

The hydromagnetic stability of a particular class of field configurations was investigated by a numerical calculation. The criterion used was derived by William A. Newcomb[1] and involved the zeros in a solution of an Euler-Lagrange equation. A maximal force configuration was considered, i.e.,

$$r\,B_\theta = \lambda\,B_z\,;$$

and the pressure gradient was represented as

$$\frac{dP}{dr} = \begin{cases} A & \text{for } 1/4 < r < 1 \\ -\dfrac{\ell}{2r}\left(\dfrac{r^2+\lambda^2}{1+\lambda^2}\right)^{\frac{\ell}{2}} & \text{for } 1 < r < 10 \end{cases}$$

where $A > 0$, $0 < \ell \leqslant 1$, and $0 < \lambda < \infty$. The system was completely specified by these three field parameters.

It was sufficient to examine the stability of the system against displacements characterized by the displacement parameter values of $m = 1$, $-\infty < k < +\infty$. Values of k were further limited to the interval $-16\,\lambda \leqslant k \leqslant -\frac{\lambda}{100}$, since the feeling was that the most malicious instabilities were connected with those displacements having associated singularities of the Euler-Lagrange equation within the interval $1/4 < r < 10$. Solutions of the Euler-Lagrange equations were examined for a representative spectrum of k values. The technique was to make a Frobenius expansion of the "small solution".[1] This was then employed to start the numerical calculation in the neighborhood of the singularity.

Early work was discouraging in that the time required to calculate out of the vicinity of the singular point was prohibitively long. Since the solution had an approximate dependence of $\xi = x^{-m}$ in this neighborhood, it was hoped that the transformation $\psi = x^m \xi$ would relieve the difficulty. Instead the cumulative effect of the six additional terms introduced into the Euler-Lagrange equation was to slow computation further. Fortunately, some rather minor changes in the coding of the problem led to a considerable shortening of machine time.

At present it is possible to discuss the instabilities of particular configurations; however, the results are not complete enough to warrant conclusions about the relation of complete stability to the values of the field parameters.

[1] William A. Newcomb, Hydromagnetic Stability of a Diffuse Linear Pinch, UCRL-5447, Aug. 1959. (Where appropriate the notation and definitions are the same as in that report.)

6. MAGNETIC SHOCKS

S. A. Zwick

In certain cases it is possible to obtain exact solutions for the magnetic behavior of a collision-free plasma. Two examples are outlined below.

(a) The One-Dimensional Steady-State Configuration

To investigate possible configurations before the arrival of a shock, we consider a neutral plasma composed of plus and minus ions of equal mass in a uniform applied magnetic field. Plasma currents affect the induction field present, so that there is a self-consistency problem to be solved.

Distributions of the particle velocity and the magnitude of the induction field are assumed to vary only with the coordinate x, transverse to the field direction z. In a reference frame at rest in the plasma, no electric induction exists in steady state. The ratio $\beta = B/B_0$ of the actual to the imposed magnetic field, and the total particle density n, may then be expressed as functions of x in the parametric form

$$\beta^2 = 1 - 4\lambda \int_0^\infty w^3\, dw \int_{-\pi/2}^{\pi/2} \cos^2\theta\, f(w, w \sin\theta - \psi)\, d\theta,$$

$$n = 4 \int_0^\infty w\, dw \int_{-\pi/2}^{\pi/2} f(w, w \sin\theta - \psi)\, d\theta, \quad \omega_0 x = \int_0^\psi \frac{1}{\beta}\, d\psi;$$

in which $\lambda = 8\pi m/B_0^2$, $\omega_0 = (-q\, B_0)/mc$.

In the integrals, $f(w, p)$ denotes the effective velocity distribution of the positive ions (mass m, charge q) at the plane $x = 0$, as a function of their speed w and velocity component p in the y direction.* The parameter ψ is a "stream function" for B.

The prototype distribution $f(w, p) = (N/4)\, \delta(w - v)\, \delta(p + \sigma)$ yields

$$\beta^2 = 1 - (N\lambda v^2)\left[1 - \left(\frac{\psi - \sigma}{v}\right)^2\right]^{1/2} \quad n = N\left[1 - \left(\frac{\psi - \sigma}{v}\right)^2\right]^{1/2}$$

over $\sigma - v < \psi < \sigma + v$, and $\beta^2 = 1$, $n = 0$ outside this range in ψ. The value of x is given by an elliptic integral, which is finite for $N\lambda v^2 < 1$. This steady-state solution represents a plasma in which each particle travels in a fixed symmetric loop oriented normal to the magnetic field. The centers of the loops are uniformly distributed on the plane $\psi(x) = \sigma$.

*Here $|p|$ may be chosen greater than w. In this case f actually refers not to $x = 0$ but to points where $|p - \psi| < w$.

The significant feature of the steady-state solution lies in the circumstance that one can construct, ad lib, configurations in which an infinite plasma density exists in stable magnetic equilibrium adjoining a vacuum, say. Such a "stationary shock" is an evident impossibility in an ordinary gas, which suggests caution in the use of shock analogies.

(b) The Zero-Temperature Pulse

The simplest initial solution of the type discussed above consists of a uniform distribution of particles at rest (e.g., $f = (N/2\pi)\,\delta(w^2)$). In this instance the trajectory equations for a plus ion in a traveling magnetic "pulse" of field ratio $\beta = B/B_0$ (at the instantaneous particle location) can be integrated:

$$\frac{x-\xi}{R} = -\frac{a \sinh a\omega_0 (t + \xi/V)}{1 + \sqrt{1 + a^2} \cosh a\omega_0 (t + \xi/V)} ,$$

$$\frac{y-\eta}{R} = \frac{\sqrt{1 + a^2} + \cosh a\omega_0 (t + \xi/V)}{1 + \sqrt{1 + a^2} \cosh a\omega_0 (t + \xi/V)} ,$$

$$1 + \beta = 2\sqrt{1 + a^2}\left(\frac{y-\eta}{R}\right) ;$$

where

$$R = \sqrt{mc^2/N\pi q^2} , \quad a = \sqrt{\frac{1}{2} N \lambda V^2 - 1} ,$$

and $\lambda = 8\pi m/B_0^2$, $\omega_0 = (-q B_0/mc)$ as above. Particle motion starts infinitely slowly at $t = -\infty$ where $\beta = 1$, builds up and then subsides again as $t \to +\infty$. Since $(x - \xi)^2 + (y - \eta)^2 = R^2$, the path is a segment of a circle of radius R, centered at (ξ, η); each plus ion undergoes a net displacement $\Delta x = -2aR/\sqrt{1 + a^2}$ around its circle during the disturbance. One notes that, inasmuch as a particle with circle centered at ξ reaches a given angular position at a time ξ/V ahead of the particle with circle centered at $x = 0$, the disturbance as a whole moves to the left with velocity V.

A mechanical counterpart to the zero-temperature pulse may be constructed of a number of cards (or dominoes) placed on end along a line, each leaning against its neighbor to the right (say). The magnetic field may be imagined as coupling the ends of the cards by springs. To create the pulse, one simply pushes the last card over to the left; the value of $\beta + 1$ appropriate to each card is proportional to the height of its moving end. Within limits, the pulse speed may be chosen arbitrarily.

The solution (and its analogy) fails for $\alpha^2 > 3$, since then the fastest particles are required to move ahead of their neighbors during part of the pulse; such "crossovers" modify the field where they occur. An attempt is now being made, by numerical methods, to clarify this aspect of the high-speed pulse.

7. THE EFFECTS OF SPACE CHARGE ON THE SHAPE OF LAMINAR BEAMS

N. W. Hetherington and C. H. Woods

Considerable attention has been directed lately to phenomena associated with beams having infinite cross section. The two-stream instability is an example. However, there seems to be no adequate discussion in the literature of the shape of finite (circular) beams, particularly when space charge of opposite sign is present, and when the beam may be relativistic. For circular beams having uniform density of charge over the cross section, we have been able to express the beam shape in terms of the error function and a less familiar quadrature, which also has been tabulated.

The result depends sharply on the ratio α of neutralizing charge density to beam charge density. Specifically, for $\alpha < \gamma^{-2}$, where γ is the mass ratio of the beam particles, one finds the envelope of Fig. 27, which represents the classical situation in which a beam is "blowing up" or expanding. This result can be applied to both relativistic and nonrelativistic beams of particles having arbitrary sign of charge. On the other hand, for $\alpha < \gamma^{-2}$, the beam radius never exceeds the nominal value, and the beam becomes pinched at periodic intervals, as shown in Fig. 28. The quantity of opposite charge and the particle energy determine the characteristic "wave length" λ.

Further acceleration of a beam leads of course to a different shape for each value of accelerating field. This case involves two parameters instead of one, and requires machine calculations. A number of solutions have been obtained for values of the parameters that cover several situations of current interest. Both the analytic and machine calculations are reported in a separate paper[1] along with some numerical examples illustrating application of the results.

---

[1] C. H. Woods and N. R. Hetherington, The Effects of Space Charge and Relativity on the Shape of Charged-Particle Beams, UCRL-6010 (in preparation).

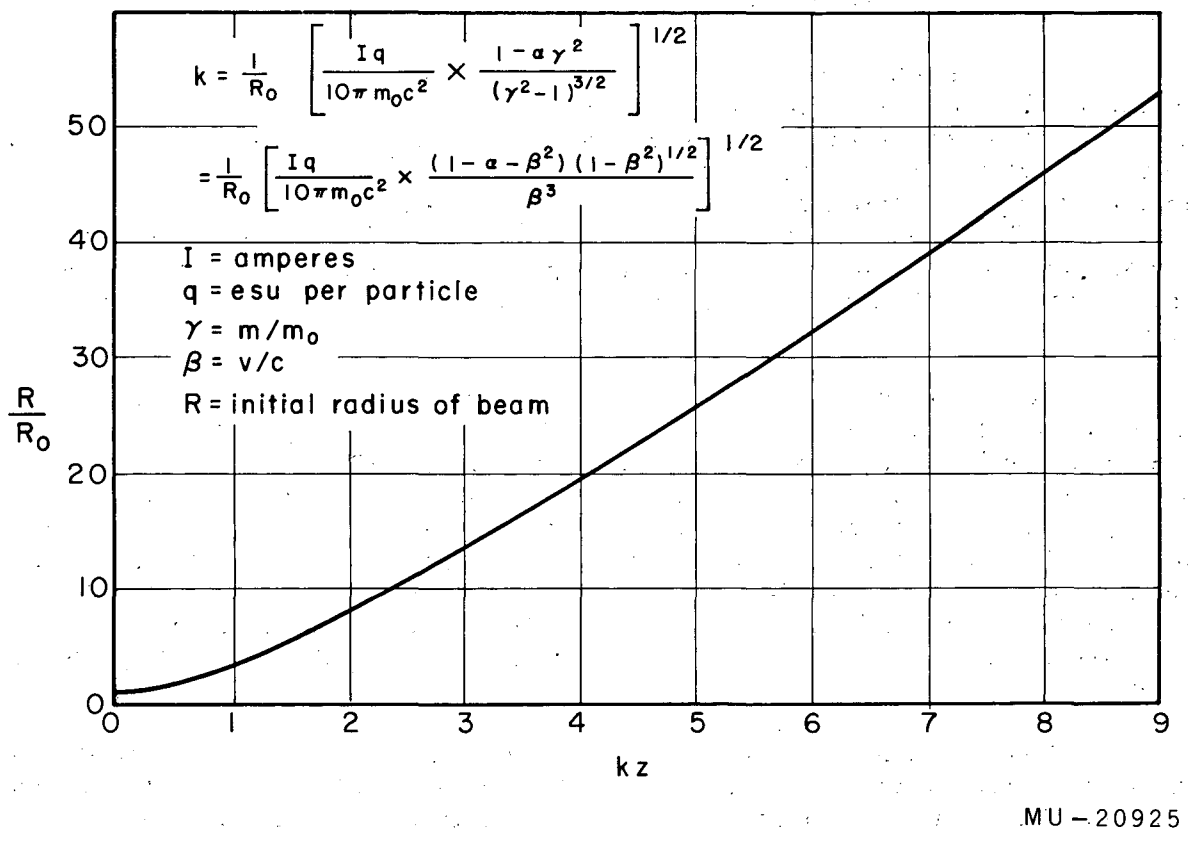

MU-20925

Fig. 34. Plot of beam radius for $\alpha < \gamma^{-2}$.

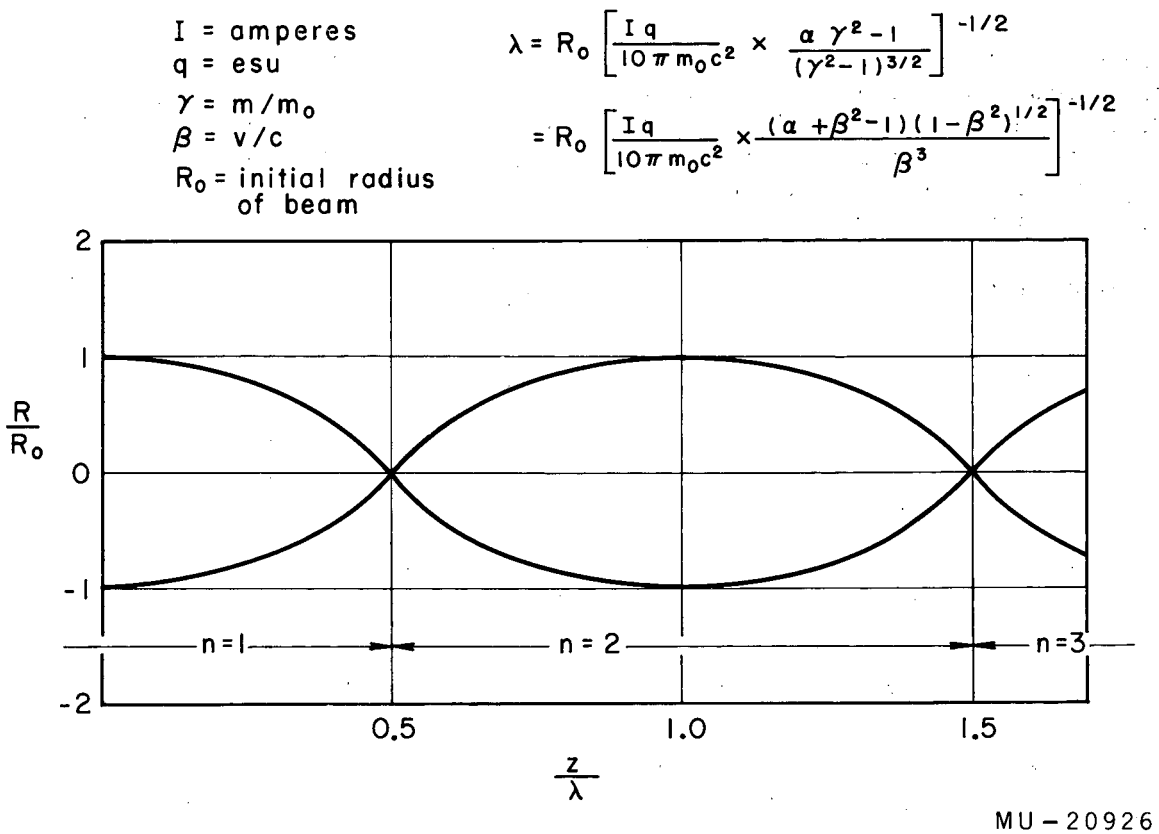

Fig. 35. Plot of beam boundary for $\alpha > \gamma^{-2}$.

8. ENERGY DEPENDENCE OF THE CRITICAL PRESSURE FOR NEUTRAL INJECTION

Gordon Gibson,* Willard C. Jordan,† and Eugene J. Lauer

The buildup of a high-energy plasma by the injection of neutral atoms into a mirror machine was analyzed previously,[1] and it was shown that if the pressure of neutral gas in the containment region is kept low enough (less than some critical pressure p_c), then the high-energy particles form a plasma of sufficient density to be of interest for study. This critical pressure depends on several parameters, some of which are functions of the energy of the incident neutral beam. A graph of the critical pressure vs the energy of the incident beam (obtained from the assumptions of Ref. 1) is presented, since there is an apparent conflict with the results of other work.[2]

The formula for the critical density[3] is

$$\rho_c = \left[\left(\frac{e/c}{2.4^2\pi}\right) \cdot \left(\frac{B}{Z}\right)\right] \frac{1}{W_0} \; j_0 \left(\frac{\sigma_t^i}{\sigma_c^n}\right) , \qquad (1)$$

where

- e is the ionic charge,
- c is the velocity of light,
- σ_t^i is the cross section for the ionization of an incident neutral atom on a trapped ion (cm^2),
- σ_c^n is the charge-exchange cross section for a trapped ion incident on a cold neutral particle (cm^2/atom),
- j_0 is the neutral beam current (atoms/sec),
- B is the magnetic field strength (gauss),
- W_0 is the energy of an incident neutral atom (ergs), and
- Z is the length of the plasma volume along the axis (cm).

For obtaining the results shown in Fig. 29, (B/Z) has been held constant (i.e., independent of energy or machine size), and set equal to 10^3 gauss/cm. This corresponds physically to the assumption that the current density (amp/cm^2) in the coils is held constant, and also that the relative dimensions (i.e., of the coils and their spacing) are held constant. This condition is chosen because Eq. (1) shows that the critical pressure increases proportionally to the field strength, and thus one wants the highest field feasible. However, the practical limitation is the rate of heat transfer, and this sets a limit on the current density.

*Westinghouse Electric Co.

†Bendix Corp.

[1] G. Gibson, W. A. S. Lamb, and E. J. Lauer, Phys. Rev. 114, 937 (1959).

[2] R. F. Post and C. C. Damm, Bull. Am. Phys. Soc. Series II, 5, No. 4, Abstr. DA3.

[3] May be obtained from the results of Ref. 1.

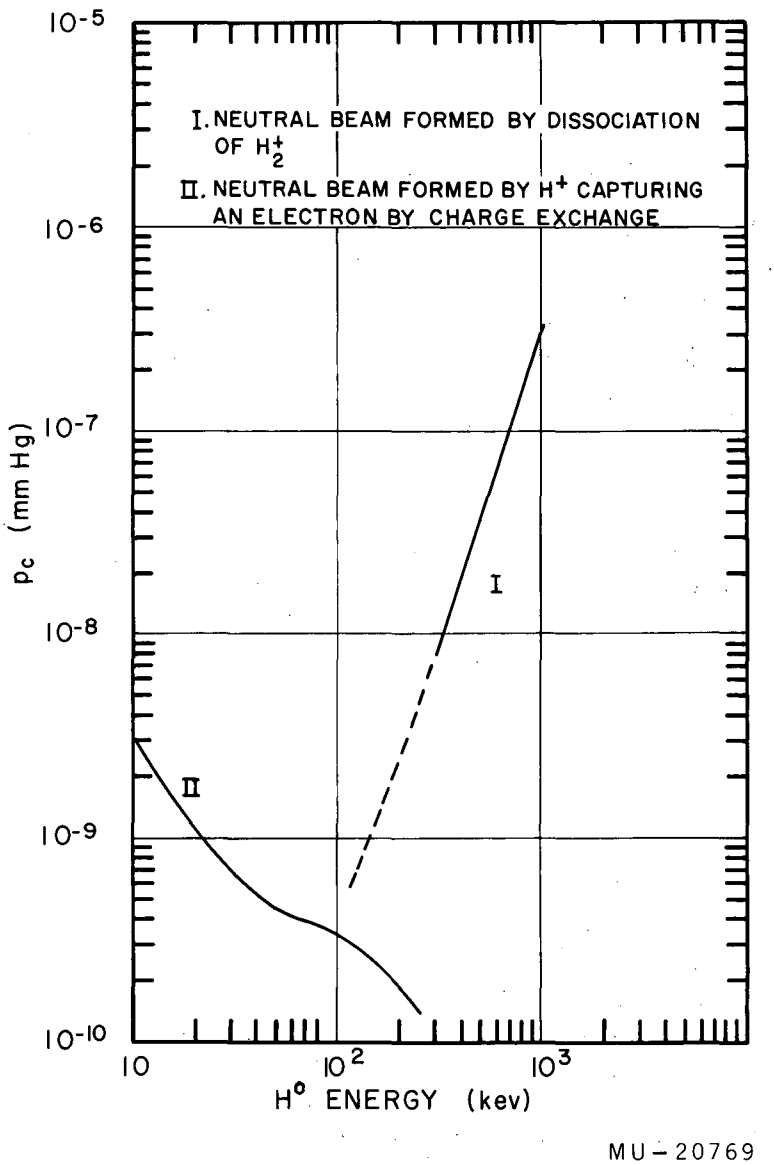

Fig. 36. Critical pressure of hydrogen gas vs hydrogen-beam atom energy.

As a result of this assumption we have

$$B \approx \frac{I}{a} \approx \frac{a^2}{a} = a ,$$

where I is the total ampere turns in a coil and a is the coil mean radius. Also $Z \sim a$. Hence B/Z = constant.

It can also be seen from Eq. (1) that the maximum beam, j_0, is desirable. One may speculate about the primary current obtainable as a function of energy; however, the useful portion of this is restricted to that which produces neutral beam atoms which pass through a region about two orbit radii wide near the axis where ρ_c is a maximum. Therefore in this calculation it is assumed that the maximum accelerated beam current, I_0, is independent of the energy of the beam and corresponds to 0.3 amp.

The neutral beam that can be obtained does depend on the energy. For energies less than 100 kev the neutral beam is formed by the charge-exchange process when a beam of protons is sent through a gas (e.g., hydrogen) target. As the particles pass through the neutralizer the protons become neutralized and the energetic neutral hydrogen atoms may be ionized, so that the neutral current produced at equilibrium is

$$j_0 = I_0 \frac{\sigma_c^{\,n}}{\sigma_c^{\,n} + \sigma_i^{\,n}} . \tag{2}$$

Here $\sigma_i^{\,n}$ is the cross section for the ionization of a neutral atom incident on a neutral target particle.

Curve 1 of Fig. 29 corresponds to this method of obtaining a neutral beam. The cross sections were obtained from published experimental data.[4, 5] As stated by Post and Damm,[2] the critical pressure does decrease with increasing energy. From Eqs. (1) and (2) it can be seen that even though the charge-exchange-loss cross section decreases rapidly with increasing energy the critical pressure at large energies is independent of this cross section, since the neutral beam is formed by this same process. However, the neutral beam may be produced in a more efficient manner at high energies.[1] Hydrogen molecular ions are sent through a gas target. Collisions result that leave the molecular ion in an excited unstable state from which it dissociates. This is unlike the other scheme in that there is an optimum area density[6] for the neutralizer because the incident beam is attenuated by ionization. For neutral-hydrogen-atom energies greater than 300 kev the charge-exchange cross section is small and may be neglected when compared with the ionization or breakup cross sections. The maximum neutral beam that may be produced is

$$j_0 = I_0 \, XY^{\frac{1}{1-Y}} , \quad Y \neq 1, \tag{3}$$

[4] C. F. Barnett and H. K. Reynolds, Phys. Rev. 109, 355 (1958).
[5] R. Curran, T. M. Donahue, and W. H. Kasner, Phys. Rev. 114, 490 (1959).
[6] G. Gibson and E. J. Lauer, "Production of a High-Energy Neutral H or D Beam", UCRL-4646, January 1956.

where I_0 is the incident H_2^+ current,

$$X = \frac{\sigma_{BU}}{\sigma_i^n} ,$$

and

$$Y = \frac{\sigma_i^n}{\sigma_{BU} + \sigma_{i_2}^n} ,$$

where σ_{BU} is the cross section for the breakup of the molecular ion which results in a neutral atom,

$\sigma_{i_2}^n$ is the cross section for the ionization of a molecular ion incident on a neutral particle.

For W_0 = 400 kev, j_0/I_0 = 0.21, as determined from published experimental cross sections.[4,7] For obtaining Curve 2 of Fig. 29, this fraction was assumed independent of energy, since the cross sections are expected to have the same energy dependence. For energies less than 300 kev, the curve is dashed to indicate that it is not justified to neglect the formation of neutral beam by charge exchange. Curve 2 rises approximately as W_0^{-3}. The curve would have the same shape for the case of "injecting" by H_2^+ breakup in the plasma without converting to H^0.

[7] D. R. Sweetman, Phys. Rev. Letters 3, 425 (1959).

9. THEORY OF SCATTERING OF CHARGED PARTICLES BY ATOMS

Marvin H. Mittleman

The problem of electron scattering from atoms as presented in four previously issued reports[1] is still being pursued in cooperation with Professor Kenneth M. Watson. The integro-differential equation resulting from this theory is being coded for the 704. A method due to Gamel is being used. Difficulties in the operation of the code are now being dealt with.

The proton-hydrogen scattering problem has been studied by an impact-parameter method. The equations have been rigorously derived and applied to the high-energy excitation scattering and the charge-exchange scattering.[2] The results are probably better than previous calculations. The low- and intermediate-energy scatterings are now being investigated.

Similar techniques are now being used to investigate charge exchange in the proton-plus-atom system. There are some additional difficulties here due to action of the Pauli principle among the electrons.

---

[1] Marvin H. Mittleman, The Scattering of Electrons by Atomic Hydrogen (UCRL-5711, Dec. 1959), submitted for publication in Proceedings of the Royal Society (London);

Marvin H. Mittleman and Kenneth M. Watson, Effects of the Pauli Principle on the Scattering of Electrons by Atoms at High Energies, (UCRL-8976, Nov. 1959), submitted to Annals of Physics;

Bernard A. Lippmann, Marvin H. Mittleman, and Kenneth M. Watson, The Scattering of Electrons by Neutral Atoms (UCRL-8774, June 1959), Phys. Rev. 116, 920 (1959);

Marvin H. Mittleman and Kenneth M. Watson, Phys. Rev. 113, 198 (1959).

[2] Marvin H. Mittleman, The Proton-Hydrogen Scattering, UCRL-5941. (To be published.)

10. ATOMIC AND MOLECULAR BEAM RESEARCH

Gilbert O. Brink

The crossed-beam machine has been essentially completed and is undergoing final vacuum tests. A large liquid nitrogen trap has been installed and it has been possible to obtain a vacuum of 5×10^{-8}mm of Hg. Refrigeration of the cooling coils on the diffusion pumps did not help the vacuum or pumping speed.

The setup for the first experiment has been completed and installed in the machine. This will be an experiment to measure the relative cross section for the production of positive ions by electrons on H_2. Since this cross section is known it will be a good one for initial testing of the machine. The experiment will be described in detail in a future report.

An ion source is being constructed to provide proton beams for cross-section measurements. As soon as this source is completed it will be installed on the crossed-beam machine.

VI. ENGINEERING AND TECHNOLOGICAL DEVELOPMENT

1. ULTRAHIGH-VACUUM DEVELOPMENT

Norman Milleron and Leonard L. Levenson

Introduction

Pursuing our goal[1] of optimizing diffusion pump systems, we worked on:

(a) reducing oil backstreaming without sacrificing pumping speed,
(b) conductance measurements,
(c) isolation properties of activated alumina traps,
(d) leak valves and motion seals.

Oil Backstreaming

Ordinarily, significant amounts of oil cannot penetrate upward through the top jet of a diffusion pump. However, in the PMC 720, made by CVC, oil from the second jet reflects from the top of the third jet and penetrates upward through both second and first jets. This source of oil backstreaming was observed and corrected by increasing the distance between jets and by making the top jet stream more dense.

Backstreaming originating in the diffusion pump boiler was found during studies of backstreaming with the NRC H-10-P using Narcoil-40 fluid. This source of backstreaming was eliminated by packing aluminum foil between the jet assembly and the pump wall just below the diffusion pump foreline.

Considerable effort was applied to setting up a pumping-speed apparatus so that backstreaming and pumping speed could be considered together. The first pump to be tested will be the NRC H-10-P.

Conductance Measurements

An attempt was made to confirm the dependence of molecular-flow conductance on the square root of the molecular weight of the diffusing gas. The gas chosen was CCl_2F_2 (Freon-12) because it can be cryo-pumped at liquid nitrogen temperature. However, after calibration data had been obtained with Freon-12, one ionization-gauge filament (iridium) broke and another gauge filament was badly corroded. This damage occurred in approximately 10 hours of operation with Freon-12 at ion gauge readings ranging between 5×10^{-5} and 3×10^{-4} mm Hg. Previous conductance runs with CO_2 totaling approximately 100 hours of operation at similar pressures produced no noticeable damage to the gauge filaments, although the other elements became blackened. The use of Freon-12 for the conductance runs has been abandoned.

---

[1] Norman Milleron and Leonard L. Levenson, in Controlled Thermonuclear Research Quarterly Report, UCRL-9002, Dec. 1959, p. 115.

New equipment is being built for conductance measurements. This new equipment was designed with use of conductance data from previous runs. It will permit eight models to be run consecutively without breaking the vacuum.

Isolation Properties of Activated Alumina Traps

An ultravacuum system can be directly connected to a dirty system by utilizing the isolation properties of activated alumina. An unbaked, baffled, rubber-gasketed oil diffusion pump, covered by a Plexiglas plate and operating at 5×10^{-7} mm Hg gauge reading, was isolated from an ion gauge through an alumina trap. Baking out and cooling the trap to room temperature yielded a pressure of 2×10^{-9} mm Hg in the isolated gauge. Cooling the alumina to liquid nitrogen temperature yielded a pressure less than the x-ray limit of the gauge, i.e., $< 1\times10^{-10}$ mm Hg.

Leak Valve

A bakable leak valve, adjustable from 10^{2} to 10^{-10} (NTP) cc of helium per sec, was built of 1/16-in.-i.d. copper tubing. A 3-in. section of tubing is squeezed closed or open with precise control by two interlocking jaws which apply force in orthogonal directions. After several cycles, annealing is necessary. A 1-in. section of 7/16-in. i.d. copper tubing was also closed to a conductance of $< 10^{-10}$ (NTP) cc/sec of helium.

Motion Seals

The small alumina trap, mentioned above, isolated a rubber O-ring shaft seal from ultravacuum. No pressure pips were detected through the trap at pressures $< 1\times10^{-10}$ mm Hg when the 3/8-in. o.d. shaft was rotatably translated. The shaft is lubricated with Octoil-S and sealed with two Hycar O rings. The space between the O rings is pumped. The oil lubricates the shaft and the Hycar O rings and acts as a surface-tension liquid seal against the guard vacuum. When the shaft is moved into the vacuum, gas adsorbed on the oil surface is wiped off by the first O ring. Gas that penetrates the first O ring is held out by the surface tension of the oil around the second O ring. Beyond the second O ring, the alumina trap takes up any oil vapor that originates from the seal.

2. MECHANICAL ENGINEERING DEVELOPMENT

Thomas H. Batzer

Beta-Ray Experiment

J. Ralph Ullman

Work has been under way since the last machine run in April to change the experimental apparatus in preparation for a a second phase of the fast-emptying experiment. These machine changes will permit

(a) extension of the search within the axially symmetric machine to larger ratios of orbit diameter to coil diameter,

(b) a check of the predictions of adiabatic theory with the coil axes tilted, and

(c) investigation of the containment properties of the cusp geometry. Measured orbit diameters will be compared with predicted orbit diameters. Changes made in the apparatus include replacing the 60-in. (mean diameter) Waldo coils with 30-in. (mean diameter) modular coil assemblies. In addition, the 20-in.-diam main vacuum vessel has been shortened in place, and a new section having a major diameter of 44 in. added. The coil-support rails were also extended 4 feet to accommodate the longer vacuum-vessel counter assembly. These changes are being concluded and the apparatus will be ready for the scheduled machine run beginning May 26. Initial measurements will be made with the central field of 1.3 kG and a mirror ratio of 1.8.

Installation of automatic trap fillers plus differential pumping on several leaks has lowered the system base pressure to 7×10^{-9} mm Hg (unbaked) in the volume between the two-bounce liquid nitrogen trap and the 20-in. fast-opening valve gate.

Hard-Core Torus

Raymond E. Keyes

A taping machine designed to wrap large toroidal shapes is in fabrication. It will be used in the assembly of the hard-core torus (Levitron).

Toy Top

John R. Benapfl

The 10-in. mercury pumping units used on the Source Test assembly and on the previous Toy Top machine have not been satisfactory, having low pumping speed and poor base pressure. Tests on a unit produced the rather low speeds of 300 to 400 liters per second for air, with a system base pressure greater than 5×10^{-6} mm Hg.

Modifications were made on a Source Test assembly unit. The modifications included removing the high-impedance Freon baffle and increasing the conductance of the liquid nitrogen baffle by removing one set of louvers, changing the "Z" array to a "V" array. Further, the cooling tubing on the upper 8 in. of the diffusion pump barrel was modified to allow it to be refrigerated. Subsequent tests indicated that the pumping speed was now 500 to 700 liters per second and the base pressure lower by a factor of 10.

Replacing the liquid nitrogen baffle by a type recommended by Bob Jobson increased the speed to 800 liters per second. As a result of these modifications and tests all the 10-in. pumping systems are being similarly modified.

Table Top

James F. Ryan

The mechanical crowbar relief switch is undergoing alterations, which include the addition of a saturable reactor and a light-beam safety interlock to the contact chamber. The saturable reactor is being installed to reduce contact erosion, and the interlock will prevent the bank from charging if the contact cylinder has not returned to open position. This protects against shorts across the contacts. The previous arrangement used only a switch that verified that the drive piston had returned to the open position.

Low-Energy Neutral Beam Experiment

William S. Neef, Jr., Eugene T. Bradley, and J. Ralph Ullman

Installation of the liquid nitrogen supply system for the Alice area in Bldg. 180 was completed. Miscellaneous support structure and vacuum plumbing are being installed as the parts come in.

A first attempt was made at vacuum-potting a coil section. The leak rate into the fixture was too high, not allowing sufficient time for complete penetration of the resin into the interior of the coil. The fixture is being reworked to permit the resin unrestricted access to all external coil surfaces and to improve the vacuum seals.

Thyrite will be used with the mirror coils to absorb some of the stored energy at the end of a pulse. An analysis indicated that cooling of these elements from peak temperatures of approximately 194°F to the initial state of 68°F would be difficult to achieve at the desired test frequency of one pulse per 3 minutes, using forced air as a cooling medium. The volume of air required, the amount of noise associated with the cooling fans, and the appreciable temperature rise of the environment adjacent to these resistors are the major objections to this type of cooling.

From the results of plotted computer data, a final choice of rectangular coil design for the source was made. These coils are about half complete. The other parts of the source vacuum chamber and support frame are about 80% complete. About half the parts for the electrical components of the beam source are designed and have been released for fabrication. Some layout work remains for the mechanism that positions the accelerating electrode.

The beam tube is being mocked-up to check its vacuum characteristics. A liquid-nitrogen-cooled evaporator tank is to be used as a dummy reaction chamber for this experiment. A new 4-in. elbow trap has been designed for beam-tube pumping, using a tube for liquid nitrogen circulation instead of the usual pot. The trap will be much simpler to fabricate, leak-hunt, and repair with no sacrifice in effectiveness. The tube will have a 4-in. bakable valve in it which has been modified in accordance with test information obtained from a 10-in. valve of identical design. New parts for this valve are now being fabricated.

The beam neutralizer in the Baby Alice experiment developed a leak due to local overheating. Previous troubles in repairing leaks in this neutralizer resulted in a new neutralizer design using the circulation-tube principle, rather than a welded and soldered liquid nitrogen pot. It was built, and is operating very satisfactorily.

The results of development work to date on the bakable vacuum seal look very promising. After completing nine successful bakeout cycles (no failures) with the differentially pumped double-pinch gasket,* using both 90-10 cupro-nickel gaskets annealed to Rockwell B-15 to B-16 and electrolytic tough pitch copper unannealed, we modified one of the titanium evaporator tanks to receive a double-pinch gasket to test a larger gasket. One flange of the evaporator tank (Dwg. No. 7HL4044A) was remachined to a double

*Refer to Fig. 42, in Controlled Thermonuclear Research Quarterly Report, UCRL-9002, Dec. 1959, p. 127.

pinch, along with a companion blind flange for use with the existing C clamps. The 90-10 copper-nickel gaskets, 16-1/8 in. o.d. and 0.050 in. thick, were fabricated and annealed in a hydrogen atmosphere to a hardness of Rockwell B-16. A single-pinch gasket was used on the opposite end of the evaporator tank and on the 6-in. side port.

This test apparatus was baked out successfully four times to temperatures between 350°C and 400°C. The heaters were arranged to heat the double pinch to 400°C and the single pinch to less than 325°C. The ultimate vacuum attained was 2×10^{-9} mm Hg. Pressure bursts with a repetition period of approximately 2 min were observed when the system pressure got into the range 10^{-8} mm Hg. On the assumption that these bursts were caused by diffusion pump oil dropping from the water baffle onto the hot jets of the diffusion pump, a refrigeration unit was connected to the water baffle and the temperature of the baffle was reduced to 0°C. This made the bursts less frequent, but did not stop them. Liquid nitrogen was then circulated through the water baffle, stopping the pressure bursts completely, indicating that the original assumption was probably correct. However, this is not a remedy, since all the pump oil would eventually collect on the baffle.

A 16-in. o.d. double-pinch gasket of unannealed electrolytic tough pitch copper was then substituted and baked out three times successfully, but pressure bursts prevented holding ultrahigh vacuum for more than several hours. However, a vacuum of 7.8×10^{-10} mm Hg was achieved.

In an attempt to prevent the pressure bursts, drip shields of stainless steel were installed on the jet assembly of the diffusion pump along with drip wires to prevent oil from dropping from the water baffle onto the hot jets. This reduced the repetition rate of the bursts but did not stop them.

A commercial seal manufactured by Cadillac Gage Co. was tested with no success. The seal and flanges were taken by Cadillac personnel for further tests by them.

The down time for the move from Bldg. 124 to Bldg. 180, is being utilized also for a change-over from the large Mopu tank end flange to a double-pinch array. A bakable 3-in.-diam aperture valve has been designed for Mopu and is being detailed. It incorporates the Marmon Conoseal as the valve seat. The application requires only fairly low conductance in the closed position, since the pressure differential is small, say 10^{-7} mm Hg, rahter than 10^{-10} mm Hg. Closing forces for the Marmon seal are less than 300 lb per linear inch, which compares very closely to rubber gasket joints.

Atomic and Molecular Beam Research

Alfred R. Taylor

All the equipment for the original cross-section-measuring system has been received and installed. Pumping speed and base-pressure measurements have been made on the trapping section and it has been found unsatisfactory. A pressure of about 10^{-8} mm Hg is now desired during operation rather than the 10^{-7} mm Hg originally specified. In order to achieve this limiting pressure the Edwards vacuum valves have been replaced with Temescal valves to increase the system pumping speed. New refrigerated baffles have been designed and fabricated to fit the Edwards diffusion pumps. An aluminum extension tank and flange have been designed, and are in production, to house an 18-filament molybdenum evaporator to fit on the end of the trapping chamber. A pressure of 5×10^{-8} mm Hg has been reached in the trapping chamber by using a liquid nitrogen trap and a temporary molybdenum evaporator.

Astron

Charles A. Hurley, James F. Ryan, James E. Blades, David C. Holten, and Edward G. Scarlett

The over-all mechanical design of the 720-kv electron gun is approximately 95% complete. The status of fabrication is as listed:

1. Pressure vessel and covers are being built by Berkeley Steel for $9,650. Approximately 90% complete.

2. Cathode Test

   a. Two complete 10-in. cathodes were delivered by Semicon Co. for $5,720.

   b. All the necessary equipment for testing the cathode has been fabricated and assembled.

   c. One cathode was tested successfully except for the heater design. The ceramic support had too much entrapped gas and the proper operating pressure and temperature were very difficult to reach. The heater has been redesigned and will be tested.

3. Fabrication of the 12-in.-diameter soldered ceramic accelerating column is approximately 25% complete. Coors Porcelain Co. was the only bidder for two units at $18,968.

4. The accelerating column which is to be built up, using O rings, is approximately 25% fabricated. The ceramic is being fabricated by Coors for $2,321.

5. The components necessary to complete the accelerating column are approximately 50% complete. Humboldt Instrument Co. was low bidder at $6,210.

6. The jigs, fixtures, and handling equipment for core and column assemblies have been released for bid.

7. The core stack support structure and secondary sheets are approximately 40% complete. Low bidder was Nor-Cal Metal at $3,995.

8. The plate which contains the 90 feed-through insulators for core-pulsing leads has been released for bid.

9. The Freon gas cooling apparatus has been released for bid. This includes a heat exchanger, blower, motor, and stand.

10. Equipment for testing a duplicate section of the core assembly (three cores) has been designed and fabricated for $2,000. These parts are awaiting the delivery of the cores.

Design has begun on the building modifications and construction requirements in Bldg. 157 for the 5-Mev Astron facility.

A cost-and-time estimate shows a completion date of Oct. 15, 1960 and total cost of $106,524.

Listed are the necessary changes.

1. Dismantling of north wall and part of east wall.

2. New footing for wall running north-south.

3. Fabrication of 27 new blocks and 25 plugs.

4. Restacking of north wall blocks, east wall blocks, and new blocks to form an L-shaped shielding.

5. Installation of Bldg. 124 crane.

6. Supply of steel support for existing crane.

7. Supply of steel support for electron gun and accelerator.

8. Installation of power for crane, lighting, etc.

9. Relocation of landing balcony on third-floor mezzanine.

Ceramic-metal column modules for the induction accelerator are being fabricated by Gladding-McBean and Company. Delivery is expected by June 30, 1960. Final design of the primary loops, secondary plates, supports, and air-cooling equipment is awaiting results of the core and tube tests being made by Electronics Engineering.

Job orders have been released for the E Layer and one resistor tank. Only the injection tank remains to be designed, and this awaits design parameters to be supplied by the physicists.

Design is complete on the main solenoid coils. A mandrel is being fabricated, and one coil will be made here to verify the process and specifications. The remainder will be purchased.

A detachable split-coil module has been designed and released for purchase. These coils will be installed over the flanged tank joints.

The outer coils are designed to provide flexibility in shaping the field. Any 6-in. (axial length) section can be powered separately if desired. Water cooling to handle up to 1900 amp (1560 gauss central field) is provided.

Engineering Notes ENA-105 and ENA-106 have been distributed, and give the electrical properties of the coils, and the power supplies, required for the next stage of Astron experiments.

Design is complete on the internal mirror coils and will be released as soon as details for attaching cooled coaxial power leads are verified by testing a model unit.

The design concept of the cantilever supports for internal coils has been decided on. Studies now are in process to arrange practical details for ease of fabrication, assembly, and maintenance.

The study of a differentially pumped pressure-transition section to be utilized in beam diagnostics of the Astron machine was initiated. This section would allow a fairly smooth pressure transition from 1 mm Hg to atmospheric pressure in a maximum distance of about 50 mm, while allowing an unobstructed beam path about 5 mm in diameter. Such a device would incorporate a series of staged orifices, whose discharge chambers would be individually vacuum-pumped. An analysis was completed which indicated that an optimum expansion ratio exists for any fixed configuration of orifice area, orifice discharge coefficient, and discharge-chamber pumping speed.

A staged orifice device, geometrically and dimensionally similar to the proposed configuration (see Fig. 30), has been constructed, and is now being connected to appropriately staged vacuum systems. Actual pressure characteristics of this system should be forthcoming in the near future.

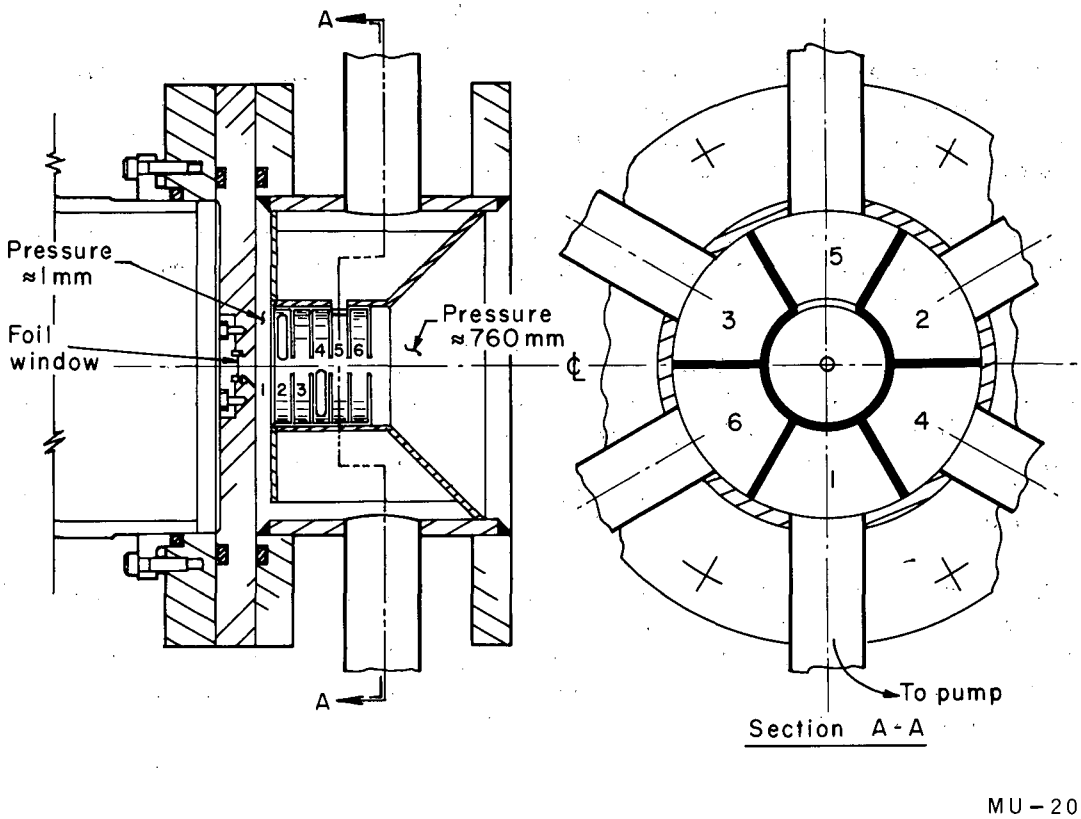

Fig. 37. Differentially pumped transition section.

Cryogenic Project

Clyde E. Taylor, Robert L. Nelson, David C. Holten, and Richard G. Mallon*

Sodium of a purity high enough to give a resistivity at 4.2°K of 1/5000 or less of its resistivity at 0°C can now be routinely produced in our vacuum still. Approximately 30 gallons (total) has been distilled. This is a satisfactory conductor metal for cryogenic coils.

A sodium sample 20 ft long by 1/2 in. diam, encapsulated in a steel tube, is now being prepared for a magneto-resistance measurement in a 20,000-gauss field.

Construction of the 8-in. i.d. sodium test coil continues at a satisfactory rate. About half of the coil test apparatus is under construction, and the remainder is about two-thirds designed. The refrigerator for this test apparatus is now completed and is operating at the Arthur D. Little Co. in Cambridge, Mass. The 20,000-std.-ft^3 helium gas recovery balloon has been received and is being installed.

The small three-stage cascade refrigerator is now operating satisfactorily at -250°F. The final stage uses a single 3/4-hp hermetically sealed methane compressor. Several months of operating experience will be necessary before the new rotary-vane-type first-stage compressors can be deemed satisfactory for this type of service.

*Consultant to UCRL from Astra, Inc., Raleigh, North Carolina.

3. ELECTRICAL ENGINEERING DEVELOPMENT

Vernon L. Smith

Pyrotron

David R. Branum

Table Top II

During the past three months the Table Top machine has been used in the experiments of Dr. Thomas Passell and Dr. Walton Perkins. For this period there were 5,335 bank operations at an average bank level of ±10 kv.

The mechanical crowbar relieving switch is awaiting modifications and has not been in use on the machine during the past quarter.

It became necessary to replace all the bank charge resistors that had been in use since 1955, but there have been no malfunctions of the machine itself.

Two types of photomultiplier-detector circuits were designed and constructed for use on the experiments by Dr. Walton Perkins. One circuit was designed without a cathode follower and for a 6-μsec response time. The second base was designed with a cathode follower to drive 150 volts into Z_0 = 1 megohm at the end of 100 feet of RG-63/U coaxial cable. The second base was designed to have less than 10% "overshoot" for a 40-msec signal.

The two Tobe Deutschmann 15-μf capacitor and type-A ignitron setups were connected to the gas valve experiment. The units functioned satisfactorily at levels up to 10 kv. At a level of 16 kv and a resultant peak current of 196,000 amp the ignitrons overheat and do not hold voltage above 10 kv. Additional capacitor-switch sections are to be added to decrease the maximum current per switch ignitron.

The dc ion-gauge power supply for the experiment by Dr. Richard F. Post was completed and installed. The unit cancelled out all pickup noise from the source.

The 50-kv electron gun bias cart was completed and is now in use on this experiment. The deflection pulser was installed and is now in use. At 46 kv, the deflection chassis failed to deflect the beam sufficiently to direct it all into the Faraday cup. The geometry of the gun structure will be changed to effect full deflection into the cup. The changed gun will require only a 1-kv deflection pulse to deflect the beam into the measuring cup. The present deflection chassis is a breadboard model and has a peak pulse amplitude of 3 kv. A new chassis will not be constructed until the complete electron gun requirements are known.

The six 3/4-in. photomultiplier detectors for the experiment by Dr. Robert Ellis are still in the shops.

Toy Top III

There has been a large amount of electronics engineering effort on Toy Top during the past three months.

One of the 300-kw dc magnet supplies has been completed and is now in use. The second 300-kw dc supply is complete in itself. The controls to the operating area are not yet complete.

The two kenotron-type dc 20-kv bank-charging supplies have been completed. Both units have been tested and used at 21 kv at 3 amp for approximately 150 operations. The two supplies, when set for 21 kv at 2.5 amp, charge one 210,000-joule section of bank No. 4 to full energy in 9 sec. Both supplies can be operated at 25 kv at 4 amp maximum if a faster charge rate is desired.

The 32,000-joule bank, known as bank No. 1, has been tested into its one-turn load coil for approximately 50 pulses at ±17 kv.

Bank No. 1 has a rise time into its 0.3-μh load coil of 4.5 μsec. The L/R crowbarred field-decay time is approximately 230 μsec. This is a ratio of field-decay time to field-rise time of 50. The average ratio on previous coil-bank systems has been 10 to 15. This bank delivers approximately 96% of its energy to the one-turn load coil.

Bank No. 4 was completed and tested on its two 3-μh load coils for 150 operations at maximum energy of 210,000 joules per load group at ±20 kv bank voltage. Additional bracing was added to the bank bus system to prevent the forces due to the high current, a maximum of 300,000 amp, from bending the bus-work.

Each section of bank No. 4 has a rise time of 50 μsec into a 3-μh load coil. The crowbarred field does not have an adequate L/R decay time and appears to be due to too large a resistance in the bank transmission line and its individual coaxial joints. The field decays to the 1/e value in 325 μsec with a nonuniform damped ring on top of the average field decay. Further work will have to be done on decreasing the transmission-line resistance without increasing the line inductance. The present line has a calculated inductance of 0.36 μh and a measured resistance of 7 milliohms. The crowbar tubes appear to have a resistance of 2 milliohms.

The rather large line resistance causes a voltage-current phase lag between the coil and the terminals of the crowbar tubes at the bank end of the transmission line. This condition makes it almost impossible to obtain a good crowbar action at the peak of the current through the load coil.

Bank No. 3C, a 210,000-joule ±20-kv bank, is approximately 80% complete. The transmission line for this bank is now under design and will have a total run of 80 ft.

P-4

There has been some electronics engineering effort in the P-4 in trying to develop a system for the analysis of the spectral lines from the beam and for analysis of the beam noise output.

Atomic and Molecular Cross Section Experiments

David R. Branum

Considerable effort has been devoted to the completion of the atomic cross section facility. All the cables and most of the chassis have been installed.

The machine has been vacuum tested and a number of minor changes in the electrical wiring have been made.

Tests have been made, using a simulated signal source, a lamp, and a diode with no anode voltage, to determine the effectiveness of the detection system.

In an effort to synchronize the chopper-wheel frequency with the band-pass frequency of the phase lock-in amplifier, a frequency-control unit fixed to 100 cps as a reference frequency was designed and is now under construction. This unit will be used as part of the detection system when completed.

The 6-in. Varian electromagnet has been received, and a matching current supply is on order.

The power supplies for the ion gun were chosen from those available commerically which most nearly approach the desired regulation. Since no manufacturer would bid on supplies with the desired regulation of 0.1% at 60 kv, power supplies with 1% regulation have been ordered and will be delivered in the latter part of June 1960.

Pyrotron

H. W. Van Ness

Baby Alice

A rapid beam-turnoff system was designed and put into operation. Investigation of instrumentation problems involved in plasma decay rate measurements is in progress.

Alice

Design of the electronics installation for Bldg. 180 continues. A thyrite discharge resistor assembly for dissipation of the stored energy in the cryogenic cooled-coil system has been designed and ordered. Tests are planned on possible switches for use in conjunction with the thyrite to terminate the current pulse in the magnet coils. The tests will determine the ability of the switches to interrupt the dc coil current satisfactorily without damage.

Sanctus

It is planned to move this experiment to Bldg. 180 very shortly. Equipment for running a beam-scattering experiment has been designed and is being fabricated.

Source Development

Design effort for source-development equipment in Bldg. 180 continues. A current-regulator scheme to control the motor generator supply for the source field coil is being studied. It will be necessary to maintain the magnetic field constant within 0.1% with the regulator.

Pinch and Collapse

H. W. Van Ness

Gamma Bank Area

Operational tests of the condenser-bank sections are under way. A protective prefire crowbar system was developed to automatically crowbar the bank in case of prefire of individual capacitor-ignitron units. In addition, a sensing system to fire all the bank crowbar tubes in the event of a gross prefire of most or all of the bank is being developed. The combination should permit safe operation of the bank up to the 20-kv level.

A modular air-core isolating inductor for use in the levitron experiment has been completed. It successfully operated as a test load for the 1.5-farad electrolytic bank at a charge level of 400 volts.

Electron-Beam Experiment

A 50-kw pulsed oscillator operating in the range of 2 to 5 Mc is currently undergoing development tests for use as the power source for multiply pulsing the electron gun. It is hoped to provide 100 kv peak in the tank circuit, which will supply the anode-cathode gun potential.

Plasma-Acceleration Experiment

All material is on hand to construct the fast bank. Construction has been postponed to permit other higher-priority jobs to be completed.

Sodium Radio-Frequency Analog Experiment

Moderate success has been achieved with the development of a variable-frequency (100- to 2000-cycle) ignitron inverter. However, somewhat erratic performance occurs at the higher frequencies. This is apparently due to the marginal nature of some of the components employed. A redesigned version will be constructed in the hopes of obtaining improved operation.

300-kv Marx Bank Area

Cornell-Dubilier provided an electrician to run reduced rating tests on a sample lot of 300 of the Tobe Deutschmann capacitors which gave unsatisfactory performance in this bank. One unit failed during the test, but the rest operated for 1000 pulses without trouble. Consequently, the manufacturers will replace 95 capacitors gratis and we will accept the rest as being useful for other applications. The 95 replacement capacitors include the 30 used in the test and others which failed previously or were otherwise determined to be defective.

Investigation of Energy-Storage System

The latest delievery date promised on the unipolar generator is June 1. Trouble experienced during assembly of the unit at the factory has resulted in considerable delay.

Work is continuing on design and tests of components for the 1.5×10^6-amp switch to be employed in the system.

Switch Development

D. B. Cummings

Mechanical Switching

The fast mechanical crowbar relief switch is being modified for the addition of a saturable reactor. This will reduce currents, during the arcing period prior to closure, that previously caused some contact erosion. This work is essentially completed.

Ignitron Development

Tube Test

All ten of the ignitrons with ceramic anode, ignitor seals, and vacuum-melted molybdenum anodes have been tested at 20 kv. As reported last time, this test established that these ignitrons are very clean, rugged tubes with some mercury wetting problems. With the completion of the testing it has been found that the tubes with copper-nickel brazing did not perform well at 20 kv but those with copper brazing had very few prefires. It is hoped that some of the experimental tubes on order will produce a reliable 20-kv tube of this type.

Nine tubes of the rounded-throat design with graphite anodes have been tested at 10 kv as crowbar tubes. The last three tubes were taken to 7,600, 8,120, and 7,665 shots. The voltage and decay time will be increased to determine the limitations of this type of tube.

Six different kinds of experimental size-A ignitrons have been ordered and are expected soon. These will establish (a) whether a single glass pantleg is as good as a double glass pantleg, (b) whether vacuum-melted steel can be substituted for vacuum-melted molybdenum as the anode

material, and (c) whether a single ceramic pantleg tube with vacuum-melted molybdenum anode can be reliable at 20 kv.

Ignitron Mechanisms Investigation

The report, Kerr-Cell Photographs of Glass Ignitrons, is being issued as UCRL-5687.

Astron

Vernon L. Smith

Introduction

The efforts of the Electronics Engineering Group associated with Astron has been divided into two separate groups, namely, a Research and Development Group (Kris Aaland, Project Engineer) and a Systems Engineering Group (C. D. Nail, Project Engineer). In this and future reports the activities of these two groups will be reported separately by the responsible Project Engineer.

The immediate objective of the Systems Engineering group is to design and construct the Astron machine and associated 5-Mev electron accelerator. Considerable design and some development still must be accomplished before this objective is met; however, procurement of major components has begun.

The Sixth Symposium on Hydrogen Thyratrons and Modulators (May 19, 20, 21) was attended by Kris Aaland and V. L. Smith. Ideas concerning contemplated switching of accelerator cores and our proposed methods were generally accepted by this specialized group as one of the best attempts consistent with the present "state of the art." The details will be found in the subsequent sections.

Research and Development

Kris Aaland

Hard-Tube Modulator Research

Investigation of hard tubes has continued in view of the stringent accuracy (±1/2% on amplitude) and repetition-rate requirements on the present accelerator. A rise-time requirement of 0.01 μsec for the first six cores plus flatness of pulse may require hard tubes. Also, a section of cores driven by hard-tube modulators could be used for correction of the pulse shape by variation of modulator outputs after beam is measured. This method assumes that a constant beam shape from pulse to pulse can be attained. This method would also eliminate the need for a fast-feedback circuit (response to 300 Mc) to operate during the pulse.

The accompanying chart shows the tubes that have been investigated and their present status. A test facility has been constructed to test large tubes in the 30-Mw peak-pulse power class. This facility is capable of

testing hard tubes as switches up to 70 kv and for 0.3-μsec pulse widths. The Westinghouse WX 4366 tube in particular looks promising. Construction has started on a cubicle using six of these tubes in parallel and capable of delivering 100 Mw peak power at 70 kv.

Metal film resistors manufactured by Filmohm and Corning Glassworks were tested for pulse (0.3-μsec width) voltage breakdown. Filmohm samples failed in the 3- to 5-kv range and the Corning samples failed at 8 kv. The application is for energy-dissipating resistors to be used in the new injection system for the Astron.

Manufacturer	Tube	Status
Eimac	4PR60	Parallel assembly (16 tubes) tested. 800 amp and 10 kv (13 Mw). 32-tube assembly performed unsatisfactorily because of voltage breakdowns and oscillations. Distributed amplifier (50-tube assembly) in process of being tested.
Central Electronics	7545/XD45	Four tubes received; all green or gassy. Tube evidently does not meet specs.
Amperex	TBL 12/40	Two tubes received. One tube tested to 30 kv and 200 amp (6 Mw).
Machlett	MB 6697	One tube received. Tested to 31 kv and 310 amp (10 Mw).
Federal	F 6920	One available tested at 30 kv and 200 amp. Covar seal cracked and tube is being repaired.
Westinghouse	WX 4366	Six tubes received. Two tested to 52 kv and 520 amp (27 Mw). Further investigation proceeding. 100-megawatt chassis using six of these tubes is being designed and constructed.

Astron Systems Engineering

C. D. Nail and V. L. Smith

Main Field Power Supplies

The dc power-supply requirements for the mirror fields in the Astron tank have been examined. There appear to be two approaches to the problem of individually adjusting the 80 outer coils and 102 inner coils. Greatest flexibility and rapid change can be obtained by using separate power supplies for each coil. This requires a large number of 10-v power supplies of about 10 kw each.

Alternatively, it seems possible to series-connect all the 80 outer coils and power them from one or two larger supplies. (Similarly for the inner coils.) The individual current adjustments can then be made by shunting each coil with a resistive element. These shunts would be constructed of stainless tubing, water cooled, and be made semi-adjustable by manually sliding a connection along the length. Maximum dissipation in any of the shunts would be about 2.5 kw. The complete mirror-coil system would require six supplies: four 500-kw at 400 v, one 250-kw at 1000 v, and one 20-kw at 40 v. All should be current-regulated. Total power required for the fields is about 2500 kw. The specifications for these supplies are under study. Ripple voltage for a polyphase full-wave supply without filters is less than 5% rms. The inductance of the coils and the flux excluding effects of the tank-wall to 5% ripple at 360 cps will reduce the ac field variation to negligible amounts.

Accelerator Cores and Switching

The following cores were ordered:

One hundred fifty, 8 in. i.d. × 24 in o.d. × 1/2 in. thick, 1 mil, 50% Ni-Fe.

Fifty, 18 in. i.d. × 33 in. o.d. × 1/2 in. thick, 1 mil, 50% Ni-Fe.

One prototype of each was received and tested, and approval was granted to Magnetic Metals to manufacture the balance of the order.

A line-type modulator consisting of one 6587 hydrogen thyratron as a switch element, seven parallel RG-8/U cables (each 97.5 ft long) as a pulse-forming network, and seven parallel RG-8/U cables to a resistive load was constructed and is being run on a life test of 60 pps, 0.3-μsec pulses for 24 hours per day. The network voltage is +32 kv and the output pulse is -16 kv with cathode grounded. The peak power output is 35 Mw. Although the 6587 is rated for only 2 Mw, the actual peak power rating is an unknown function of anode dissipation, peak current, pulse width, anode voltage, rise and fall times of voltage and current, and reservoir voltage.

The manufacturers of thyratrons cannot rate tubes accurately for our application. Since we are of the opinion that the manufacturers' peak power rating can be exceeded for short pulses of low repetition rate we are going to build the accelerator with small thyratrons. The cost difference between three hundred 6587 tubes and three hundred GL-7390 tubes (a General Electric thyratron of comparable rating per their specification data) is about $430,000. It is believed this is a sound decision if a life of 300 hours can be obtained per thyratron. The reliability requirement stipulates that 98% of tubes must work simultaneously. This means six failures can be tolerated continuously. Using tube costs only as a comparison, the GL-7390 would have to have an average life of at least 15,000 hours to be equal on a replacement-cost basis.

The design for a test section of the accelerator utilizing cores and thyratrons has been started, and construction should be finished by mid-June.

The test modulator also revealed that RF-8/U cable had an average life of only 70 hours for this pulse duty when used as a pulse-forming network and charged positive to 32 kv. Failed cables were examined and the preludes to additional failures were noticed as small craters starting from the outside and digging towards the center of the cable. RG-17/U has been substituted for RG-8/U and no failures have been recorded with 100-hour tests on three cables. No failures of the RG-8/U cables on the load side were reported for more than 300 hours of testing on seven cables.

VII. TALKS AND PUBLICATIONS

American Nuclear Society, Iowa State College, Ames, Iowa, March 14, 1960

D. O. Kippenhan, Thermonuclear Research at Livermore, invited paper.

Radio Station KPFA, Berkeley, California, March 15, 1960

R. F. Post, Fusion Power (UCID-4144, March 25, 1960).

U. S. Naval Research Company 12-2 Meeting, UCLRL, Livermore, California, April 4, 1960

Lewi Tonks, Fusion, invited paper.

Spring Meeting of the American Chemical Society, Symposium on the Chemistry of Solid-State Phenomena, Cleveland, Ohio, April 11-14, 1960

R. A. Pasternak and H. U. D. Eisendanger, Interaction of Nitrogen and of Hydrogen with a Molybdenum Surface, invited paper.

American Physical Society Meeting, Washington, D. C., April 25-28, 1960

A. H. Futch, C. C. Damm, W. Heckrotte, and John Killeen, High-Energy Plasma Production by Neutral Atom Injection (UCRL-5872-T Abst., Feb. 8, 1960).

R. F. Post and C. C. Damm, Parametric and Scaling Relations for Plasma Production by Neutral Atom Injection (UCRL-5874-T Abst., Feb. 8, 1960).

H. P. Furth, Sufficient Conditions for Hydromagnetic Stability of a Diffuse Linear Pinch (UCRL-5865-T Abst., Feb. 2, 1960).

John Killeen and W. M. Hess, Densities of Electrons from Neutron Decay Trapped by the Geomagnetic Field (UCRL-5875-T Abst., Feb. 8, 1960).

Harvard University, Physics Department Colloquium, May 2, 1960

H. P. Furth, Controlled Fusion and Its Application in High-Energy Physics, invited paper.

IRE Meeting, Melville, Long Island, New York, May 3, 1960

N. C. Christofilos, Astron High-Current Electron Accelerator (UCRL-5883-T Abst., Feb. 16, 1960).

Journal Publications

Journal of Applied Physics

Charles B. Wharton and Donald M. Slager, Microwave Determination of Plasma Density Profiles, 31, 428 (1960).

The Physical Review

T. G. Northrop and Edward Teller, Stability of the Adiabatic Motion of Charged Particles in the Earth's Field, 117, 1 (1960).

Gordon Gibson and E. J. Lauer, Radiation Damping of an Electron in a Uniform Magnetic Field, 117, 5 (1960).

Lewi Tonks, Self-Consistent Field and Motion of Electrons Which Have a Range in Canonical Angular Momentum in a Uniform Magnetic Field, 118, 2 (1960).

The Physics of Fluids

W. A. Newcomb, Magnetic Differential Equations, 2, 4 (1959).

The Review of Scientific Instruments

Alan W. DeSilva and John M. Wilcox, Method for Defining Position of Magnetic Field Lines, 31, 455 (1960).

IRE Transactions on Nuclear Science

V. L. Smith, Electronic Engineering Design Problems in Fusion Research, NS-7, 1 (March 1960).

This report was prepared as an account of Government sponsored work. Neither the United States, nor the Commission, nor any person acting on behalf of the Commission:

A. Makes any warranty or representation, expressed or implied, with respect to the accuracy, completeness, or usefulness of the information contained in this report, or that the use of any information, apparatus, method, or process disclosed in this report may not infringe privately owned rights; or

B. Assumes any liabilities with respect to the use of, or for damages resulting from the use of any information, apparatus, method, or process disclosed in this report.

As used in the above, "person acting on behalf of the Commission" includes any employee or contractor of the Commission, or employee of such contractor, to the extent that such employee or contractor of the Commission, or employee of such contractor prepares, disseminates, or provides access to, any information pursuant to his employment or contract with the Commission, or his employment with such contractor.